Physiological and behavioural responses of a keystone intertidal predator, *Pisaster ochraceus*, to periodic aerial heat stress

by

Lydia Walton

BSc, University of Victoria, 2021

A Thesis Submitted in Partial Fulfillment of
the Requirements for the Degree of

MASTER OF SCIENCE

in the Department of Biology

We acknowledge and respect the Lək̓ʷəŋən (Songhees and Esquimalt) Peoples on whose territory the university stands, and the Lək̓ʷəŋən and W̱SÁNEĆ Peoples whose historical relationships with the land continue to this day.

Physiological and behavioural responses of a keystone intertidal predator, *Pisaster ochraceus*, to periodic aerial heat stress

by

Lydia Walton
BSc, University of Victoria, 2021

Supervisory Committee

Dr. Amanda Bates (Department of Biology)
Supervisor

Dr. Rana El-Sabaawi (Department of Biology)
Departmental Member

Dr. Iain McGaw (Department of Ocean Sciences, Memorial University)
Outside Member

Abstract

Extreme heat events are becoming more frequent and intense, requiring a better understanding of how temperature variability influences species performance and interactions. When temperatures approach critical thermal limits, disruptions to individual behaviour and physiology, such as reduced prey consumption and suppressed metabolic activity, can have cascading effects on ecosystem functioning. These effects can be especially widespread when keystone predators are negatively impacted, as they exert a disproportionate effect on their community relative to their biomass. My thesis investigates how periodic aerial heat stress relates to mortality, feeding, metabolism, and body surface temperature in juvenile *Pisaster ochraceus* (ochre sea star, hereafter *Pisaster*), a keystone intertidal predator. Through controlled laboratory experiments, I show that exposure to extreme aerial temperatures (~30°C) increases mortality by 33% and reduces mussel consumption to half of that observed in animals experiencing typical aerial temperatures (~20°C or 25°C). Furthermore, cooler seawater (~15°C) exacerbates these adverse effects, leading to a 17% increase in mortality, and ~50% reductions in feeding and metabolic rates compared to individuals exposed to high aerial temperatures (~30°C) under warmer seawater (~20°C). To further assess the effects of temperature variability, I use infrared thermography (IRT) to examine the body surface temperatures of *Pisaster* (n = 738) from eight beaches during summer low tides on Vancouver Island and relate these temperatures to biological factors and environmental conditions. I found that *Pisaster* use several strategies to minimize thermal stress in the field. Specifically, the selection of shaded microhabitats and the use of evaporative cooling allow *Pisaster* to maintain body surface temperatures up to 14°C degrees cooler than the ambient air and up to 6°C cooler than ambient sea surface temperatures. Even so, some individuals were found in sun exposed microhabitats, and in those rare cases,

body surface temperatures exceeded ambient air temperatures by 2°C. The integration of manipulated experiments with field monitoring reveals that increasing air-sea surface temperature disparities could reshape community dynamics through shifts in keystone predation, however, the severity of thermal stress may be reduced through behavioural and physiological buffering strategies.

Table of Contents

List of Tables

Chapter 2

Chapter 3

Appendix 1: Supplementary Materials for Chapter 2

List of Figures

Appendix 1: Supplementary Materials for Chapter 2

Fig. S1 (A) Daily measurements of the maximum air temperature and sea surface temperature for Barkley Sound during the boreal summer (May – August) of 2022. **(B)** Air temperatures were collected by an EnvLogger temperature sensor deployed at Eagle Bay, Bamfield (48.833739, -125.146825 in the intertidal zone (Baum Lab research group, University of Victoria)). Sea surface temperatures (SST) were obtained from the Amphitrite Point Lightstation (48.921138, -125.540979) dataset (https://www.dfo-mpo.gc.ca/science/data-donnees/lightstations-phares/index-eng.html).

Fig. S2 A polynomial regression relating the dry tissue weight (g) and shell size (mm) of Mytilus trossulus (n = 70).

Fig. S3 The percent drop in oxygen by juvenile *Pisaster ochraceus* over 2-hours of aerial exposure in Experiment 2 (May 2024).

Fig. S4 Set up of the metabolic kit **(A)** prior to and **(B)** during measurements of oxygen consumption.

Appendix 3

Fig. 1 Kaplan-Meier survival curves for juvenile *Pisaster ochraceus* (n = 56). *Pisaster* were separated into four treatments (+mussels/25°C air, +mussels/30°C air, -mussels/25°C air, -mussels/30°C air).

Fig. 2 Feeding activity of *Pisaster ochraceus* (n = 11) during the metabolic rate experiment conducted in August 2023.

Fig. 3 The cumulative consumption of *Mytilus* spp. by juvenile *Pisaster ochraceus* in "+ mussels" treatments (+mussels/25°C air, +mussels/30°C air) of the metabolic rate experiment conducted in August 2023.

Fig. 4 The metabolic rates of juvenile *Pisaster ochraceus* that survived the metabolic rate experiment conducted in August 2023. *Pisaster* were assigned to four different treatments: 25°C air/+mussels, 30°C air/+mussels, 25°C air/-mussels, 30°C air/-mussels.

Appendix 4

Fig. 1 The relationship between *Pisaster* body size (ash-free dry mass) and **(A)** the percent drop in aerial oxygen and **(B)** aquatic metabolic rate (estimated using aquatic oxygen consumption).

Fig. 2 The body surface temperatures of juvenile *Pisaster* immediately after a 6-hour emersion in 20°C air (actual air temperature = 18.8°C; pink), a 6-hour emersion in 30°C air (actual air temperature = 28.8°C; red), and an 18-hour submersion in 15°C seawater (actual water temperature = 15.2°C; blue).

Acknowledgements

I am grateful to the Huu-ay-aht people, whose land this research was conducted on, as well as to the Lək̓ʷəŋən people, where the University of Victoria is situated. Thank you to my supervisor Amanda, for believing in me, for always encouraging my ideas, and for showing me what type of scientist I should aspire to be. Thank you to my committee, Drs. Ian McGaw and Rana El-Sabaawi, who have supported me throughout this process and to my co-authors, Jasmin, Viola, and Valesca, who made conducting this science feel like anything but work. Thank you to the Bates Lab for watching countless presentations and helping me work through the highs and lows of this project. To everyone in the biology department, it has been a pleasure to be a part of this community for so long.

Thank you to my friends, who have made these past years some of my most memorable. From boogie boarding in the freezing ocean to hiking through sea caves at low tide, my time in Bamfield would not have been the same without the amazing people who call it home (including the visiting locals). To Chloe and Emma, thank you for taking the most incredible breaks with me, I couldn't ask for two better people to travel the world with. To Valesca and Brittnie, thank you for making me laugh; seeing you both was always the best part of my work day. Thank you to my roommate Wesley, who has supported me through the craziness of not one, but two thesis submissions; going through grad school together has been wonderful. To Leigh, thank you for being both an amazing role model and friend. To my friends back home, particularly Kyra and Brianne, thank you for always being there, even though we are miles away.

Thank you to my parents, who now have an in-depth understanding of sea star biology and intertidal climate change. The countless facetime calls and visits have always kept me moving forwards and I owe my success to your unwavering support. Finally, to my partner Logan, thank you for pushing me to accomplish things I never thought I could, and for being there alongside me every step of the way.

Chapter 1 – General Introduction

Species interactions are fundamental to biodiversity and ecosystem functioning, with competition and predation regulating resource use and promoting ecosystem stability and species richness (Estes *et al.*, 2011; Åkesson *et al.*, 2021). Keystone predators, in both terrestrial and marine systems, are particularly important for maintaining ecological balance by preventing prey populations from overgrazing critical resources and triggering environmental phase shifts (Paine, 1966). Terrestrial grasslands and kelp forests where gray wolves (*Canis lupus*) and sea otters (*Enhydra lutris*) are present exhibit greater biodiversity and habitat quality, as these predators regulate herbivore activity (Estes and Palmisano, 1974; Estes and Duggins, 1995; Ripple and Beschta, 2012; Boyce, 2018). This increased biodiversity enhances ecosystem stability and resilience, as greater redundancy in species traits and trophic roles helps communities resist and recover from environmental disturbance (Peterson *et al.*, 1998). Preserving high-diversity systems through the maintenance of predator-prey relationships will therefore be crucial in the face of ongoing human-driven environmental change, however, this area of research remains understudied (*e.g.*, Alexander *et al.*, 2016).

1.1 Metabolism, predation, and temperature

Predator-prey dynamics are heavily influenced by species' metabolism, which governs resource acquisition from the environment, conversion of these resources into energy, and allocation of that energy toward maintenance, growth, and reproduction (Brown *et al.*, 2004). The metabolic theory of ecology (MTE) describes the relationship between metabolism and predation and links both processes to temperature, predicting that basal metabolic rates and predation rates should increase equally with temperature (Gillooly *et al.*, 2001; Brown *et al.*, 2004). Warmer conditions heighten metabolic demands, requiring greater prey consumption to

sustain physiological processes (Brown *et al.*, 2004). Conversely, colder temperatures slow metabolic processes, placing organisms in a more energy-efficient state where less food is needed (Fernandes and McMeans, 2019). Although MTE provides a strong foundation to connect temperature, metabolism, and predation, empirical studies show that metabolic and feeding rates may not rise proportionally with temperature (Sohlström *et al.*, 2021; Csik *et al.*, 2023). Disparities in thermal sensitivity between metabolism and consumption could destabilize populations, particularly if metabolic demands exceed feeding capacity and cause predator starvation (Rall *et al.*, 2010; Fussmann *et al.*, 2014). Alternatively, heightened predation under warming temperatures may cause severe reductions in prey populations (Vasseur and McCann, 2005). Despite its significance for ecosystem stability, few studies have simultaneously measured metabolic and predation rates under typical or extreme warming conditions.

Even though metabolic and predation rates do not always scale proportionally with warming temperatures, aspects of MTE remain valuable for predicting organismal responses to thermal stress. Physiological traits, such as oxygen consumption, movement, and digestion, typically follow a unimodal thermal performance curve (Padfield *et al.*, 2016; Silbiger *et al.*, 2019). Performance rises with temperature from a critical lower thermal limit to a thermal optimum, before falling sharply towards the critical upper thermal limit, beyond which proteins and membranes are disrupted, and oxygen capacity is greatly reduced (Huey and Stevenson, 1979; Angilletta *et al.*, 2002; Angilletta, 2009). Most species inhabit environments where ambient temperatures remain below their thermal optimum, allowing them to avoid sublethal and lethal conditions amid daily and seasonal temperature fluctuations (Martin and Huey, 2008). However, if temperatures exceed critical thresholds, species may employ buffering strategies, such as altering activity in time or space to avoid extreme temperatures (Whitman, 1987; Petes *et*

al., 2008; Richards *et al.*, 2023). Unfortunately, climate warming coupled with increasingly frequent and intense heat events are pushing many species closer to or beyond their thermal optimums, heightening the risk of thermal stress and potentially reducing the efficacy of thermal buffering strategies (*e.g.*, Deutsch *et al.*, 2008; Kingsolver *et al.*, 2013; Pinsky *et al.*, 2019)

Understanding how species interactions will shift in response to thermal stress is important for predicting the impacts of climate warming and extreme heat events on ecosystem functioning. Higher trophic levels are particularly vulnerable to warming, as consumers face greater metabolic demands in comparison to primary producers with elevated temperatures (López-Urrutia *et al.*, 2006; Murphy *et al.*, 2020). Declines in predators due to climate warming can cascade through lower trophic levels, providing critical case studies to assess the broader ecological consequences of warming and extreme heat events. The effects of warming and predator loss can vary across communities, depending on the thermal vulnerability of different trophic groups. For instance, in a plankton community, warming caused population declines in predators but not in mesopredators (Murphy *et al.*, 2020). Instead, changes in mesopredator and herbivore densities were primarily driven by top-down effects following predator loss (Murphy *et al.*, 2020). Similarly, a microcosm experiment found that warming led to extinctions of top predators and herbivores, while primary producers and bacterivores were largely unaffected by elevated temperatures (Petchey *et al.*, 1999). These multi-trophic approaches are vital for understanding how warming will reshape communities, and more studies are needed to examine the effects of thermal stress across a wider array of species.

1.2 Climate-driven declines of the original keystone predator

The keystone predator hypothesis, first introduced by Robert T. Paine, demonstrated how the removal of predatory sea stars from a north temperate (*Pisaster ochraceus*) and subtropical

(*Heliaster kubiniji*) habitat led to decreased species diversity and reduced food web complexity (Paine, 1966). Since its inception, this concept has been applied broadly across ecosystems, consistently showing that the loss of top predators triggers cascading negative effects on lower trophic levels, disrupts resource availability, and impairs ecosystem functioning (Estes *et al.*, 2011). As climate change drives an increasing number of species extinctions, understanding how keystone species respond to and endure extreme temperature fluctuations will be critical.

Although studies of *Pisaster ochraceus* and *Heliaster kubiniji* founded the keystone predator hypothesis in the 1960s, disease-driven mass mortalities associated with climate warming have brought these predatory sea stars back to the forefront of ecological research. Recent mass die-offs are caused by sea star wasting disease (SSWD), an infection characterized by white lesions, loss of body turgor, tissue degradation, body fragmentation, and eventual death (*e.g.*, Bates *et al.*, 2009). One of the earliest reported outbreaks of SSWD drove *Heliaster kubiniji* to near extinction in the Gulf of California by the late 1970s (Dungan *et al.*, 1982). While the exact cause of SSWD remains unclear, high seawater temperatures have been linked to more severe and rapidly progressing symptoms, making future climate warming particularly concerning for these keystone predators (Bates *et al.*, 2009; Eisenlord *et al.*, 2016; Menge *et al.*, 2016).

The largest recorded SSWD epidemic began in the summer of 2013 along the West Coast of North America, severely affecting more than 20 species of sea stars from Baja California, Mexico to Alaska, USA (Menge *et al.*, 2016). This outbreak coincided with abnormally high seawater temperatures (2 – 3°C above average in some areas) associated with a marine heatwave known as “The Blob” and the 2014-2016 El Niño event (Eisenlord *et al.*, 2016). While the direct causes of the SSWD epidemic are debated, the impacts were far reaching due to the loss of top

marine predators. For instance, the collapse of the sunflower sea star (*Pycnopodia helianthoides*) has been linked to the proliferation of sea urchin barrens, which have replaced kelp forests along the west coast of North America (Galloway *et al.*, 2023). *Pisaster ochraceus* (hereafter *Pisaster*) populations were also severely depleted by the SSWD outbreak, which has negative implications for intertidal community structure due to possible reductions in mussel predation (Paine, 1966, 1974; Eisenlord *et al.*, 2016). However, unlike some other species of sea star, *Pisaster* populations exhibited a surge in recruitment immediately following the epidemic, potentially contributing to their slow but relatively successful recovery in rocky shore habitats (Menge *et al.*, 2016). Despite the repopulation of *Pisaster* along its range, future extreme heat events still threaten this keystone predator and a better understanding of its response and ability to persist under high temperatures is needed.

1.3 Responses to thermal stress in *Pisaster ochraceus*

As an intertidal species, *Pisaster* experiences both aquatic and aerial conditions daily, making it vulnerable to the impacts of climate warming in both environments. Despite this challenge, the natural temperature variability of intertidal habitats has equipped *Pisaster* and other intertidal organisms with adaptations to withstand a wide range of thermal conditions. Notably, the upper thermal limit of adult *Pisaster* in air is approximately 35°C (estimated as the air temperature at which 50% of adult *Pisaster* die of heat death during a 6 hr emersion period; Pincebourde *et al.*, 2008), demonstrating its resilience to extreme heat. This heat tolerance may also help explain *Pisaster*'s relatively successful recovery following the SSWD epidemic, in contrast to strictly subtidal species like *P. helianthoides*, which have remained at persistently low abundances across their range (Hamilton *et al.*, 2021).

Although *Pisaster* has a relatively high thermal tolerance limit, several studies have documented significant sublethal effects under warming aerial and aquatic conditions, including changes in behaviour and physiology (*e.g.*, Pincebourde *et al.*, 2008; Fly *et al.*, 2012; McGaw *et al.*, 2015). For example, chronic exposure to aerial body temperatures exceeding 23°C reduced mussel consumption in adult *Pisaster*, whereas acute exposure to the same conditions temporarily increased feeding due to heightened metabolic demands (Pincebourde *et al.*, 2008). Such shifts in predation have important ecological implications, as mussels, though a foundation species, are competitive dominants that often exclude other species from settlement, thereby reducing biodiversity of intertidal ecosystems (Paine, 1966). Metabolic studies further reveal that *Pisaster*'s oxygen consumption is more sensitive to warming seawater than to elevated air temperatures, with aerial oxygen consumption reaching only about 50% of aquatic levels (Fly *et al.*, 2012). Together, these findings suggest that extreme heat events may significantly alter keystone predation in the intertidal, as *Pisaster* adjusts its feeding rates to balance the varying energetic demands imposed by its environment.

Research on *Pisaster*'s thermal biology has primarily focused on adults, leaving its juvenile life stage relatively understudied. This gap is significant, as early life stages are often more vulnerable to extreme environmental conditions than adults (Harley *et al.*, 2006; Byrne, 2011; Przeslawski *et al.*, 2015). In intertidal ecosystems, many juvenile invertebrates exhibit lower resistance to heat and desiccation compared to their adult counterparts (Jenewein and Gosselin, 2013). High juvenile mortality, driven by environmental stress, predation, competition, and limited food availability (Gosselin and Qian, 1997), is a natural process that may have a limited impact on overall population change. However, extreme juvenile mortality due to climate related stressors could lead to recruitment failures and subsequent population declines (Cavole *et*

al., 2016). To predict the long-term stability of key populations under climate change, a deeper understanding of juvenile thermal tolerance and resilience is needed.

1.4 Thesis Research

This thesis aims to examine how thermal stress affects the physiology and behaviour of a keystone predator during its juvenile life stage. In Chapter 2, I test how periodic aerial heat stress affects mortality, feeding, and oxygen consumption in juvenile *Pisaster* by manipulating air and seawater temperatures representing typical and heatwave conditions in Barkley Sound, British Columbia. I predict that high air temperatures near the upper thermal tolerance limit of *Pisaster* (~35°C in adult *Pisaster*; Pincebourde *et al.*, 2008) will lead to higher mortality, reduced feeding, and decreased oxygen consumption. I also expect that any effects of aerial heat exposure will be minimized when *Pisaster* are housed in cool seawater representative of spring conditions (~15°C) during daily submersion. To contextualize these results, I monitor intertidal air and sea surface temperatures, and quantify *Pisaster* body surface temperatures and the condition of animals in the field (*i.e.*, observations of moribund individuals in a near-death state). Appendices 3 – 5 contribute to the work conducted in this chapter by addressing related questions through targeted supporting experiments. Specifically, Appendix 3 tests the combined effects of food availability and air temperature on the aquatic oxygen consumption of juvenile *Pisaster* to determine if fasted individuals are more vulnerable to aerial heat stress. Appendix 4 investigates the relationship between *Pisaster* body size, body surface temperature, and metabolic rate during aerial and aquatic exposures. Lastly, Appendix 5 tests for the presence of anaerobic respiration under oxygen-limited conditions by measuring the concentration of lactic acid in *Pisaster* coelomic fluid. My research is the first to directly test the responses of juvenile *Pisaster* to

manipulations of both air and seawater temperatures, and contributes to the limited number of studies which examine metabolism and predation simultaneously under thermal stress.

Chapter 3 examines the body surface temperatures of adult and juvenile *Pisaster* during summer low tides at sites near Bamfield and Sidney, British Columbia using infrared thermography (IRT). I investigate how body size, aggregating behaviour, microhabitat selection, and environmental conditions (*i.e.*, air temperature, sea surface temperature, substrate temperature, humidity, and wind speed) influence *Pisaster* body surface temperatures *in situ*. I predict that larger *Pisaster*, and *Pisaster* within aggregations, will buffer heat more effectively due to greater thermal inertia (*i.e.*, the ability to resist temperature change). I also predict that *Pisaster* will preferentially occupy heat-protected microhabitats in order maintain body temperature near their thermal optimum. This chapter provides valuable insights into *Pisaster*'s thermal biology in the field while also validating the experimental treatments outlined in Chapter 2. Moreover, my work highlights key insights that can be gained from infrared thermography over traditional and biomimetic temperature loggers for accurately measuring ectotherm body surface temperatures.

Chapter 2 – Cool ocean temperatures fail to provide thermal refuge for a heat-stressed keystone predator

Lydia N. Walton*[1], Viola R. Watts[1], Jasmin M. Schuster[1,2,3], Amanda E. Bates[1]

[1]Department of Biology, University of Victoria, Victoria, British Columbia, Canada

[2]Department of Anthropology, University of Victoria, Victoria, British Columbia, Canada

[3]Hakai Institute, Calvert Island, British Columbia, Canada

In prep as:

Walton, L.N, Watts, V.R., Schuster, J.M. and A.E. Bates. Cool ocean temperatures fail to provide thermal refuge for a heat-stressed keystone predator.

Acknowledgements: We thank the staff and researchers at the Bamfield Marine Sciences Centre (BMSC) for hosting our research and providing essential resources for our experiments. We thank Mike Delsey for building the temperature-controlled incubators used in our experiments. We also thank Mara Bohm, Emily Braun, Valesca de Groot, and Logan O'Reilly for supporting animal collections and field surveys. We thank Julia Baum, Matthew Csordas, Chris Neufeld and Sam Starko for contributing the air temperature data from Eagle Bay.

Funding: This work was supported by the National Science and Engineering Research Council (NSERC) Discovery Grant (DGECR-2019-00032) and University of Victoria Institutional Funds (Impact Chair 71809) to AEB.

Ethics approval: All applicable institutional and/or national guidelines for the care and use of animals were followed. Research on *Pisaster ochraceus* was conducted under approval of the Department of Fisheries and Oceans Canada (Licence numbers for 2023: XR 123 2023 and 134459; for 2024: XR 52 2024 and 138371), the Huu-ay-aht First Nations Department of Lands and Permitting (HFN permit number: 2023-017), and following the guidelines for animal care outlined by the Bamfield Marine Sciences Centre (BMSC) and the Canadian Council on Animal Care (CCAC).

2.1 Abstract

The increasing frequency and intensity of extreme climatic events demands a better understanding of how organisms respond to temperature shifts and how these responses shape species interactions. Temperature related disruptions in individual behaviour and physiology can signal broader community change and this is particularly true for keystone species, whose impact on their ecosystem is disproportionately large. We tested how periodic aerial heat stress affects mortality, feeding, and metabolism in juvenile *Pisaster ochraceus* (ochre sea star; hereafter *Pisaster*), a keystone intertidal predator, by manipulating air and seawater temperatures representing typical and heatwave conditions in Barkley Sound, British Columbia. To contextualize these findings, we also quantified local environmental temperatures paired with *Pisaster* body surface temperatures and physical condition in the field. We found the highest mortality (42%) in treatments exposed to cool seawater (~15°C) with high air temperatures (~30°C), which corresponded with ~50% reductions in both mussel consumption and metabolic rate. In contrast, warmer seawater (~20°C) mitigated these effects, supporting higher feeding and metabolic rates, even under extreme air temperatures (~30°C). These findings refute the assumption that a combination of warm seawater and high air temperatures would lead to greater cumulative heat damage. Thus, we predict that *Pisaster* will be vulnerable to aerial heatwaves in spring and early summer when ocean temperatures remain cool. The timing of extreme heat events therefore plays a critical role in predicting species responses, particularly as warming air temperatures actively alter community dynamics by changing rates of keystone predation.

2.2 Introduction

Climate change is complex, and ongoing analysis of its impacts on natural environments is needed to understand and respond to the accelerating pace of change. Global surface temperatures are not only rising, they are becoming more variable with increasingly frequent and intense climatic events. Unpredictable fluctuations in temperature can be damaging for numerous taxa, causing reduced metabolic functioning, suppressed feeding, reproductive failure, and mortality (*e.g.,* Pincebourde *et al.* 2008, McKechnie *et al.* 2012, Zeh *et al.* 2012, Menge *et al.* 2016, Kim *et al.* 2024). Such impacts can cascade through entire communities, leading to local species declines and extinctions, altered species interactions, and diminished ecosystem functioning (Kordas *et al.*, 2011; Wernberg *et al.*, 2013; Stoks *et al.*, 2017; Vázquez *et al.*, 2017).

Despite the physiological challenges related to environmental variability, many organisms can adapt, often relocating to more favourable thermal habitats or altering their daily rhythms to shut down during extreme exposures (Beever et al. 2017, Fey et al. 2019, Gilbert et al. 2022). Some insects take refuge in shaded locations during the hottest parts of the day while others shift activity patterns between day and night to avoid unfavourable conditions (Whitman, 1987; Huey and Pascual, 2009). Likewise, lizards, birds, and mammals can buffer extreme heat or cold by shading in burrows or basking on sun-exposed surfaces (*e.g.*, Moore *et al.* 2018, Hieb *et al.* 2023, Richards *et al.* 2023). Such behavioural strategies allow organisms to conserve energy and vital resources, and may improve their capacity to cope with sudden temperature changes.

Intertidal ecosystems, where ocean and land meet, have long been a model for studying the effects of temperature variability. Many intertidal areas experience extreme temperature shifts daily, with resident organisms facing changes upwards of 20°C between submersion and emersion (Helmuth and Hofmann 2001, McGaw et al. 2015). Similar to terrestrial animals,

mobile marine species generally avoid such thermally stressful conditions through movement (Helmuth and Hofmann, 2001; Szathmary *et al.*, 2009; Sun *et al.*, 2023). For example, predatory sea stars move with the tides to avoid high temperatures, and position themselves lower on the shore to minimize emersion time (Robles *et al.*, 1995; Robles, 2013).

The strong link between behaviour and thermal conditions underscores the importance of temperature on organismal performance, influencing everything from metabolic rates to foraging efficiency. In ectotherms, performance typically rises with temperature from a critical lower thermal limit (CT_{min}) up to a thermal optimum (T_{opt}) before declining sharply near a critical upper thermal limit (CT_{max}), beyond which death occurs (Gillooly *et al.*, 2001; Brown *et al.*, 2004; Dell *et al.*, 2011; Rebolledo *et al.*, 2021). When temperatures approach CT_{max}, ectotherms may conserve oxygen by suppressing non-critical behaviours like feeding, prioritizing energy for survival over digestion (Dahlhoff et al. 2001, Pincebourde et al. 2008). However, this trade-off can reduce survivorship over time and have bottom-up effects on community composition and species diversity when predator-prey interactions are altered (Paine 1966).

We were interested in temperature variability typical of extreme climatic events and how this would affect the behaviour and physiology of a keystone predator. We tested whether warmer ocean temperatures (~20°C) combined with high air temperatures (~30°C) would lead to greater cumulative heat damage in a predatory intertidal sea star (the ochre sea star: *Pisaster ochraceus,* hereafter *Pisaster*). We designed two experiments to determine the responses of mortality, feeding rate (mussel consumption), and metabolic rate (oxygen consumption) under typical air and ocean temperatures, crossed with warm exposures representing heatwave conditions. First, we predicted that higher air temperatures near the upper thermal tolerance limit of *Pisaster* would lead to higher mortality and reduced mussel (*Mytilus* spp.) consumption. We

also expected that any effects of heat exposure would be minimized when organisms were housed in relatively cool seawater (~15°C) during daily submersion. Second, we investigated the role of metabolic suppression as an indicator of poor physiological condition and increased susceptibility to thermal stress (Dahlhoff et al. 2001). We predicted that elevated aerial temperatures would lower oxygen consumption and impair locomotory function (*i.e.*, *Pisaster*'s ability to attach to surrounding substrates). We also monitored intertidal air and sea surface temperatures, and quantified *Pisaster* body surface temperatures and the condition of animals in the field (*i.e.*, observations of moribund individuals in a near-death state) to provide real-world context for our experimental treatments.

2.3 Materials and Methods

2.3.1 Collections

Juvenile *Pisaster ochraceus* (hereafter *Pisaster*) were haphazardly collected from Eagle Bay, Bamfield, British Columbia (48°50'01.9"N, 125°08'47.7"W; **Fig. 1**) in early June 2023 (Experiment 1; n = 72) and early May 2024 (Experiment 2; n = 72). Animals were transported by boat (in water-filled buckets) to the Bamfield Marine Sciences Centre (BMSC; **Fig. 1**) and housed in flow-through seawater tables. *Pisaster* were measured upon collection, including arm length (measured from the centre of the aboral disc to the tip of the arm ray closest to the madreporite in mm), disc diameter (diameter of the aboral disc in mm), and wet mass (g). Wet mass ranged from 1 to 30 g (mean ± SD = 8.2 ± 6.5 g) in 2023 and from 5 to 16 g (mean ± SD = 8.9 ± 3.0 g) in 2024. *Pisaster* were classified as juveniles based on size (sexual maturation at wet masses of 70 to 150 g; Mauzey, 1966; Menge and Menge, 1974; Robles, 2013). Mussels (*Mytilus* spp.) were provided as a food source and were collected from docks and pilings within the Bamfield Inlet (48°49'48.0072"N, 125°8'17.5884"W; **Fig. 1**).

2.3.2 Experimental set-up

Four sea tables (40 L each) were used for seawater treatments and were supplied with continuous flow-through seawater at ~0.625 L min^{-1}. Two sea tables were heated to ~15°C using 200 W aquarium heaters (AEH3617090 Jager aquarium thermostat heater, Eheim), while the other two were heated to ~20°C using 250 W aquarium heaters (3618090 Jager aquarium thermostat heater, Eheim). Each sea table housed 18 animals in individual 750 mL containers. Containers were swapped daily between sea tables to minimize sea table effects while preserving treatment conditions (*i.e.*, individuals in the 15°C seawater treatment alternated between both 15°C sea tables).

Three temperature-controlled incubators (95 L Coleman cooler fitted with a LANTRO JS Thermoelectric Cooler (B094NMHPGJ)) circulated and heated air (using 12V, 12A Peltier cells) to achieve target temperatures of ~20°C, 25°C, and 30°C. Each incubator housed 24 *Pisaster* containers. Air and sea surface temperatures in Barkley Sound, described below under "Body surface temperatures and Field observations", were used to parameterize air and seawater treatment temperatures (see **Appendix 1: Supplementary Materials for Chapter 2** for a detailed explanation).

The tidal cycles in Barkley Sound are mixed semidiurnal (*i.e.*, two low and two high tides of differing size each day), with *Pisaster* typically exposed only during the lowest tide lasting ~6 hours. To expose animals to air, *Pisaster* were cycled (*i.e.*, containers were moved by hand) between an 18-hour submersion in sea tables and a 6-hour aerial emersion in incubators. Temperature probes (INKBIRD IBS-TH2 Plus) monitored conditions at the inflow and outflow of each sea table and inside each incubator throughout the experiment.

2.3.3 Experiment 1 (June 2023): Effects of air and seawater temperatures on juvenile Pisaster feeding rates

Juvenile *Pisaster* were randomly assigned to one of six treatments (n = 12 per treatment) crossing two seawater exposures (15 and 20°C) and three air exposures (20, 25, 30°C), resulting in combinations of 15/20, 15/25, 15/30, 20/20, 20/25, 25/30 (water/air temperatures in °C). Mean body size (disc diameter) differences among treatments were less than 3 mm. Before treatment exposures, *Pisaster* were submerged in seawater (~13°C) which was pumped from the bottom of the Bamfield Inlet into experimental sea tables through a flow-through system, allowing animals to adjust to laboratory conditions. During heat stress, seawater temperatures were raised to better represent conditions present at the collection site (*i.e.*, 15°C representing SST recorded at Eagle Bay in May and June, 20°C representing SST recorded at Eagle Bay in August; **Table 2)**. Juvenile *Pisaster* were fasted for eight days prior to heat stress, ensuring all animals had evacuated food from their digestive systems and returned to basal levels of metabolic rate (Vahl, 1984; McGaw and Twitchit, 2012; McGaw *et al.*, 2015).

Heat stress began on day nine, with *Pisaster* cycled between 18 hours submerged in sea tables (~15°C or 20°C seawater) and 6 hours emersed in incubators (~20°C, 25°C or 30°C air). Heat stress lasted for 16 consecutive days, and *Pisaster* were fed mussels *ad libitum* (*i.e.*, minimum 3 mussels in every container). Empty shells (*i.e.*, consumed mussels) were counted and replaced with fresh mussels daily. *Pisaster* survival was also monitored, and any deceased individuals were removed from the experiment. Following heat stress, sea table temperatures returned to ambient (~13°C) for an eight-day recovery with continued *ad libitum* feeding and daily removal of empty shells. All surviving *Pisaster* were returned to the collection site at the end of the experiment.

2.3.4 Experiment 2 (May 2024): Effects of air and seawater temperatures on juvenile Pisaster feeding rates, metabolism, and attachment tenacity

Juvenile *Pisaster* were randomly assigned to one of four treatments (n = 18 per treatment) crossing two seawater exposures (15 and 20°C) and two air exposures (25 and 30°C), resulting in combinations of water/air temperatures in °C as follows: 15/25, 15/30, 20/25, 20/30. Mean body size (disc diameter) differences among treatments were less than 1 mm. Before treatment exposures, *Pisaster* were cycled between 18 hours submerged in sea tables (heated to 15°C) and 6 hours emersed in incubators (heated to 20°C) for a ten-day adjustment period. Heat stress began on day 11, with animals alternating between 18 hours submerged in 15°C or 20°C seawater, and 6 hours emersed in 25°C or 30°C air. Heat stress lasted for 20 consecutive days. Following heat stress, seawater temperatures returned to 15°C and air temperatures to 20°C, and *Pisaster* continued to cycle through 18 hours of submersion and 6 hours of emersion for a nine-day recovery period. We fed *Pisaster* mussels *ad libitum* during the entire experiment (adjustment, heat stress, and recovery) to assess whether the mortality and feeding rates in Experiment 1 were related to fasting prior to treatment exposures. Elevated temperatures can also impair locomotory function in sea stars (Kidawa 2005), therefore, *Pisaster* attachment to their holding container was used as an additional indicator of thermal stress. We monitored attachment by gently pulling each animal from the holding container following 6 hours of aerial emersion, and recorded them as “attached” or “unattached”.

Measurements of aerial and aquatic oxygen consumption (metabolic rate)

Nine *Pisaster* were randomly selected from each treatment (15/25, 15/30, 20/25, and 20/30) for measurements of aerial and aquatic oxygen consumption. Oxygen consumption was measured four times during the experiment. Assays took place at the end of adjustment (day 9), in the middle of heat stress (day 19), at the end of heat stress (day 29), and at the end of recovery

(day 38). All *Pisaster* were fasted surrounding the oxygen consumption assay (*i.e.*, 48 hours prior, 24 hours during, and 24 hours after completing the assay) to avoid rapid increases in metabolic rate after feeding (*i.e.*, the specific dynamic action of food; SDA) (Vahl, 1984; Schuster *et al.*, 2022)

Experimental assay system for measuring oxygen consumption

A custom-built experimental system was used to measure the oxygen consumption ($\dot{M}O_2$) of individual *Pisaster* (**Fig. S4;** described in detail: Schuster et al. 2022, Schuster and Bates 2023). In brief, the system consisted of a table with 10 removable acrylic chambers (240 mL, 6.5 cm in diameter) and magnetic stir plates, placed inside either a temperature-insulated incubator (aerial $\dot{M}O_2$) or temperature-insulated seawater tank (aquatic $\dot{M}O_2$). The seawater tank was fitted with a heater, chiller, water pump and air stone. Each acrylic chamber was fitted with its own temperature and fiber-optic oxygen dipping probe (PreSens Pt1000 and DP-PSt7-10-L2.5-ST10-YOP). Temperatures and oxygen levels (% saturation) were made every second via PreSens software (PreSens Measurement Studio 2, Version 3.0.3; Precision Sensing GmbH, Regensburg, Germany); oxygen measurements were automatically temperature-corrected by the software. Probe calibration was done using air-saturated seawater (100% O_2) and room temperature distilled water containing sodium sulfite (no O_2; 1 g Na2SO3 dissolved in 100 mL of water).

Aquatic oxygen consumption ($\dot{M}O_2$)

The wet mass (g) and volumetric displacement (volume of seawater with *Pisaster* - volume without *Pisaster*) of each individual was measured the evening before the assay. The seawater tank was filled with fresh, filtered (10 µm) seawater at the start of each assay day, and heated to the treatment temperature. Treatment temperatures were 15°C for the first assay day (adjustment), 15°C or 20°C for the second and third assay days (heat stress), and 15°C for the

fourth assay day (recovery). A maximum of nine individuals could be assayed at a time (due to space constraints of the respirometry system), thus measurements of aquatic $\dot{M}O_2$ were staggered over a ~6-hour period. Animals were randomly assigned to each of the nine chambers, with the tenth chamber remaining empty to account for background respiration (*i.e.*, due to microorganisms). All ten chambers were covered with mesh-fabric to prevent escape and left undisturbed inside the seawater tank for 15 minutes. To initiate an assay, the lids to each chamber (9 *Pisaster*, one blank) were sealed. Oxygen consumption ($\dot{M}O_2$ in % air saturation) was recorded until oxygen levels dropped by 5 to 10%. The total assay time varied from ~30 min to ~90 min, with longer times for *Pisaster* with lower masses of metabolically active tissue. Following each assay, *Pisaster* were returned to their holding containers and placed into temperature-controlled incubators for a 6-hour aerial emersion. The seawater tank was emptied and rinsed with warm freshwater before the next assay day. *Pisaster* were frozen at -20°C following the last oxygen consumption assay (day 39).

Aerial oxygen consumption (% drop in O_2)

Aerial oxygen consumption was measured immediately after aquatic $\dot{M}O_2$ assays using temperature-controlled incubators and following the same procedures as above. Oxygen levels dropped by a maximum of 3% over a 2-hour measurement period across all treatments during the first (adjustment, day 9) and second (heat stress, day 19) assay days. Given early results, we did not continue to measure aerial oxygen consumption during the third and fourth assay days to minimize handling stress.

Ash-free dry mass (AFDM)

Pisaster AFDM was determined to quantify the amount of organic tissue, or metabolically active tissue, of each animal. Empty aluminum weigh boats were placed in a

muffle furnace (500°C) for 12 hours to remove any organic matter and stored in a sealed container. Animals were thawed and placed on pre-weighed (to 0.01 g accuracy) weigh boats prior to drying. *Pisaster* were dried in a combustion oven (60°C) for 12 – 24 hours until their dry mass had stabilized and then ashed in a muffle furnace (500°C) for 24 – 48 hours. AFDM (*i.e.*, metabolically active tissue) was calculated as the dry mass (including the weigh boat) minus the ashed mass (including the weigh boat) while individual dry mass (*i.e.*, organic and inorganic mass) was calculated as the dry mass minus the weight of the empty weigh boat. The inorganic mass, primarily representing the animal's calcified endoskeleton, was calculated as the ashed mass minus the weight of the empty weigh boat.

Data processing (calculating $\dot{M}O_2$ values)

We calculated the mass-specific $\dot{M}O_2$ for each individual *Pisaster* using the "respR" package in R (Carey and Harianto 2023). $\dot{M}O_2$ measurements were adjusted for salinity and water volume in the chamber by correcting for each individual's volumetric displacement. The $\dot{M}O_2$ values in the blank chamber of each run (<0.1 mL O_2 h^{-1}) were used to correct for background respiration. Mass-specific values were adjusted for ash-free dry mass (*i.e.*, absolute $\dot{M}O_2$ divided by mass). The $\dot{M}O_2$ data was visually inspected to ensure that a linear decrease of 5 – 10% occurred and a minimum r^2 of 0.98 was set to identify nonlinear measurements (Schuster et al., 2022). Measurements that did not meet the r^2 requirement were not included in subsequent analyses (n = 14/144 measurements). Animals failed to meet a minimum drop of 5% air saturation during the 2-hour aerial measurement period, and thus we did not calculate aerial $\dot{M}O_2$.

2.3.5 Body surface temperatures and field observations

We recorded body surface temperatures of experimental animals in 2024 using a thermal imaging camera (FLIR ONE Pro (iOS), Teledyne FLIR; iPhone 13 Pro, Apple Inc.). The camera had a pixel resolution of 19200px (160 x 120px) and an accuracy of ±3°C or ±5% when the unit was within 15°C - 35°C and the scene was within 5°C - 120°C. Emissivity was set to 0.95 in line with studies showing intertidal substrates and invertebrates have emissivity values between 0.95 and 1 (Denny and Harley, 2006; Chapperon and Seuront, 2011; Cox and Smith, 2011). To validate the infrared measurements, we randomly selected 20 *Pisaster* from several sites near BMSC and measured their internal body temperatures with a digital thermometer (Taylor 9848E Safe-T-Guard digital pocket thermometer with antimicrobial sleeve) inserted into the coelomic cavity (midway down one arm ray). The difference in temperature between infrared and thermometer readings was 0.65 ± 0.4°C (mean ± SD; n = 20).

Two infrared images were taken per animal (n = 72) on day 30 (end of heat stress) and on day 39 (end of recovery). The first image was taken immediately after an 18-hour submersion in seawater, and the second immediately after a 6-hour emersion in air. Images were analyzed in Thermal Studio Pro (Teledyne FLIR) using spot measurements (on the central disc and on each visible arm ray) to determine the body surface temperatures of juvenile *Pisaster*.

Field observations of *Pisaster* were conducted monthly (May, June and August) in 2023 at three sites in Barkley Sound (Eagle Bay, Grappler Narrows, and Strawberry Point; **Fig. 1**) during the lowest daily tide. We surveyed *Pisaster* along walking belt transects (three to four transects per site) from the waterline (at tidal datum of 0.33 m to 0.71 m) up to the highest occurring individual. *Pisaster* within one meter on either side of the transect were counted and assessed for signs of moribundity (*i.e.*, animals in a near-death state); animals were recorded as

"moribund" if they displayed white lesions on the body surface or abnormal body turgor (Bates et al., 2009). *Pisaster* were subsequently classified as adults or juveniles based on body size. Air and sea surface temperatures were recorded at each site using a temperature probe (INKBIRD IBS-TH2 Plus) at the start and end of each survey (**Table 2**).

2.3.6 Statistical analysis

All statistical analyses were conducted in R version 4.3.3 (R Core Team 2021). Survival probabilities were determined using Kaplan-Meier survival curves and Cox proportional hazards models from the "survival" and "survminer" packages (Kassambara et al. 2021 and Therneau et al. 2023 respectively). Deceased *Pisaster* and those with fewer than five intact arms were excluded from the feeding and metabolic rate analyses (n = 9 in 2023; n = 0 in 2024).

The effect of air and seawater temperatures on feeding was assessed using generalized linear mixed models ("glmmTMB" package; Brooks et al. 2017) with poisson distributions. Mussel consumption was compared between treatments across the experimental period and within treatment blocks (adjustment, heat stress, recovery). A change point analysis ("changepoint" package; Killick et al. 2022) detected shifts in feeding during the transition from heat stress to recovery. Attachment to the aquaria (a measure of thermal stress) was compared across treatments during heat stress and recovery using a generalized linear mixed model ("glmmTMB" package) with a binomial distribution. The effect of air and seawater temperatures on aquatic $\dot{M}O_2$ was evaluated using a linear mixed-effects model ("nlme" package; Pinheiro et al. 2012) and Tukey post-hoc test ("lsmeans" package; Lenth 2016). Aerial oxygen consumption (% drop in O_2) was compared across treatments and assay days using an ANOVA and Tukey HSD post-hoc test. *Pisaster* body surface temperatures were compared to treatment temperatures

using Kendall tau correlation tests. We used a significance value of $p < 0.05$ as the threshold for all statistical tests.

2.3.7 Pseudoreplication

We recognize that in an ideal experimental set-up, each juvenile *Pisaster* would be assigned to an individual sea table and incubator to avoid pseudoreplication (Hurlbert, 1984), however, this approach was not logistically possible. Instead, we used several methods to reduce the potential errors associated with pseudoreplication in our experiments. *Pisaster* were alternated between sea tables of the same temperature treatment to reduce tank effects. As the number of temperature-controlled incubators was limited in our experiment (n = 1 per air temperature) we included "group" (*i.e.*, animals that were swapped between the same sea tables and incubators were recorded as a distinct group) in statistical models as a random effect to account for variation between incubators and sea tables. We also compared feeding rate and mortality across experiments (Experiment 1, Experiment 2, and Appendix 3) for replicated treatments (*i.e.*, 15°C water/25°C air, 15°C water/30°C air, 20°C water/25°C air, 20°C water/30°C air). Patterns in mussel consumption were very similar between experiments, demonstrating the same trends across temperature treatments despite new cohorts of animals and potential differences in heating equipment between years. While mortality differed between each experiment, this was likely due to environmental factors, such as the timing of collections, as opposed to sea table or incubator effects. This is supported by field observations made during the same months as our experiments, which showed similar mortality in experimental *Pisaster* and those observed in the field at our collection site (Eagle Bay). For these reasons, we do not believe that our experimental results were an artifact of sea table or incubator effects.

2.4 Results

2.4.1 Experimental mortality

Pisaster ochraceus mortality occurred only in the 30°C air treatments during Experiment 1 (June 2023). Five (of 12) animals died in the 15°C water/30°C air treatment and three (of 12) animals died in the 20°C water/30°C air treatment, all during the first half of the heat stress period (days 1-8; June 2023). *Pisaster* in the 30°C air treatments thus had a significantly higher probability of mortality (Cox proportional-hazards model; $p < 0.01$) than those in the 20°C or 25°C air treatments (**Fig. 2**). *Pisaster* mortality in the two 30°C air treatments did not differ, however, there was a trend towards higher mortality in the 15°C water treatment compared to the 20°C water treatment (**Fig. 2**).

2.4.2 Experiment 1 (June 2023): Effects of air and seawater temperatures on juvenile Pisaster feeding rates

Feeding (total mussels consumed per individual) differed between temperature treatments. *Pisaster* in the 15°C water/30°C air treatment consumed the fewest mussels during heat stress and recovery (**Fig. 3A, Table S2A;** $p < 0.001$). However, *Pisaster* from the 15°C water/30°C air treatment did consume significantly more mussels during recovery than during heat stress, consistent with other treatments (**Fig. 3A, Table S2A;** $p < 0.001$).

We also detected differences in feeding rates within each eight-day "trial block" (*i.e.*, first half of heat stress: days 1-8, second half of heat stress: days 9-16, and recovery: days 17-24). *Pisaster* in the 25°C and 30°C air treatments consumed fewer mussels than those in the 20°C air treatment during the first half of heat stress (**Fig. 3A, Table S2B;** $p < 0.01$ and $p < 0.001$ respectively), with a significant air-seawater temperature interaction (**Fig. 3A, Table S2B;** $p < 0.05$). In the second half of heat stress, feeding rates were higher in the 20°C water treatments compared to the 15°C water treatments (**Fig. 3A, Table S2C;** $p < 0.05$), except for *Pisaster* in the

30°C air treatments which consumed fewer mussels regardless of water temperature (**Fig. 3A, Table S2C;** $p < 0.01$).

Change point analysis showed a shift in feeding for *Pisaster* in the 15°C water/30°C air treatment on day 18, with significantly higher feeding during recovery than during heat stress (Kruskal-Wallis test, $p < 0.05$). All other treatments showed change points before the recovery period, and no further analyses were conducted.

2.4.3 Experiment 2 (May 2024): Effects of air and seawater temperatures on juvenile Pisaster feeding rates, metabolism, and attachment tenacity

Feeding rates were monitored throughout the experimental period. As in Experiment 1 (June 2023), *Pisaster* in the 15°C water/30°C air treatment consumed the fewest mussels during heat stress and recovery, and a significant interaction between air and seawater temperatures was observed (**Fig. 3B, Table S3A**).

Feeding differed within each "trial block" (*i.e.*, adjustment: days 1-10, first half of heat stress: days 11-20, second half of heat stress: days 21-30, and recovery: days 31-39). During adjustment, *Pisaster* in the 30°C air treatments consumed slightly more mussels than those in the 25°C air treatments (**Fig. 3B, Table S3B;** $p < 0.05$). Throughout heat stress and recovery, *Pisaster* in the 30°C air treatments consumed fewer mussels than those in the 25°C air treatments (**Fig. 3B, Table S3C, Table S3D, Table S3E;** $p < 0.001$). There was a significant effect of scaled body size (disc diameter) on feeding during the second half of heat stress and recovery, but not during adjustment or the first half of heat stress.

Attachment tenacity

The number of *Pisaster* attached to their holding containers varied significantly across treatments and trial blocks. Fewer *Pisaster* remained attached to their container when assigned to 30°C air compared to 25°C air, and during heat stress compared to recovery (**Fig. 4, Table S4**).

Within the 30°C air treatments, fewer *Pisaster* were attached during the second half of heat stress compared to the first half of heat stress or recovery (**Fig. 4, Table S4**). The percentage of attached *Pisaster* across treatments (water/air temperature in °C) and trial blocks (first half heat stress, second half heat stress, and recovery) was: 85.6% (15/25, first half heat stress), 81.7% (15/25, second half heat stress), 94% (15/25, recovery); 49.5% (15/30, first half heat stress), 10.6% (15/30, second half heat stress), 78.3% (15/30, recovery); 91.7% (20/25, first half heat stress), 90% (20/25, second half heat stress), 96.1% (20/25, recovery); 70% (20/30, first half heat stress), 30.6% (20/30 second half heat stress), and 88.9% (20/30, recovery).

Aquatic oxygen consumption ($\dot{M}O_2$)

The aquatic $\dot{M}O_2$ of *Pisaster* differed across treatments and between assay days. In the adjustment assays, $\dot{M}O_2$ was lower in the 15°C water/25°C air treatment compared to the 15°C water/30°C air treatment (**Fig. 5A, Table S5;** $p < 0.05$). During the first half of heat stress, *Pisaster* in the 15°C water treatments exhibited significantly lower $\dot{M}O_2$ than animals in the 20°C water treatments (**Fig. 5B, Table S5;** $p < 0.05$). In the second half of heat stress, both the 15°C water/25°C air treatment and the 15°C water/30°C air treatment had a lower $\dot{M}O_2$ than the 20°C water/25°C air treatment (**Fig. 5C, Table S5;** $p < 0.01$). During recovery, $\dot{M}O_2$ did not differ significantly between treatments (**Fig. 5D, Table S5**).

Temporal differences in $\dot{M}O_2$ were also observed. For *Pisaster* in the 15°C water/25°C air treatment, $\dot{M}O_2$ was significantly lower during heat stress compared to adjustment or recovery ($p < 0.05$). In the 15°C water/30°C air treatment, $\dot{M}O_2$ was significantly lower during heat stress compared to adjustment ($p < 0.05$), but not recovery. *Pisaster* in the 20°C water/25°C air treatment had significantly higher $\dot{M}O_2$ values during heat stress compared to adjustment ($p <$

0.01), but not recovery. In the 20°C water/30°C air treatment, $\dot{M}O_2$ was higher during the first half of heat stress compared to the second half ($p < 0.05$).

Aerial oxygen consumption (% drop in O_2)

Aerial oxygen consumption was minimal during the 2-hour measurement period, with a percent drop in oxygen ranging from 0.5% to 2.6% during adjustment and 0.6% to 2.9% during the first half of heat stress. There was no significant difference in aerial oxygen consumption between treatments, however, *Pisaster* consumed slightly more oxygen during heat stress compared to adjustment (**Fig. S3**; $p < 0.001$). Further investigation found that even over a 6-hour measurement period (representing a full 6-hour low tide), oxygen saturation failed to drop beyond 8% in air (**Appendix 4**).

2.4.4 Body surface temperatures

The body surface temperatures of juvenile *Pisaster* were highly correlated with environmental temperatures (*i.e.*, seawater and air temperatures; $p < 0.001$). Body surface temperatures were generally within 2°C of the seawater temperature and 3°C of the air temperature (**Fig. 6, Table S6**).

2.4.4 Natural moribundity in Pisaster

All sites displayed very low levels of moribund *Pisaster* during the summer, peaking at 9.6% of adults in Eagle Bay in August (**Table 2**). Eagle Bay showed the highest percentage of moribund adults and juveniles, with signs of lesions and tissue degradation present in adults during all surveyed months and in juveniles during August. Moribundity was only noted for adults and juveniles in Grappler Narrows in August, and no moribund individuals were ever present at Strawberry Point during surveys (**Table 2**). Air temperatures (recorded using the INKBIRD IBS-TH2 Plus temperature probe) ranged from 15.4°C (May) to 21.8°C (June) at

Eagle Bay, 17.8°C (May) to 23.5°C (August) at Grappler Narrows, and 14.3°C (June) to 21°C (May) at Strawberry Point while SST ranged from 14.7°C (May) to 19.5°C (August) at Eagle Bay, 14.6°C (June) to 17.6°C (August) at Grappler Narrows, and 14.7°C (June) to 17.5°C (August) at Strawberry Point (**Table 2**).

2.5 Discussion

Overall, our results highlight the influential nature of temperature variability on a key intertidal species, *Pisaster ochraceus*. Specifically, we found that exposure to cool ocean temperatures (~15°C) during an aerial heatwave increased juvenile *Pisaster* mortality risk, reduced feeding, and suppressed metabolic rates. In contrast, warmer ocean conditions (~20°C) mitigated some of these negative effects, lowering mortality risk and elevating feeding and metabolism, even under extreme air temperatures (~30°C). It appears that *Pisaster* are vulnerable to heatwaves in the spring and early summer months, when ocean temperatures remain cooler, revealing a seasonal window of heightened risk. These findings illustrate a critical gap in our understanding of how fluctuating thermal environments impact behaviour, physiology, and survival. Moreover, they emphasize the need to consider both the timing and interaction of air and ocean temperatures in predicting species responses to climate change.

Prolonged aerial heat stress led to complex feeding and metabolic responses in juvenile *Pisaster*. When extreme air temperatures (~30°C) were paired with cooler seawater (~15°C), mussel consumption and aquatic metabolic rates dropped sharply, and remained low for the duration of heat stress. This sustained decline likely reflected an accumulation of physiological damage and a reduced capacity to recover in cooler waters. When these same air temperatures were paired with warmer seawater (~20°C), the decline in feeding and metabolic rates was less pronounced and recovery was accelerated, suggesting warmer ocean conditions provide partial

protection against aerial heat stress. These findings were unexpected, as they contradict the assumption that warmer ocean conditions, combined with aerial heat stress, would result in greater cumulative heat damage (Martínez-De León and Thakur, 2024). We suggest that, while high air temperatures disrupt feeding and metabolism, the severity and duration of these impacts will be strongly modulated by ocean temperatures.

Despite the positive effects of warmer seawater on feeding and metabolic rates, mortality still occurred in juvenile *Pisaster* exposed to ~30°C air temperatures across both cool and warm seawater treatments. Mortality risk was likely impacted by additional factors such as thermal history and food availability. Sublethal heat exposure can either boost thermal tolerance through acclimatization (Lindquist and Craig, 1988; Somero, 2002; Sørensen *et al.*, 2003) or reduce tolerance by depleting energy reserves (Pörtner 2010, Sokolova et al. 2012). As a result, extreme heat events following stressful conditions are more likely to cause mortality than those following favourable conditions (Siegle et al. 2018). *Pisaster* mortality was higher in 2023 (33%) than in 2024 (0%), likely due to a late-May heatwave in Barkley Sound which may have suppressed feeding and metabolism, exacerbating sensitivity to experimental heat stress. In contrast, well-fed animals in 2024 showed lower mortality rates, emphasizing the critical role of energy reserves for surviving extreme temperatures (Donelson et al. 2010, McLeod et al. 2013). During recovery, *Pisaster* exposed to ~30°C air continued to show suppressed feeding and metabolic rates compared to animals in lower air temperature treatments, further supporting the theory of reduced tolerance post heat stress.

Juvenile *Pisaster* proved to be more thermally sensitive, with mortality occurring at body surface temperatures around 27°C, compared to 35°C in adults (Pincebourde et al. 2008). This aligns with findings in other intertidal invertebrates (*e.g.*, mussels, barnacles, snails; Jenewein

and Gosselin 2013, Hamilton and Gosselin 2020), where juveniles typically exhibit lower heat tolerance and desiccation resistance. These differences may stem from habitat use, as juveniles often occupy shaded and protected areas (*e.g.*, filamentous algae, mussel beds, underneath rocks), whereas adults reside in more exposed areas (Hunt and Scheibling, 1996; Gosselin, 1997; Jenewein and Gosselin, 2013). Most juveniles in our study were found shaded, underneath rocks, or deep in crevices and may not experience extreme heat as often as adults. Additionally, juvenile *Pisaster* lack the thermal inertia of larger adults, which can buffer heat stress by circulating cool coelomic fluid throughout their body (Pincebourde et al. 2009).

The results of this study suggest that high air temperatures during spring low tides can have cascading effects on *Pisaster* populations by disrupting feeding and metabolic processes. Reduced food intake during heatwaves may lower energy reserves, which are critical for sustaining physiological functions and ensuring successful gamete production during reproductive development in the winter (Mauzey, 1966; Sanford and Menge, 2007; Robles, 2013; Robles *et al.*, 2021). In fact, the mass of pyloric caeca prior to winter is almost proportional to the mass of gametes released during the following spring spawn, meaning diminished summer feeding rates directly impacts recruitment (Sanford and Menge, 2007; Robles *et al.*, 2021). Conversely, periods of high air and ocean temperatures may enhance feeding and boost energy stores, potentially improving reproductive output and promoting population growth. The timing and severity of heatwaves, particularly during critical windows for energy acquisition and reproductive development, thus play a pivotal role in shaping *Pisaster* reproductive success and long-term population trajectories.

Extreme heat events also have broader implications for community structure, as *Pisaster* can exert top-down control on intertidal ecosystems through keystone predation (Paine 1966).

Elevated feeding rates under optimal thermal conditions may intensify mussel predation, clearing mussel beds and opening settlement space for other species; a phenomenon which has already been shown to increase biodiversity in intertidal ecosystems (Paine 1966). However, if air temperatures surpass *Pisaster*'s thermal limits, feeding rates decline, reducing predation pressure and allowing mussels to outcompete other species for space (Paine 1969, 1966, Robles 2013 Robles et al. 2021). In this case, the destabilization of predator-prey dynamics decreases intertidal biodiversity and ultimately reduces ecosystem functioning. The strength of this top-down control likely varies across *Pisaster*'s range and between sites (*e.g.*, Menge *et al.*, 1994), as factors such as prey diversity and abundance influence *Pisaster*'s role as a keystone species. Investigating the effects of temperature variability across the geographical range of key predators will be an important next step in assessing community structure under future climate stressors.

2.6 Conclusion

The responses of a predatory sea star to different exposures of air and seawater temperatures suggest that spring and summer heatwaves will affect survival, feeding and metabolism in ways that can not always be predicted based on theory. Hot air temperatures during low tide in the spring months, when ocean temperatures are relatively cool, may lead to the most harmful impacts. This finding underscores a knowledge gap in how other species may respond to increased temperature variability, especially when exposed to both air and ocean conditions. We further highlight the thermal sensitivity of juveniles in comparison to adults, and advocate for future studies to examine thermal stress responses across life stages. Widespread understanding of species responses, at various life stages, to extreme heat events will be crucial for predicting large-scale impacts on ecosystem functioning and for developing effective monitoring and management strategies.

2.7 Figures and Tables

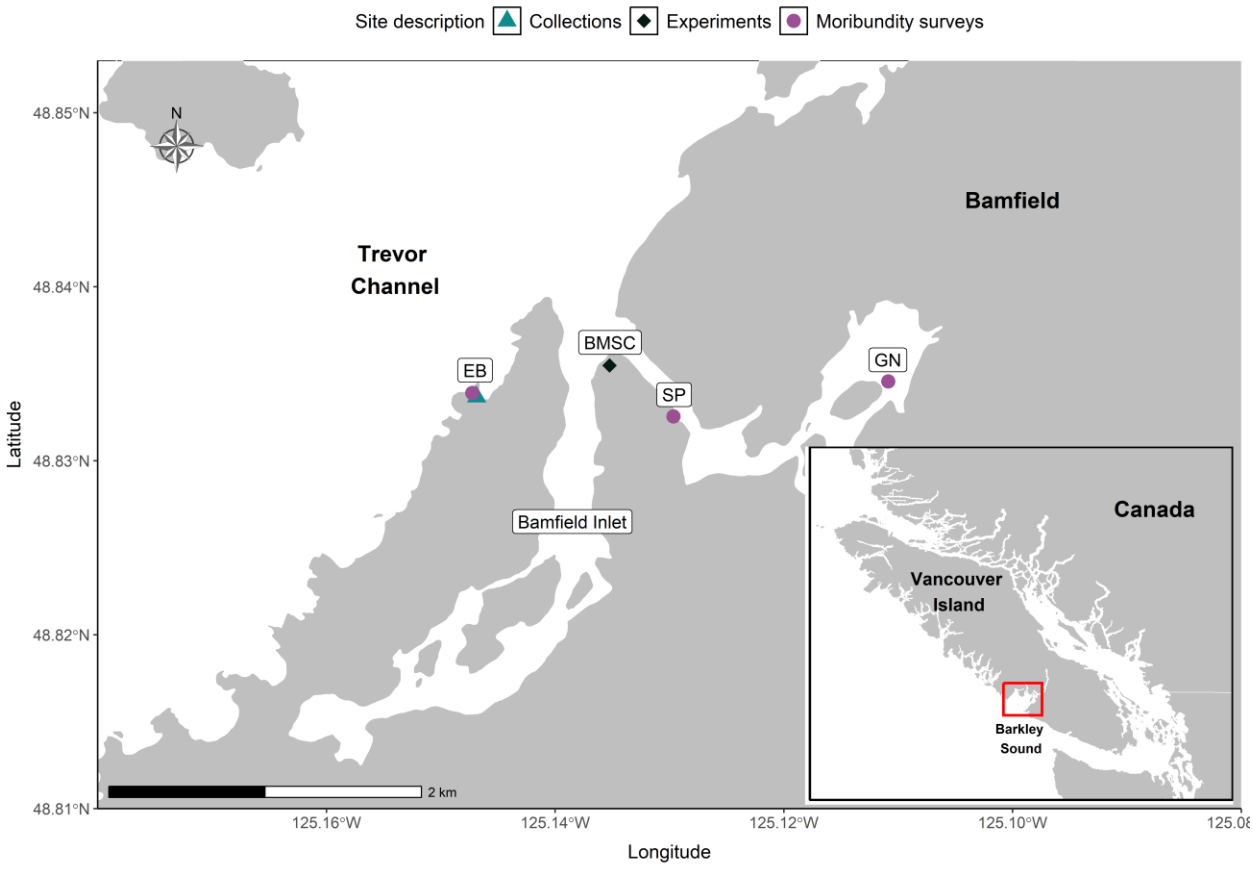

Fig. 1 Map of sites near the Bamfield Marine Sciences Centre (BMSC; black diamond) in British Columbia, Canada used for experiments and field observations in the summers of 2023 and 2024. Eagle Bay (EB) was selected as the collection site (blue triangle) for juvenile *Pisaster ochraceus* used in experiments, and all experiments were conducted at the Bamfield Marine Sciences Centre (BMSC). Three sites (Eagle Bay (EB), Strawberry Point (SP), and Grappler Narrows (GN); pink circles) were surveyed for the presence of moribund adult and juvenile *Pisaster ochraceus*.

Table 1. Summary of experiments and observational studies undertaken in this research. Experiment 1 investigated the effects of air and seawater temperatures on juvenile *Pisaster ochraceus* feeding. The number of mussels (*Mytilus* spp.) consumed per individual and the number of *Pisaster* mortalities per treatment was recorded throughout the experiment. Experiment 2 investigated the effects of air and seawater temperatures on juvenile *Pisaster* metabolism. The number of mussels consumed per individual and attachment to the holding container (indicator of thermal stress) was recorded daily during the experiment. Measurements of aquatic oxygen consumption and aerial oxygen consumption were conducted at set times throughout Experiment 2. Field observations included infrared imaging of *Pisaster* body surface temperature during Experiment 2 and observations of *Pisaster* moribundity at three sites near the Bamfield Marine Sciences Centre (BMSC) in 2023.

Study approach	**Measurement(s)**	**Parameter(s)**	**Year**
Experiment 1: Effects of air and seawater temperatures on juvenile *Pisaster* feeding	1. Mortality: number of deceased *Pisaster* during the experiment; n = 8 mortalities/72 total individuals	Seawater x air temperatures; heat stress, recovery	2023
	2. Feeding: total and cumulative consumption of mussels per individual *Pisaster*; 6 treatments, n = 12 per treatment	Seawater x air temperatures; heat stress, recovery	2023
Experiment 2: Effects of air and seawater temperatures on juvenile *Pisaster* metabolism	1. Mortality: number of deceased *Pisaster* during the experiment; n = 0 mortalities/72 total individuals	Seawater x air temperatures; adjustment, heat stress, recovery	2024
	2. Feeding: total and cumulative consumption of mussels by individual *Pisaster*; 4 treatments, n = 18 per treatment	Seawater x air temperatures; adjustment, heat stress, recovery	2024
	3. Attachment to holding container: measure of thermal stress; 4 treatments, n = 18 per treatment	Seawater x air temperatures; heat stress, recovery	2024
	4. Aquatic oxygen consumption: estimation of metabolic rate; 4 treatments, n = 9 per treatment	Seawater x air temperatures; adjustment, heat stress, recovery	2024
	5. Aerial oxygen consumption: percent drop in aerial O_2; 4 treatments, n = 9 per treatment	Seawater x air temperatures; adjustment, heat stress	2024
Field observations	1. Body surface temperature: infrared imaging of *Pisaster* body surface temperature immediately following periods of submersion and aerial emersion; 4 treatments, n = 18 per treatment	Seawater x air temperatures; heat stress, recovery	2024
	2. Natural moribundity: walking belt transect of moribund adult and juvenile *Pisaster*; 3 sites, n = 1339	Site (Eagle Bay, Grappler Narrows, Strawberry Point)	2023

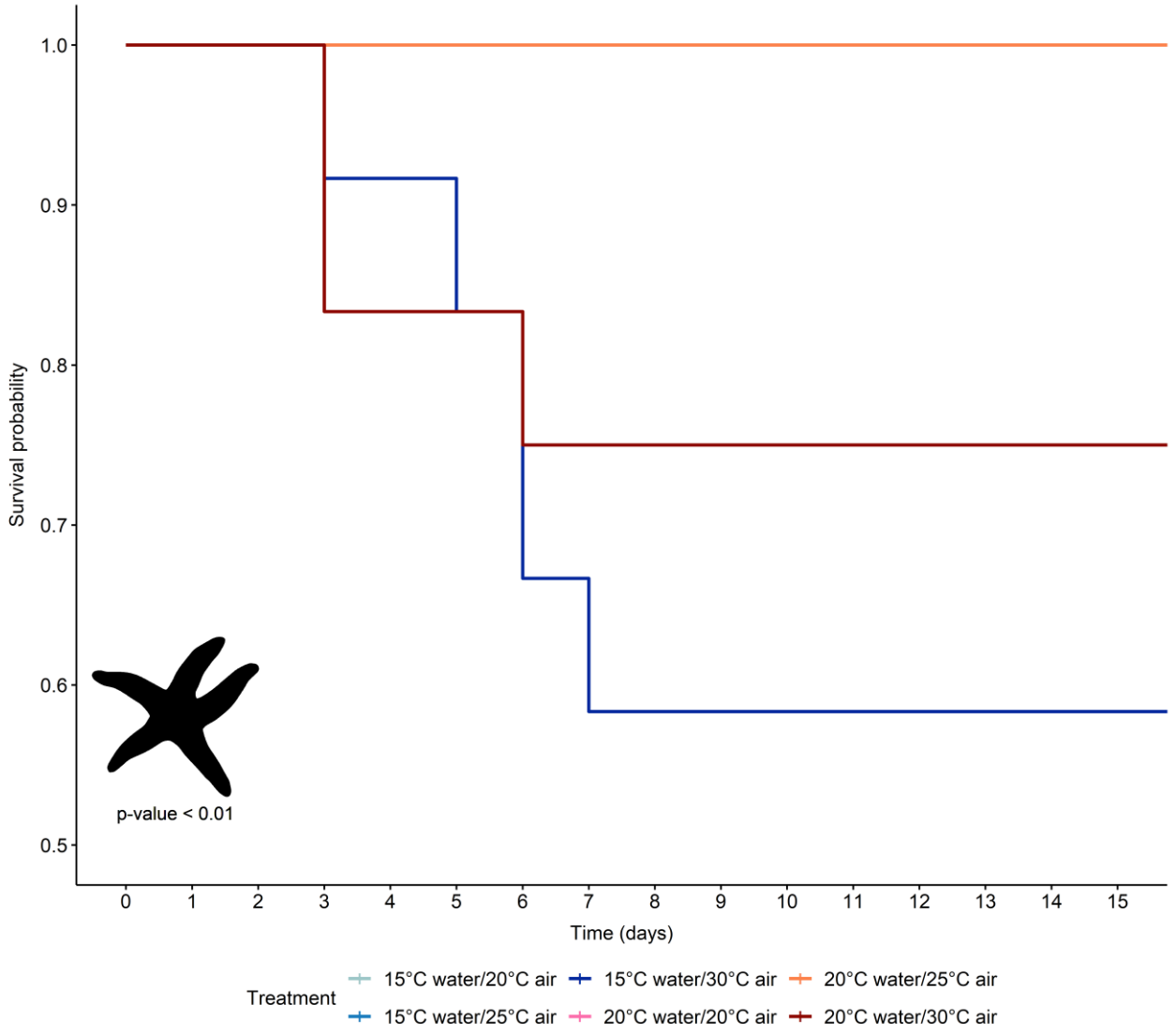

Fig. 2 Kaplan-Meier survival curve for juvenile *Pisaster ochraceus* (n = 12 per treatment) in Experiment 1 (June 2023); no mortality was observed in Experiment 2 (May 2024). Coloured lines represent each temperature treatment; as there was no mortality observed in four treatments (15°C water/20°C air, 15°C water/25°C air, 20°C water/20°C air, and 20°C water/25°C air) during Experiment 1, the lines for these treatments overlap at a survival probability of 1.0. Time (days) represents the 16 days of the heat stress period where sea stars were fed mussels *ad libitum* and alternated between seawater temperatures (~15°C or 20°C) and air temperatures (~20°C, 25°C, or 30°C) in a simulated high-tide (submerged for 18 hours) and low-tide (emersed for 6 hours) cycle. *Pisaster* in the 30°C air treatments had a significantly higher probability of mortality than animals in the 20°C or 25°C air treatments (Cox proportional-hazards model; $p < 0.01$). Five *Pisaster* in the 15°C water/30°C air temperature treatment and three *Pisaster* in the 20°C water/30°C air temperature treatment died during the experiment.

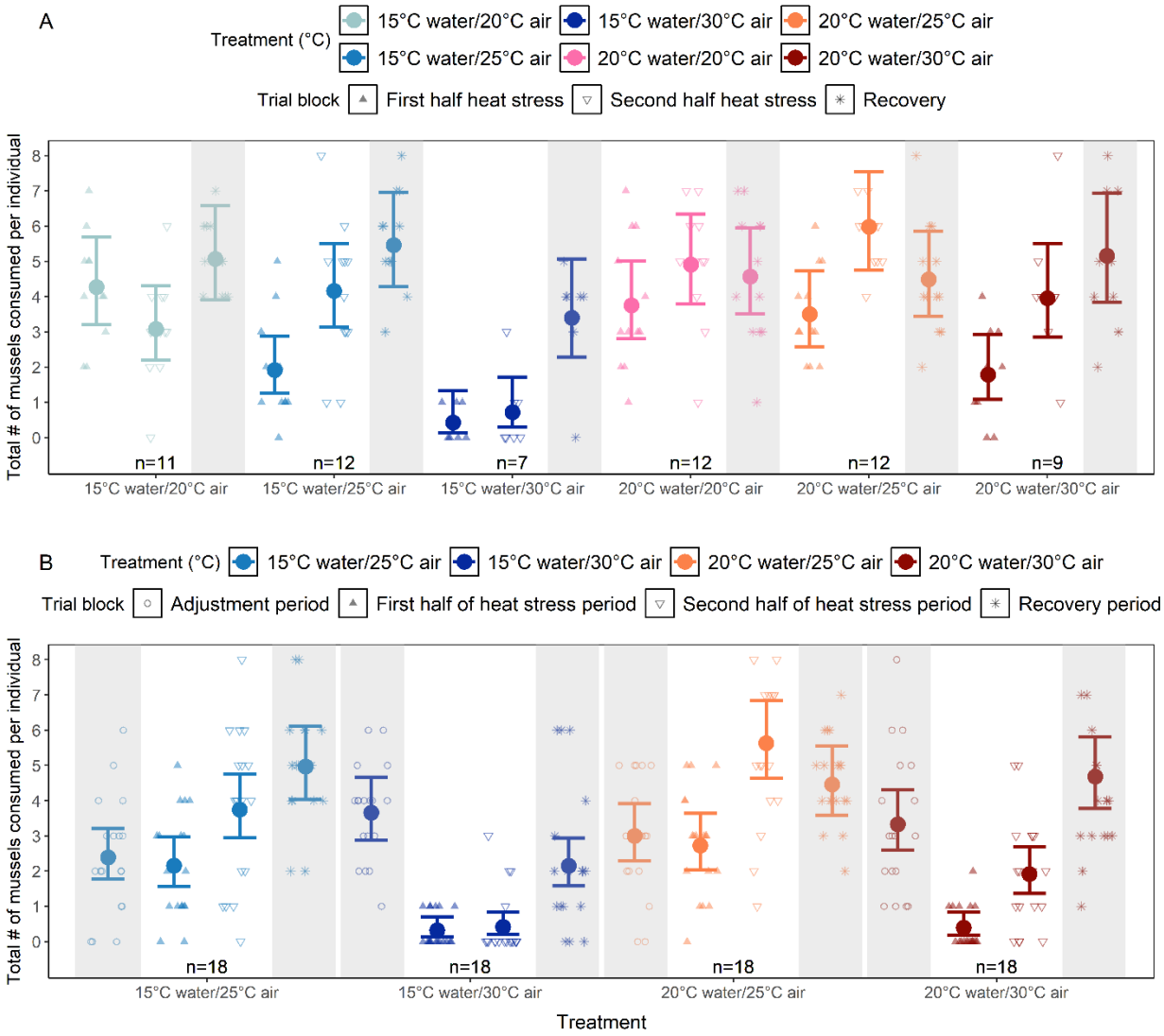

Fig. 3 The total number of *Mytilus* spp. consumed by juvenile *Pisaster ochraceus* in **(A)** Experiment 1 (June 2023; n = 63) and **(B)** Experiment 2 (May 2024; n = 72). Only sea stars that survived until the end of the experiment and retained five intact arms were included in analyses. White background shading represents the heat stress period of the experiment where sea stars were fed mussels *ad libitum* and alternated between water temperatures (~15°C or 20°C) and air temperatures (Experiment 1: ~20°C, 25°C, or 30°C; Experiment 2: ~25°C or 30°C) in a simulated high-tide (submerged for 18 hours) and low-tide (emersed for 6 hours) cycle. Grey background shading represents the adjustment (Experiment 2) and recovery (Experiments 1 and 2) periods of the experiment. In **(A)** Experiment 1, animals were fully submerged in ambient seawater (~13°C) during the adjustment and recovery periods, while in **(B)** Experiment 2 animals alternated between ~15°C seawater temperatures and 20°C air temperatures in a simulated high tide (18-hour) and low-tide (6-hour) cycle during the adjustment and recovery periods. Dots and confidence intervals represent the model estimates produced by a generalized linear mixed model investigating differences in mussel consumption between treatments. Jittered points represent the total number of mussels consumed by each individual over three (Experiment 1) or four (Experiment 2) "trial blocks". Each trial block was 8-10 days long, and represented adjustment (open circles), the first half of heat stress (triangles), the second half of heat stress (open triangles), and recovery (asterisks). Sample sizes for each treatment are included.

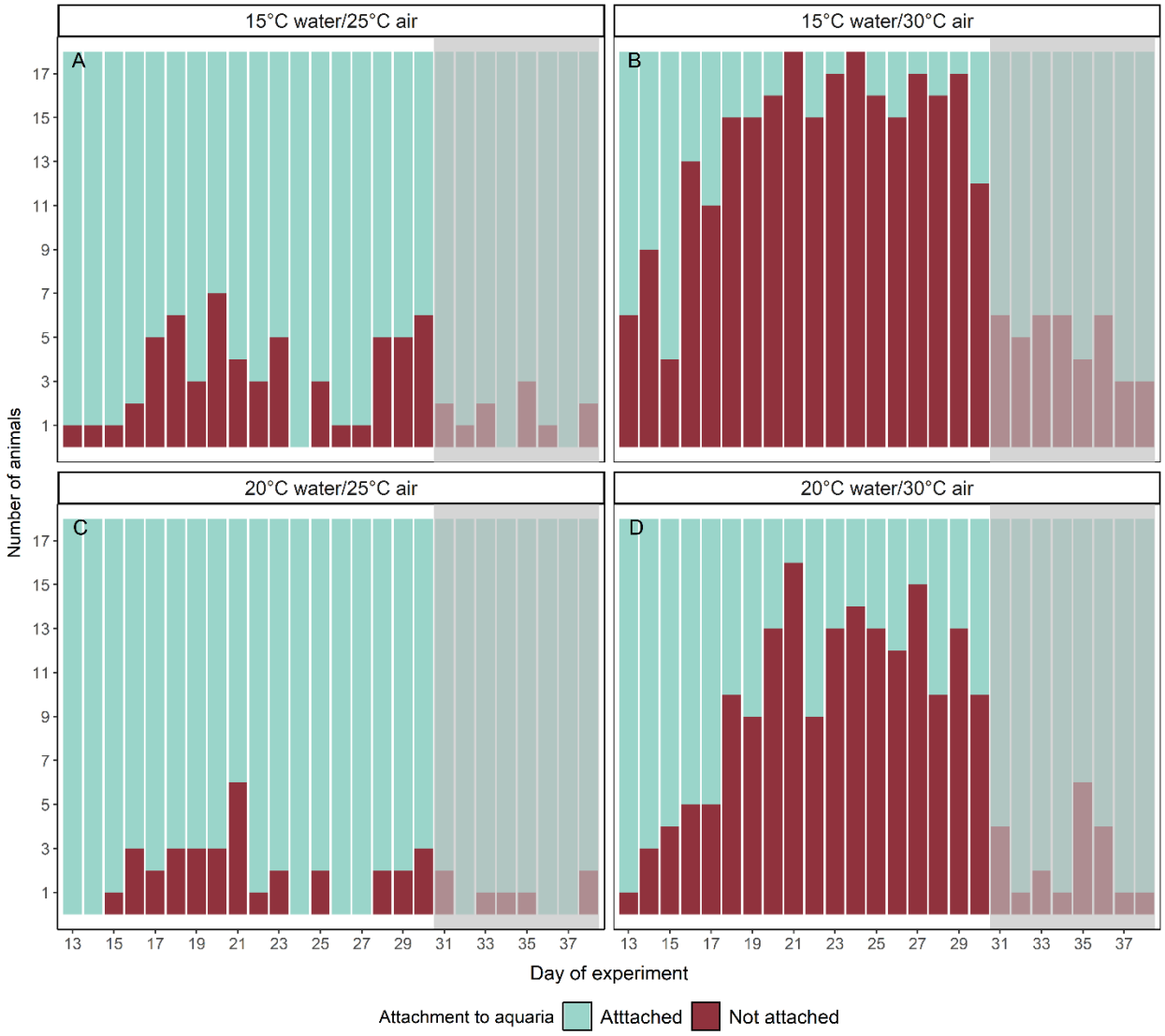

Fig. 4 The number of animals attached or not attached to experimental holding containers on each day of Experiment 2 (May 2024) across four different temperature treatments (**A:** 15°C water/25°C air, **B:** 15°C water/30°C air, **C:** 20°C water/25°C air, **D:** 20°C water/30°C air). Animals were pulled gently by hand following a 6-hour aerial emersion and were recorded as "attached" if not easily removed from the container or "not attached" if easily removed from the container. During heat stress (days 13 – 30) *Pisaster* were fed *ad libitum* and alternated between seawater (15°C or 20°C) and air temperatures (25°C, or 30°C) in a simulated high-tide (submerged for 18 hours) and low-tide (emersed for 6 hours) cycle. Grey background shading represents the recovery period (days 31 – 38) where sea stars continued to feed *ad libitum* and alternated between 15°C water temperatures and 20°C air temperatures in a simulated high-tide (submerged for 18 hours) and low-tide (emersed for 6 hours) cycle.

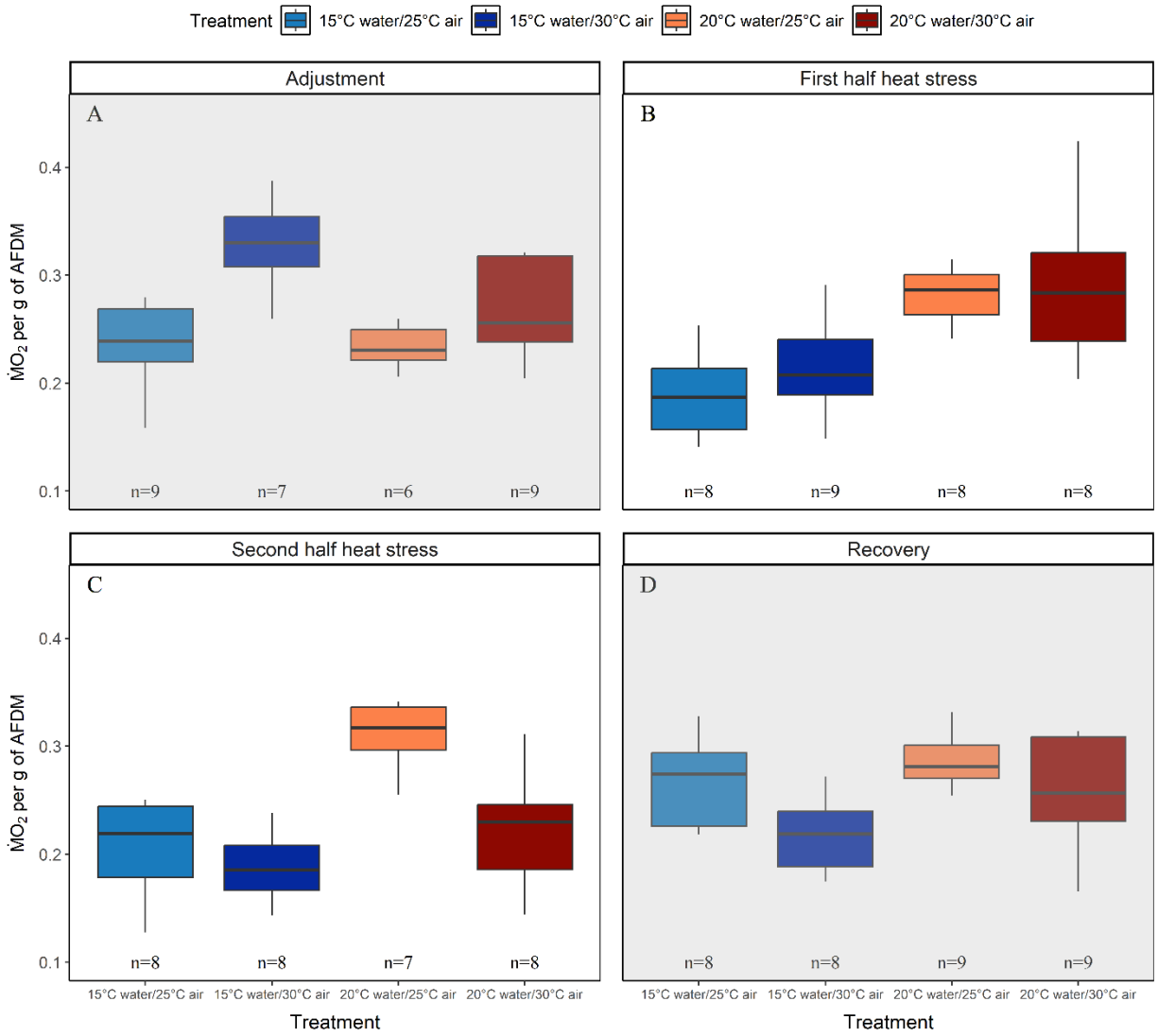

Fig. 5 The aquatic metabolic rates ($\dot{M}O_2$ per gram of ash-free dry mass; estimated using a 5-10% drop in oxygen while submerged in seawater) of juvenile *Pisaster ochraceus* measured at the end of four "trial blocks". Treatment (colour) corresponds to the assigned temperature treatments crossing different seawater (15 and 20°C) and air (25 and 30°C) temperature exposures (respectively, water/air temperatures in °C: 15/25, 15/30, 20/25, 25/30). Metabolic rates were corrected for *Pisaster* body size by including the volumetric displacement and ash-free dry mass of each animal in the calculations of $\dot{M}O_2$. Only measurements meeting the r^2 requirement of 0.98 were included in the analysis; sample sizes per treatment per measurement are included. Outliers were not plotted but were included in statistical models. **(A)** Adjustment: days 1-10; cycled between ~15°C seawater (18-hours) and ~20°C air (6-hours), **(B)** first half of heat stress: days 11-20; cycled between ~15°C or 20°C seawater (18-hours) and ~25°C or 30°C air (6-hours), **(C)** second half of heat stress: days 21-30; cycled between ~15°C or 20°C seawater (18-hours) and ~25°C or ~30°C air (6-hours), and **(D)** recovery: days 31-39; cycled between ~15°C seawater (18-hours) and ~20°C air (6-hours).

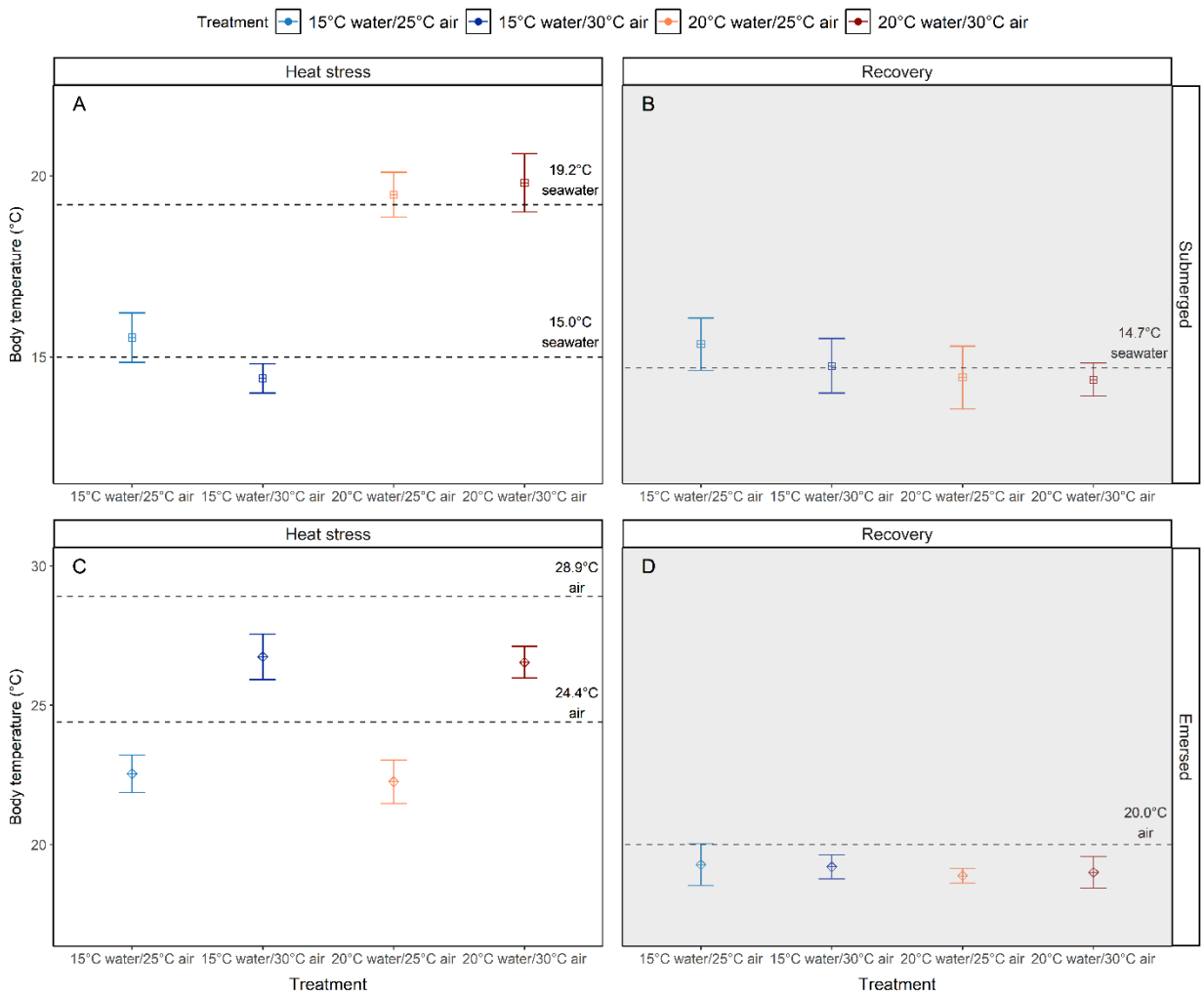

Fig. 6 The body surface temperatures of juvenile *Pisaster ochraceus* (n = 72) measured using an infrared camera during Experiment 2 (May 2024). Treatment (colour) corresponds to the assigned temperature treatments crossing different seawater (15 and 20°C) and air (25 and 30°C) temperature exposures (respectively, water/air temperatures in °C: 15/25, 15/30, 20/25, 25/30). Shape corresponds to the type of body surface temperature measurement with "submerged" measurements taken immediately after an 18-hour submersion in seawater and "emersed" measurements taken immediately after a 6-hour emersion in air. Points and confidence intervals represent the mean (± standard deviation) body surface temperature of *Pisaster* in each temperature treatment. Black dotted lines represent the actual measured temperatures of the sea table (for submerged measurements) or the temperature-controlled incubator (for emersed measurements) where *Pisaster* were housed during simulated tidal cycles. **(A, C)** Heat stress: days 11-30; animals cycled between ~15°C or 20°C seawater (18-hours) and ~25°C or 30°C air (6-hours). **(B, D)** Recovery: days 31-39; animals cycled between ~15°C seawater (18-hours) and ~20°C air (6-hours).

Table 2. The percent of moribund adult and juvenile *Pisaster ochraceus* observed at three sites (Eagle Bay, Grappler Narrows, and Strawberry Point) near Bamfield, British Columbia in May, June and August 2023. *Pisaster ochraceus* were counted along walking belt transects at each site during a midday low tide. The percentage of moribund adults and juveniles was recorded during each survey. Air temperature and sea surface temperature (SST) was recorded at each site at the start of the survey (INKBIRD IBS-TH2 Plus temperature probe).

Site (n = sample size)	Month	Moribund adults (%)	Moribund juveniles (%)	Air temperature (°C)	SST (°C)
Eagle Bay (n = 247 adults, 5 juveniles)	May	0.8	0	15.4	14.7
Eagle Bay (n = 332 adults, 13 juveniles)	June	0.6	0	21.8	16.7
Eagle Bay (n = 198 adults, 48 juveniles)	August	9.6	8.3	21.1	19.5
Grappler Narrows (n = 38 adults, 5 juveniles)	May	0	0	17.8	15.2
Grappler Narrows (n = 56 adults, 61 juveniles)	June	0	0	19	14.6
Grappler Narrows (n = 79 adults, 70 juveniles)	August	5.1	2.9	23.5	17.6
Strawberry Point (n = 76 adults, no juveniles)	May	0	0	21	16.7
Strawberry Point (n = 50 adults, 1 juvenile)	June	0	0	14.3	14.7
Strawberry Point (n = 59 adults, 1 juvenile)	August	0	0	18.3	17.5

Chapter 3 – Infrared thermography reveals persistent evaporative cooling in a keystone predator (*Pisaster ochraceus*)

Lydia N. Walton*[1], Valesca de Groot[1], Amanda E. Bates[1]

[1]Department of Biology, University of Victoria, Victoria, British Columbia, Canada

In prep as:

Walton, L.N, de Groot, V. and A.E. Bates. Infrared thermography reveals persistent evaporative cooling in a keystone predator (*Pisaster ochraceus*).

Acknowledgements: We thank the staff and researchers at the Bamfield Marine Sciences Centre (BMSC) for hosting our research and providing essential resources for our surveys. We also thank Janet Ferguson-Roberts and Viola Watts for assisting with the field surveys near Sidney, BC.

Funding: This work was supported by the National Science and Engineering Research Council (NSERC) Discovery Grant (DGECR-2019-00032) and University of Victoria Institutional Funds (Impact Chair 71809) to AEB.

Ethics approval: All applicable institutional and/or national guidelines for the care and use of animals were followed. Research on *Pisaster ochraceus* was conducted under approval of the Department of Fisheries and Oceans Canada (Licence numbers for 2023: XR 123 2023 and 134459; for 2024: XR 52 2024 and 138371), the Huu-ay-aht First Nations Department of Lands and Permitting (HFN permit number: 2023-017), and following the guidelines for animal care outlined by the Bamfield Marine Sciences Centre (BMSC) and the Canadian Council on Animal Care (CCAC).

3.1 Abstract

Climate change amplifies temperature variability, driving more frequent and intense extreme heat events that threaten to push species beyond their thermal limits. Ectotherms, which rely on external sources to regulate their body temperatures, are especially vulnerable to heat stress. Understanding the range of body surface temperatures ectotherms experience in the field is essential for assessing their resilience to climate change. However, traditional temperature loggers fail to capture the complexity of temperature regulation in living organisms, making field measurements challenging. Infrared thermography (IRT) offers a portable, cost-effective alternative for measuring the body surface temperatures of terrestrial and intertidal species. Using IRT, we examined how biological factors (body size, aggregating behaviour) and environmental conditions (air, sea surface, and substrate temperatures; humidity, wind, and microhabitat type) influenced the body surface temperatures of the keystone predator *Pisaster ochraceus* during summer low tides on Vancouver Island, British Columbia. Body size and aggregation had minimal effects on body surface temperature, suggesting that thermal inertia has a limited role in *Pisaster* thermoregulation. However, the availability of shaded microhabitats and the use of evaporative cooling allowed *Pisaster* to maintain body surface temperatures up to 14°C degrees cooler than the ambient air and up to 6°C cooler than ambient sea surface temperatures. Even so, some individuals were found in sun-exposed microhabitats, where body surface temperatures reached thresholds (≥ 23°C) associated with reduced feeding and growth under chronic exposure. These findings highlight the utility of IRT in capturing both behavioural and physiological thermoregulation strategies, and show the importance of considering how body surface temperatures match with air and sea surface temperatures in the field.

3.2 Introduction

Temperature is a key driver of biological processes at all scales, from molecules to species interactions and global species distributions. Climate change is amplifying temperature variability, creating more extreme and unpredictable patterns that threaten biodiversity and ecosystem functioning. Even brief exposures to high temperatures (*e.g.*, 30 minutes) can have harmful physiological effects, and in the long term lead to reproductive failure and mortality (*e.g.*, Fitzhenry *et al.*, 2004; Pörtner *et al.*, 2006; Szathmary *et al.*, 2009). Thermal stress also disrupts community dynamics, altering interactions like predation and competition as organisms adjust feeding rates under stress (*e.g.*, Traill *et al.*, 2010; Monaco *et al.*, 2016; Colby *et al.*, 2022). To mitigate these impacts, many organisms use buffering strategies, such as producing heat shock proteins or shifting their activity in time or space to avoid peak temperatures (*e.g.*, Whitman, 1987; Petes *et al.*, 2008; Richards *et al.*, 2023). Since these responses are typically activated when body temperatures approach critical thresholds, an accurate means of measuring body temperature is essential for predicting species resilience under thermal stress.

Ectothermic organisms may be particularly vulnerable to increased temperature variability as they rely on external sources (*e.g.* sunlight, heated surfaces, or water bodies) to regulate their body temperatures. Aquatic ectotherms typically match the temperature of the surrounding water when immersed, while terrestrial ectotherms are influenced by factors such as solar radiation, heat conduction from the ground, and evaporative cooling (see review by Helmuth, 2002). Notably, these factors allow ectotherms to maintain body temperatures several degrees above or below the ambient air, optimizing physiological processes and emphasizing the importance of temperature as a resource (Helmuth, 1998). Such decoupling from environmental temperatures complicates thermal limit estimations in scenarios where body temperatures exceed air temperature, but physiological thresholds are assessed using environmental conditions

(Marshall *et al.*, 2015; Kish *et al.*, 2016). To address this, infrared thermography (IRT) has emerged as a non-invasive tool for directly measuring body surface temperatures (see review of IRT applications by Lathlean and Seuront, 2014). Initially developed for use on reptiles (Jones and Avery, 1989), IRT has since been applied across various taxa, primarily in terrestrial ecosystems but also including intertidal habitats (*e.g.*, Pincebourde *et al.*, 2009; Caddy-Retalic *et al.*, 2011; Aguilera *et al.*, 2019).

Intertidal ecosystems, which experience significant daily fluctuations in temperature due to tidal cycles, host many organisms living near their critical thermal limits (Somero, 2002; Harley, 2008). Extreme climatic events may push these organisms beyond their physiological thresholds, leading to potentially devastating impacts on ecosystem functioning if key species are lost. One such species is *Pisaster ochraceus* (ochre sea star; hereafter *Pisaster*), a keystone predator that regulates rocky shore communities by controlling mussel populations (Paine, 1966, 1974). Despite *Pisaster*'s ecological importance, direct measurements of body temperature during aerial exposures remains scarce (but see Currie-Olsen *et al.*, 2023 for a winter example), and little is known about how *Pisaster* regulate their body temperatures in the field. Additionally, research has largely focused on adults, leaving a substantial knowledge gap regarding juvenile responses to aerial exposures. To estimate *Pisaster* body temperatures during low tide, researchers have primarily relied on biomimetic instruments designed to replicate the species' thermal properties (Pincebourde *et al.*, 2008; Broitman *et al.*, 2009; Szathmary *et al.*, 2009). Biomimetic loggers for *Pisaster* purportedly have an average absolute error of <1°C, and have estimated *Pisaster* body temperatures between 12 – 28°C across a four day tidal cycle (Szathmary *et al.*, 2009). However, these tools have notable limitations: they cannot account for evaporative cooling due to water loss, are effective only for a narrow range of size classes, and

are difficult to deploy in the microhabitats where *Pisaster* typically shelter during low tide (*e.g.*, underneath rocks or in rock crevices) (Judge *et al.*, 2018). We propose that IRT could be a more effective method for measuring *Pisaster* body temperatures in the field, as this approach has already been successfully applied to intertidal bivalves, crustaceans, and gastropods (Helmuth, 1998; Caddy-Retalic *et al.*, 2011; Lathlean *et al.*, 2012; Chapperon *et al.*, 2013).

The present study examined body surface temperatures of *Pisaster ochraceus* during summer low tides at eight rocky intertidal sites on Vancouver Island (British Columbia, Canada) using infrared thermography. We investigated whether body size and/or aggregating behaviour influenced body surface temperature, predicting that larger *Pisaster*, and *Pisaster* within aggregations, would buffer heat more effectively due to greater thermal inertia (*i.e.*, the ability to resist temperature change). We also compared body surface temperatures of *Pisaster* at the low tide line to those higher on the shore, and predicted that individuals farthest from the waterline would be warmer, as they are exposed to solar radiation for the longest interval. We recorded the type of microhabitat *Pisaster* were photographed in, and predicted that animals in heat-protected microhabitats would have lower body surface temperatures than those in sun-exposed microhabitats. Finally, we related observed *Pisaster* body surface temperatures to the environmental conditions (*i.e.*, sea surface temperature, air temperature, substrate temperature, humidity, and wind speed) recorded during each survey interval. The present study improves our understanding of *Pisaster*'s thermal biology and contributes a reproducible survey method for measuring body surface temperatures of intertidal organisms using IRT.

3.3 Materials and Methods

3.3.1 Study region and species

This study took place on sheltered and moderately exposed rocky shores along Vancouver Island, British Columbia, Canada during the boreal summer (June to August, 2024; **Fig. 1**). Vancouver Island is characterized by mixed semidiurnal tides (*i.e.*, two low and two high tides of differing sizes each day) with the lowest summer tides typically occurring during daylight for up to 6 hours. We focused on the predatory sea star *Pisaster ochraceus*, a keystone species which influences community structure disproportionate to its biomass (Paine, 1966, 1969, 1974). *Pisaster* ranges from Alaska, USA to Baja California, Mexico (Ricketts *et al.*, 1985) and regulates body temperature behaviourally by seeking out submerged or shaded microhabitats during low tide (Petes *et al.*, 2008; Szathmary *et al.*, 2009). These animals often form large aggregations, which is believed to be a general adaptation to thermal stress (Chapperon and Seuront, 2012; Chapperon *et al.*, 2013; Lathlean and Seuront, 2014); however, the thermal benefits of this behaviour has not been empirically tested in echinoderms.

We recorded the body surface temperatures of live *Pisaster* at four sites near Bamfield (48.824830034, -125.13583279; **Fig. 1**) and four sites near Sidney (48.6502411, -123.399005; **Fig. 1**), at the latitude of highest *Pisaster* abundance across its range (Sagarin and Gaines, 2002). Sites were classified as moderately exposed (Bamfield: Brady's Beach, Eagle Bay; Victoria: Glass Beach, Seabreeze Road) or sheltered (Bamfield: Bamfield Inlet, Grappler Narrows; Victoria: Chalet Beach, Moses Point) based on wave exposure.

3.3.2 Infrared imaging

Pisaster body surface temperatures were estimated using a handheld infrared camera (FLIR ONE Pro (iOS), Teledyne FLIR; iPhone 13 Pro, Apple Inc.) along two ~30 m band transects. The first transect, along the lowest occurring band of *Pisaster* (~0 – 6 m from the waterline, **Table 1**), was surveyed near low tide to capture reference temperatures for individuals

recently exposed to air. The second transect, along the highest occurring band of *Pisaster* (~1.5 – 10 m from the waterline, **Table 1**), was surveyed during the hottest part of the day (12:00 – 15:00) to measure body surface temperatures after prolonged aerial exposure. Tidal datums during each survey ranged from 0.1 m to 0.8 m. To account for reflectance, all animals were shaded during infrared measurements (Lathlean *et al.*, 2012; Lathlean and Seuront, 2014). A ruler was also included in each image for scale. Sea surface temperature, air temperature, and humidity were recorded at the start of each transect using a handheld probe (INKBIRD IBS-TH2 Plus, **Table 1**), and wind conditions were obtained from local weather stations (Bamfield Marine Sciences Centre, Bamfield: https://victoriaweather.ca/station.php?id=161 and Victoria International Airport, Sidney: https://www.wunderground.com/history/daily/ca/sidney/ISIDNE2/date/2024-2-17).

3.3.3 Camera settings and temperature validation

The infrared camera had a pixel resolution of 19200px (160 x 120px) and an accuracy of ±3°C or ±5% when the unit was within 15°C - 35°C and the scene was within 5°C - 120°C. Emissivity was set to 0.95, consistent with studies showing intertidal substrates and invertebrates have emissivity values between 0.95 and 1 (Denny and Harley, 2006; Chapperon and Seuront, 2011; Cox and Smith, 2011). To validate the infrared measurements, we randomly selected 35 *Pisaster* across the surveyed sites and measured their internal body temperatures with a digital thermometer (Taylor 9848E Safe-T-Guard digital pocket thermometer with antimicrobial sleeve) inserted into the coelomic cavity (midway down one arm ray). The difference in temperature between infrared and thermometer readings was 0.64 ± 0.4°C (mean ± SD; n = 35).

3.3.4 Image processing

Thermal images were analyzed using Thermal Studio Pro (Teledyne FLIR), and spot measurements were used to measure *Pisaster* body surface temperature. Spot measurements were placed on the central disc (aboral side) and on each visible arm ray (¾ down from the disc) (**Fig. 2**). The central disc temperature was ultimately chosen to represent body surface temperature in statistical models, as the number of visible arms was inconsistent among individuals (ranging from 1-5 visible arms). Although body temperature can vary across an animal's surface, survival in *Pisaster* is closely tied to central disc temperature, making it a critical point for analysis (Pincebourde *et al.*, 2013). Line measurements (~3 cm) were placed on the nearby substrate, and the average temperature across each line was used in statistical models to represent substrate temperature (**Fig. 2**). Microhabitat types were classified based on the animal's exposure to solar radiation (*i.e.*, exposed: receiving direct solar radiation across the entire aboral surface; partly exposed: receiving direct solar radiation across 1 to 99% of the aboral surface; shaded: receiving no solar radiation across the aboral surface; under rock: animals found underneath rocks or cobbles that had to be flipped over to obtain measurements; or tidepool: animals with part of their body surface submerged in water). *Pisaster* were categorized as "aggregated" (in physical contact with at least one other conspecific) or "solitary" (no physical contact with conspecifics) to assess aggregation effects on body surface temperature. We measured the size of each individual from the centre of the aboral disc to the tip of the longest arm using Fiji image processing software (Schindelin *et al.*, 2012). *Pisaster* were excluded from analyses if the central disc was not visible or if size could not be measured (Bamfield: 8.5% excluded (n = 52/614); Sidney: 7.8% excluded (n = 15/193)).

3.3.5 Statistical analysis

We performed all statistical analyses using R version 4.3.3 (R Core Team, 2021). Generalized linear mixed models with Gaussian distributions ("glmmTMB" package; Brooks *et al.*, 2017) were used to test the effects of predictors on *Pisaster* body surface temperature. We first modeled the separate effects of arm length (**Table S1**), aggregation behaviour (**Table S2**), and transect (**Table S3**) on body surface temperature between locations (Bamfield and Sidney), with site included as a random effect. We then incorporated these predictors into a final model alongside measured environmental variables. The dredge function ("MuMIn" package; Bartoń, 2024), which ranks all possible predictor combinations by AIC (Akaike Information Criterion), was used to inform final model selection. The global model included the following fixed effects: arm length, aggregating behaviour (aggregated or solitary), microhabitat type (exposed, partly exposed, shaded, under rock, or tidepool), transect, substrate temperature, sea surface temperature, air temperature, humidity, average wind speed, and maximum wind speed, with site included as a random effect. Based on the model selection table produced by dredge, we dropped arm length, transect, and maximum wind speed from the final model (**Table S4**). Collinearity between predictors was tested using the vif (variance inflation factor) function in the "car" package (Fox *et al.*, 2024) and model residual diagnostics were conducted using the "DHARMa" package (Hartig *et al.*, 2024).

3.4 Results

3.4.1 Body surface temperatures and environmental conditions during surveys

Pisaster body surface temperature (surface temperature of the central disc) ranged from 12.2 – 24.9°C (16.6 ± 2.1°C; mean ± SD) in Bamfield (n = 562) and from 10.1 – 25.4°C (18.0 ± 2.2°C; mean ± SD) in Sidney (n = 176). Air temperature ranged from 20.6 – 26.6°C (23.2 ±

2.4°C; mean ± SD) in Bamfield and from 19.9 – 25.6°C (22.9 ± 1.4°C; mean ± SD) in Sidney, while sea surface temperature ranged from 14.5 – 18.9°C (16.2 ± 1.4°C; mean ± SD) in Bamfield and 14.7 – 20.7°C (17.5 ± 2.2°C; mean ± SD) in Sidney. Humidity ranged from 45.1 – 64.9% (56.7 ± 6.4%; mean ± SD) in Bamfield and from 35.9 – 70.3% (59.9 ± 8.3%; mean ± SD) in Sidney.

Across all sites, 11.6% of *Pisaster* (n = 86) had body surface temperatures below the coolest recorded sea surface temperature (14.5°C) and 0% of *Pisaster* had body surface temperatures higher than the hottest recorded air temperature (26.6°C). We also found that 1.9% of surveyed *Pisaster* (n = 8) reached body surface temperatures equal to or above 23°C, which is a threshold for reduced feeding and growth in adults (Pincebourde *et al.*, 2008).

3.4.2 Relationship between predictors and body surface temperature

Arm length ranged from 1.0 cm to 16.8 cm in Bamfield (6.3 ± 3.1 cm; mean ± SD) and 1.5 cm to 13.1 cm in Sidney (5.0 ± 2.4 cm; mean ± SD). Despite this large range of sizes, arm length had no significant effect on body surface temperature (**Fig. 3A; Table S1**). Aggregation behaviour had no effect in Bamfield, but in Sidney, solitary *Pisaster* had slightly higher body surface temperatures than aggregated individuals (**Fig. 3B; Table S2**; $p < 0.01$). Microhabitat type also affected body surface temperatures, with *Pisaster* in heat-protected categories (partly exposed, shaded, tidepool, and under rock) being significantly cooler than those in sun-exposed areas (**Fig. 4; Table S4**; $p < 0.001$). *Pisaster* had cooler body surface temperatures on the lower transect (closest to the waterline), except at Chalet Beach and Glass Beach, where body surface temperatures were lowest on the higher transect (**Fig. 5; Table S3**). Body surface temperature increased with substrate temperature (**Table S4**; $p < 0.001$), but wind speed (daily average) had no effect. Air temperature and humidity both had a positive effect on *Pisaster* body surface

temperature (**Table S4;** $p < 0.001$) while sea surface temperature had a negative effect (**Table S4;** $p < 0.01$).

3.5 Discussion

Temperature variability directly affects ectotherm body temperature, often pushing animals closer to their thermal limits during extreme fluctuations. Here, we show that the keystone predator *Pisaster ochraceus* can be up to 14°C cooler than ambient air when found in shaded microhabitats on hot summer days after ~6 hours of aerial exposure. Even so, some sun-exposed individuals reached body surface temperatures exceeding 23°C, which could become harmful with prolonged exposure (Pincebourde *et al.*, 2008). As heatwaves become more frequent and intense, early detection of thermally stressed populations will be increasingly critical for conservation and management strategies. Our findings establish a baseline for *Pisaster* body surface temperatures under typical summer conditions and highlight the value of infrared thermography (IRT) for studying thermal biology in the field.

Contrary to expectations, we found no relationship between *Pisaster* size and body surface temperature, and observed aggregation effects on body surface temperature at only one of the two study locations. This is surprising given that larger animals, and those within aggregations, typically exhibit greater thermal inertia, which is an organism's ability to resist changes in temperature (Monteith and Unsworth, 2008). One explanation is that *Pisaster* modulate thermal inertia by circulating cool seawater through their coelomic cavity, a strategy observed in adult *Pisaster* under lab conditions (Pincebourde *et al.*, 2009), that could also apply to juveniles (defined here as animals with arm length < 6 cm; Gooding and Harley, 2015). Alternatively, *Pisaster* may regulate body surface temperatures through occupying heat-protected microhabitats, as our study found a high proportion of individuals in shaded locations compared

to sun-exposed ones. The use of shaded microhabitats may also confound any benefits of aggregating behaviour, as no aggregations were fully sun-exposed in our study. The small aggregations (<15 animals) we did observe may only provide limited thermal benefits as most animals were positioned on the "edge" of the aggregation, unlike studies comparing "edge" versus "centre" individuals in larger aggregations of gastropods and bivalves (Helmuth, 1998; Chapperon and Seuront, 2012; Chapperon *et al.*, 2013). This may explain why aggregating behaviour has thermally benefitted other intertidal ectotherms (Chapperon and Seuront, 2012; Chapperon *et al.*, 2013) and *Pisaster* in winter (Currie-Olsen *et al.*, 2023), but showed no major advantages under typical summer conditions at our sites. Our surveys were conducted on days with cloud cover and moderate air temperatures, which are typical of summer on Vancouver Island. Under these conditions, the thermal benefits of aggregation may be less pronounced than they would be during an extreme heat event. Future IRT surveys during aerial heatwaves where air temperatures would be higher, would clarify if aggregating influences *Pisaster* thermoregulation under more stressful conditions and what proportion of individuals are reaching body temperatures of concern (*i.e.*, sublethal effects at ≥23°C and lethal effects at >35°C for adults; Pincebourde *et al.*, 2008, 2013).

Although size did not directly affect body surface temperature, it may influence *Pisaster* thermoregulation through microhabitat selection. Juvenile *Pisaster* prefer structurally complex, heat-protected microhabitats that offer refuge from both thermal stress and predators, whereas adults often inhabit more sun-exposed areas where prey is abundant (Rogers and Elliott, 2013). Our findings align with this pattern: 98% of juveniles were observed in shaded habitats, and 89% of sun-exposed *Pisaster* were adults. However, most adults (80%) still occupied shaded habitats, suggesting site-specific factors, such as prey availability and climate, shape the trade-offs

between heat stress, predation risk, and feeding opportunities. Interestingly, *Pisaster* were often cooler than the surrounding substrate, particularly when found underneath rocks. Despite ectotherms typically relying on heat conduction from substrates to warm their body temperatures (Porter and Gates, 1969), *Pisaster* were up to 7°C cooler than adjacent rocks. This unexpected observation suggests additional variables, like air temperature and humidity, contribute to thermal regulation, potentially through evaporative cooling.

Pisaster body surface temperatures increased with air temperature and humidity, indicating that hot, humid conditions are particularly stressful. High humidity impedes evaporative cooling by reducing the gradient for water vapor loss between the body surface and the air (Bulova, 2002). Since *Pisaster* likely use dermal papulae (*i.e.* extensions of the coelomic cavity) for evaporative cooling (Pincebourde *et al.*, 2013), reduced evaporative potential on humid days may explain elevated body surface temperatures. For instance, Moses Point, which had the highest humidity (70.3% at the low tide line), also had the highest recorded body surface temperature (25°C). Reduced evaporative potential may also explain why *Pisaster* at Chalet and Glass Beach were cooler at the high tide line despite longer exposure to solar radiation; between the low and high tide line surveys, humidity decreased by 12.8% and 18.4%, respectively. Even though humidity plays a critical role in thermoregulation, it is rarely measured in field surveys or included in predictive models (but see Szathmary *et al.*, 2009 for inclusion in a heat budget model). Additionally, biomimetic loggers, which do not account for evaporative cooling, are likely underestimating body temperatures on humid days. Although our survey method and models incorporated humidity, continuous measurements and comparisons across microhabitats are needed to better understand the link between water balance and thermoregulation in *Pisaster*.

Microhabitat selection and evaporative cooling are both effective strategies for regulating body temperatures, and *Pisaster* seem to rely on both to avoid thermal stress. Remarkably, 46% of *Pisaster* had body surface temperatures several degrees cooler than the seawater they had been submerged in at high tide (n = 341; temperature difference ranged from 0.1 to 5.9°C). This is surprising, as aquatic ectotherms typically match the temperature of the surrounding water when immersed, and sea stars retain significant seawater in their coelomic cavity during low tide. While we did not expect *Pisaster* to match sea surface temperatures during low tide, it was unexpected to find individuals cooler than seawater, particularly since air temperatures were consistently 5 – 10°C warmer than the ocean. Laboratory experiments show that *Pisaster* can lose large volumes of water under extreme heat, likely as a fundamental cooling mechanism to prevent body temperatures from exceeding upper thermal limits (Pincebourde *et al.*, 2013). We did not conduct surveys during days of extreme heat, but we find that evaporative cooling may be occurring even under typical summer low tide conditions, translating to body temperatures that are much lower than expected. In fact, approximately 99% of surveyed *Pisaster* were cooler than ambient air, with the few individuals warmer than air (n = 10) found mostly in exposed habitats. These observations align with the "suboptimal is optimal" theory (Martin and Huey, 2008), which posits that ectotherms tend to maintain body temperatures below the threshold for maximal fitness to optimize long-term performance. In thermally variable environments like the rocky intertidal, *Pisaster* and other ectotherms likely maintain cooler body temperatures to mitigate heat stress and reduce mortality risks (Hui *et al.*, 2022). Our findings highlight the importance of considering how body temperatures match with air and sea surface temperatures, as this could explain gaps in simple model predictions.

3.6 Conclusion

This study is the first to measure the range of body surface temperatures experienced by *Pisaster* in the field during typical summer low tides on Vancouver Island. These baseline measurements provide an important reference for identifying abnormal body temperatures, which we expect to occur more frequently with climate change. We also contribute to a better understanding of the juvenile life stage, showing that even small *Pisaster* can buffer thermal stress during aerial exposure, mainly through microhabitat selection. Microhabitat selection and evaporative cooling allow *Pisaster* to maintain body temperatures several degrees cooler than ambient air and seawater, emphasizing the importance of behavioural and physiological strategies to thermal stress. These findings demonstrate the value of infrared thermography for accurately assessing ectotherm body surface temperatures in the intertidal, and highlight IRT's ability to capture both physiological and behavioural regulation strategies.

3.7 Figures and Tables

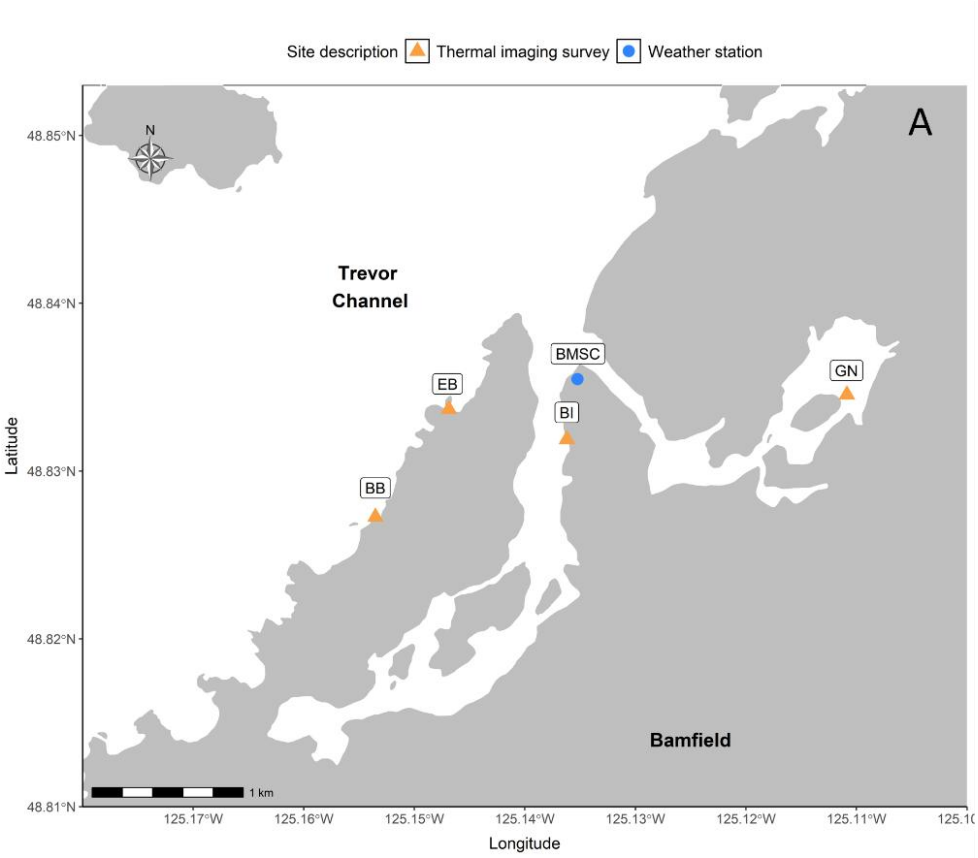

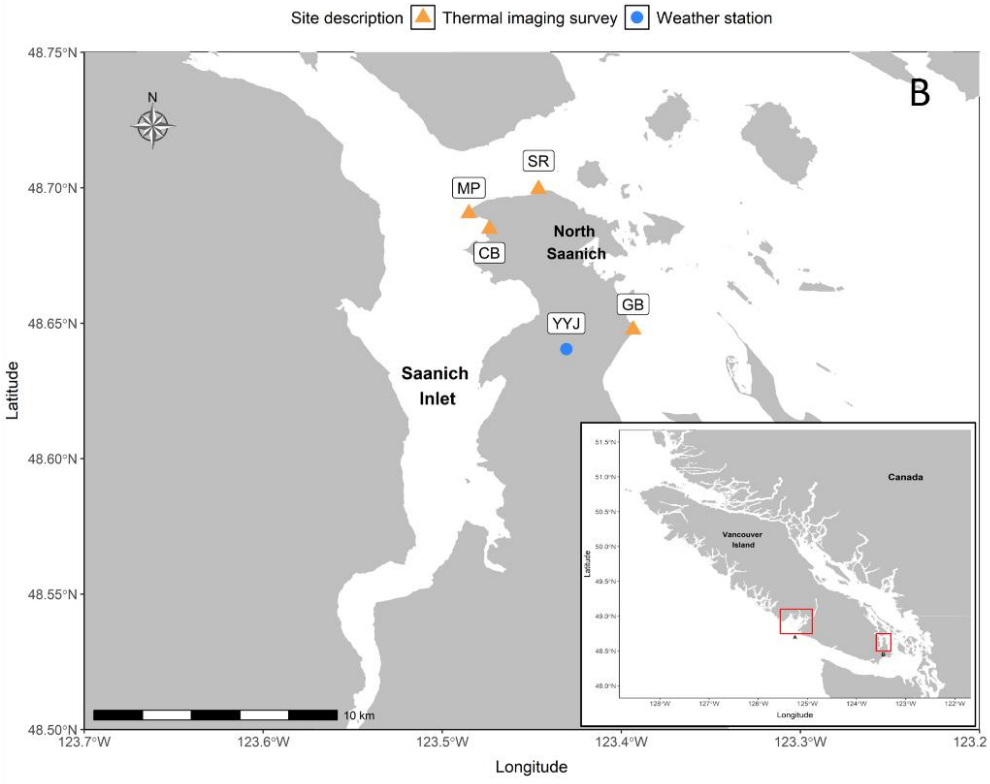

Fig 1. Map of sites near **(A)** Bamfield and **(B)** Sidney in British Columbia, Canada where infrared thermography surveys were conducted in summer of 2024. Orange triangles represent survey sites **(A)** Brady's Beach (BB), Bamfield Inlet (BI), Eagle Bay (EB), Grappler Narrows (GN) and **(B)** Chalet Beach (CB), Glass Beach (GB), Moses Point (MP), and Seabreeze Road (SR). Blue circles represent weather stations where wind data was retrieved from: Bamfield Marine Sciences Centre (BMSC) and Victoria International Airport (YYC). Environmental data (air temperature, sea surface temperature, and humidity) was collected from each site during the time of the survey.

Table 1. Observed *Pisaster ochraceus* body surface temperatures and environmental conditions at eight survey sites near Bamfield and Sidney, British Columbia, Canada.

Location	Site	Transect	Transect distance from waterline	*Pisaster* body surface temperature (min – max; mean ± SD °C)	SST (°C)	Air (°C)	Humidity (%)	Wind (km/h)
Bamfield (n = 107)	Bamfield Inlet	Low tide line	1 m	12.9 – 16.8; 14.7 ± 0.9	15.3	20.6	59.2	6
Bamfield (n = 91)	Bamfield Inlet	High tide line	4.5 m	13.6 – 19.5; 16.1 ± 1.0	15.7	21.1	62.8	6
Bamfield (n = 74)	Brady's Beach	Low tide line	2 m	12.3 – 18.6; 15.4 ± 1.5	14.5	21.8	56.3	3
Bamfield (n = 85)	Brady's Beach	High tide line	7 m	13.1 – 24.9; 16.9 ± 2.1	16.3	26.6	45.1	3
Bamfield (n = 87)	Eagle Bay	Low tide line	0 m	14.8 – 24.0; 17.6 ± 1.9	18.9	25.8	60.7	5
Bamfield (n = 36)	Eagle Bay	High tide line	8 m	16.0 – 21.0; 18.3 ± 1.3	18.2	25.1	64.9	5
Bamfield (n = 38)	Grappler Narrows	Low tide line	0.5 m	12.2 – 23.1; 17.4 ± 3.0	15.5	20.8	54.2	3
Bamfield (n = 44)	Grappler Narrows	High tide line	1.5 m	16.8 – 22.2; 19.2 ± 1.4	15.6	24.6	48	3
Sidney (n = 10)	Chalet Beach	Low tide line	5.8 m	15.6 – 20.2; 18.4 ± 1.3	20.7	24.3	60.6	15
Sidney (n = 13)	Chalet Beach	High tide line	10 m	14.8 – 17.1; 16.0 ± 0.7	20.7	25.6	47.8	15
Sidney (n = 9)	Glass Beach	Low tide line	0 m	10.2 – 17.3; 14.4 ± 2.1	14.7	23.3	54.3	12
Sidney (n = 4)	Glass Beach	High tide line	7.1 m	10.1 – 14.4; 12.6 ± 1.8	15.2	19.9	35.9	12
Sidney (n = 49)	Moses Point	Low tide line	5.5 m	16.4 – 25.0; 19.6 ± 1.4	19.2	23.9	70.3	13
Sidney (n = 17)	Moses Point	High tide line	9.5 m	17.2 – 25.4; 20.1 ± 2.4	19.6	23.5	66.4	13
Sidney (n = 68)	Seabreeze Road	Low tide line	2 m	14.7 – 21.1; 17.5 ± 1.3	15.4	21.5	55.3	13
Sidney (n = 6)	Seabreeze Road	High tide line	10 m	17.3 – 18.5; 17.7 ± 0.5	16.5	22.5	56.9	13

Transect: low tide line transects were conducted along the band of *Pisaster* closest to the water line, high tide line transects were conducted along the highest occurring band of *Pisaster* on the shoreline; Transect distance from waterline: the distance in metres of the transect tape from the waterline, measured at the start of the survey; Body surface temperature: temperature of the central aboral disc in °C; SST: sea surface temperature measured at the start of each transect in °C; Air temperature: air temperature measured at the start of each transect in °C; Humidity: humidity measured at the start of each transect in %; Average wind speed: the average daily wind speed recorded by the Bamfield Marine Sciences weather station (for sites in Bamfield) and the Victoria International Airport weather station (for sites in Sidney) on the day of each survey in km/h.

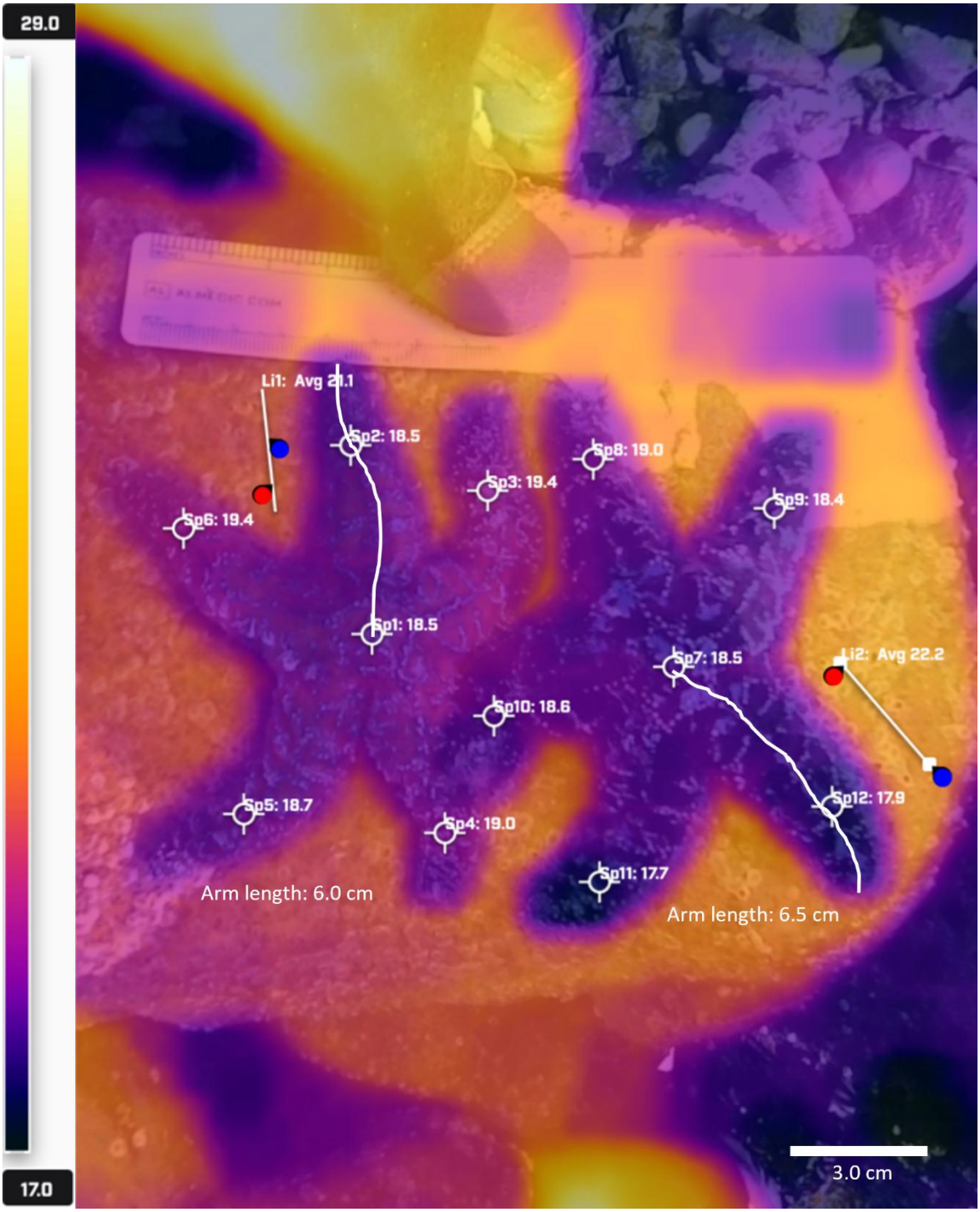

Fig 2. Example of a processed thermal image (Eagle Bay, Bamfield) used to determine the body surface temperature (°C) of *Pisaster ochraceus*. Spot measurements were placed on the central disc and on each visible arm ray (Thermal Studio Pro software; Teledyne FLIR). Line measurements were placed beside each animal and the average temperature of the line was used as an estimate for substrate temperature. The length (in cm) of the longest, straightest and/or most visible arm was measured for each *Pisaster* using Fiji (ImageJ) software. The range of temperatures observed across the entire image is represented by the temperature scale on the left.

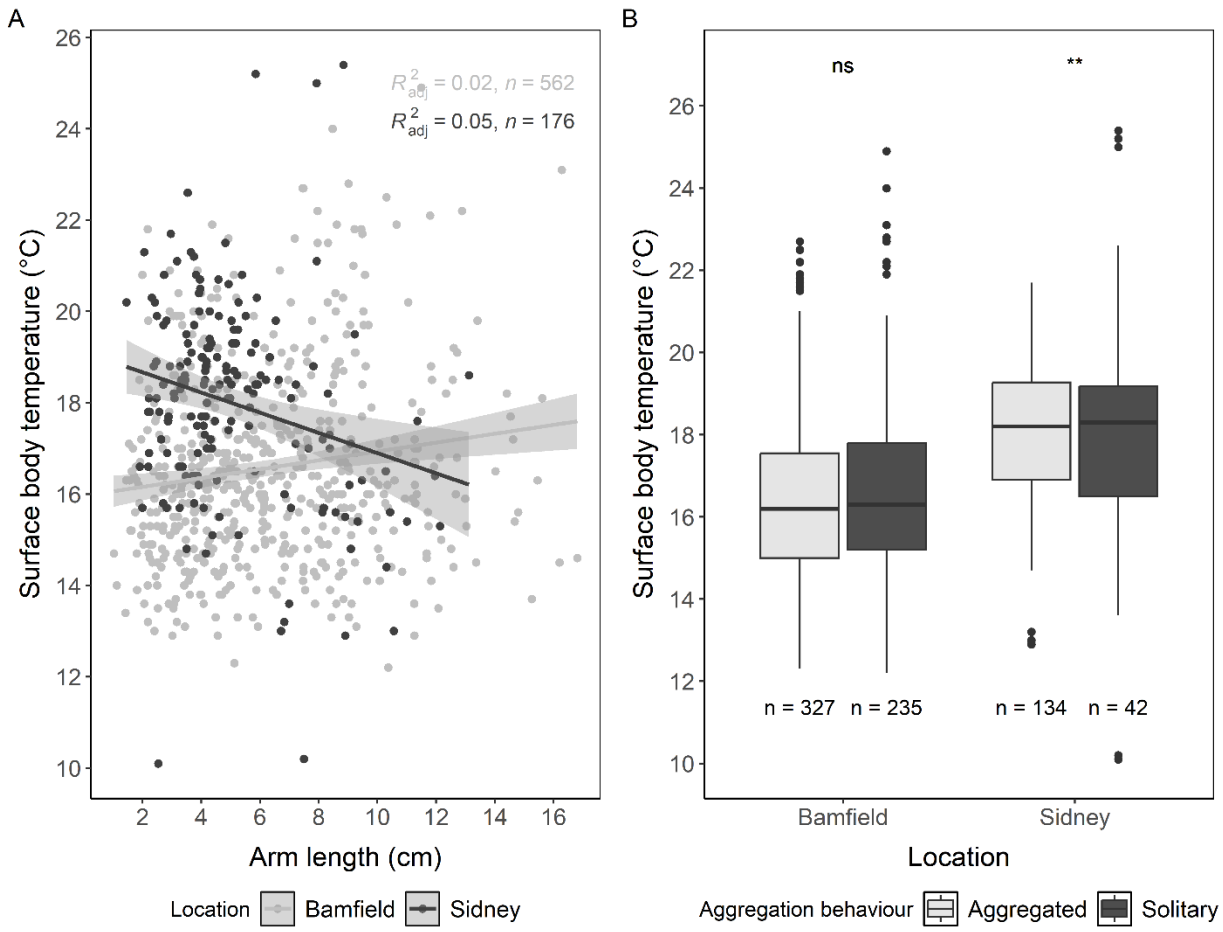

Fig 3. The body surface temperature of *Pisaster ochraceus* compared to **(A)** the arm length (cm) of *Pisaster* and the **(B)** aggregation behaviour of *Pisaster*. Body surface temperatures were estimated from thermal images and represent the temperature of the animal's central disc. Arm length was measured from the center of the body to the tip of the longest, flattest and/or most visible arm ray. *Pisaster* were identified as "aggregated" if they were touching at least one other conspecific and "solitary" if they were not touching any conspecifics. There was no relationship found between body surface temperature and arm length in *Pisaster*. There was no difference in body surface temperature between aggregated and solitary *Pisaster* in Bamfield, however, solitary *Pisaster* in Sidney had slightly higher body surface temperatures than aggregated *Pisaster* (glmm, $p < 0.01$).

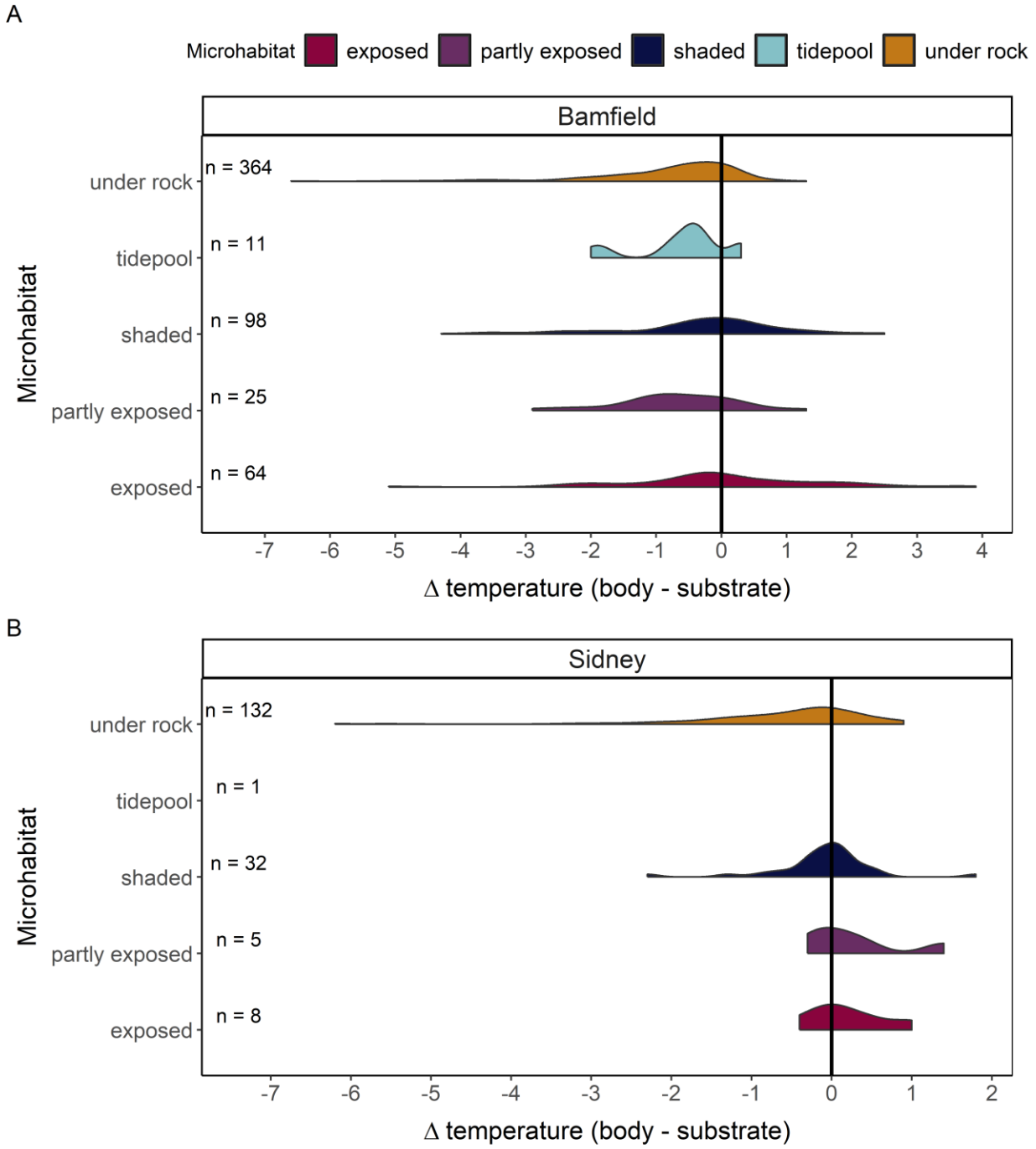

Fig 4. The difference in *Pisaster ochraceus* body surface temperature to substrate temperature at surveyed sites in **(A)** Bamfield and **(B)** Sidney, BC. The zero line represents no difference between body surface temperature and substrate temperature. Values above the zero line indicate body surface temperatures were warmer than substrate temperatures, while values below the zero line indicate body surface temperatures were cooler than substrate temperatures. Colours represent microhabitat type (*i.e.*, exposed: receiving direct solar radiation across the entire aboral surface; partly exposed: receiving direct solar radiation across 1 to 99% of the aboral surface; shaded: receiving no solar radiation across the aboral surface; under rock: animals found underneath rocks or cobbles that had to be flipped over to obtain measurements; or tidepool: animals with part of their body surface submerged in water).

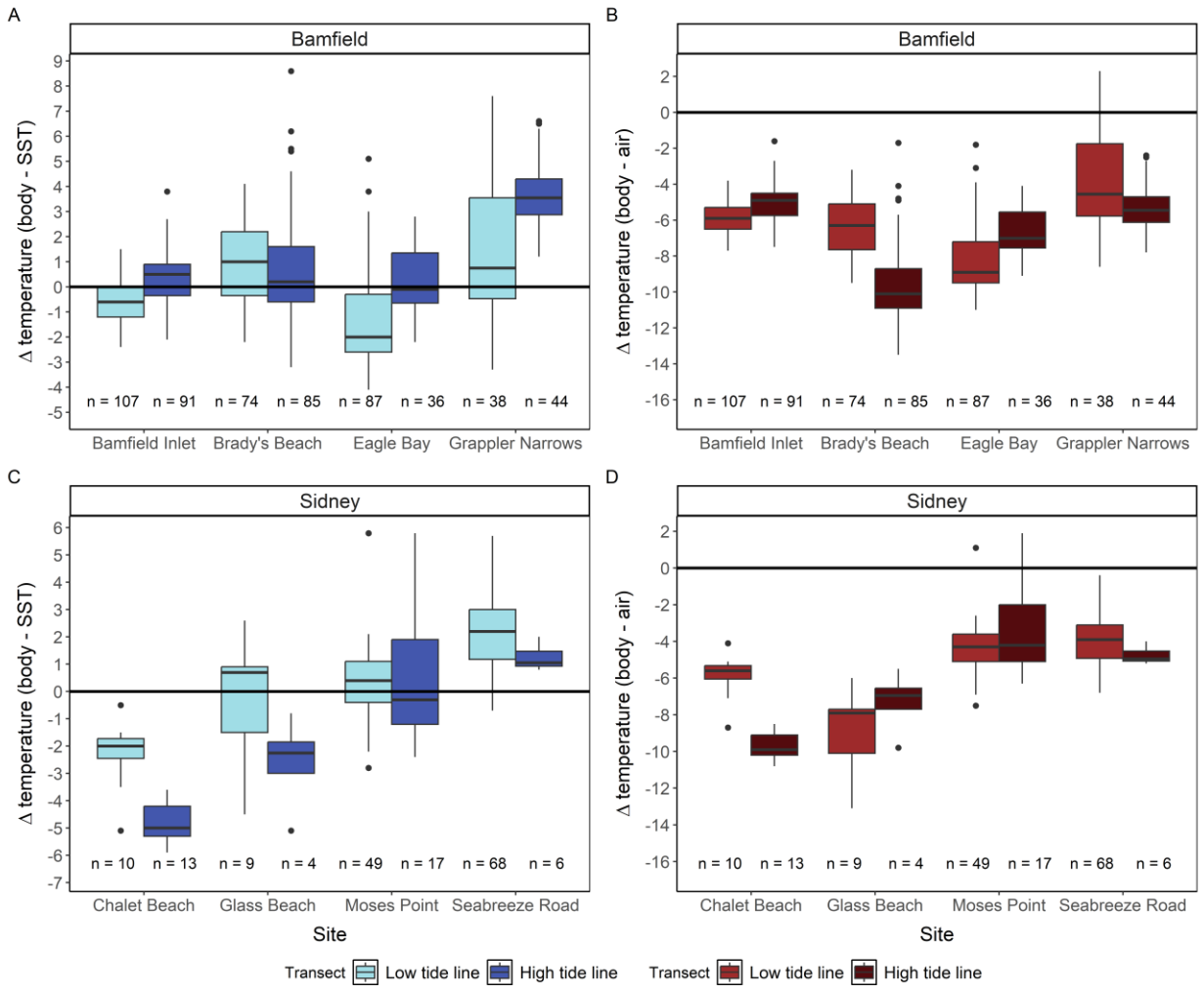

Fig 5. The difference in *Pisaster ochraceus* body surface temperature to **(A, C)** sea surface temperature (SST) and to **(B, D)** air temperature (Δ temperature) across surveyed sites in Bamfield and Sidney. The zero line represents no difference between body surface temperature and environmental temperature. Values above the zero line indicate body surface temperatures were warmer than environmental temperatures, while values below the zero line indicate body surface temperatures were cooler than environmental temperatures. Colours represent transects, with low tide line transects surveying the band of *Pisaster* closest to the waterline, and high tide line transects surveying the highest band of *Pisaster* on the shoreline.

Chapter 4 – General Conclusion

In this thesis, I integrate laboratory experiments with field monitoring to investigate the physiological and behavioural responses of a keystone predator, *Pisaster ochraceus*, to increasing temperature variability at the land-ocean interface. My findings reveal a seasonal window of heightened thermal vulnerability, occurring when cool ocean temperatures coincide with aerial heatwave conditions. During these periods, *Pisaster* experience significant physiological stress, evidenced through increased mortality, reduced mussel consumption, and suppressed metabolism. These findings indicate that the absolute difference in temperature between the air and ocean is a major factor to consider in climate change predictions, as our findings do not support a simple model of heat damage accumulation with higher temperatures (*e.g.*, Martínez-De León and Thakur, 2024). In fact, we found that when ocean temperatures were warmer, typical of late summer conditions in our study area (July and August), *Pisaster* exhibited a positive metabolic and feeding response, which may reflect seasonal acclimatization, potentially enhancing thermal tolerance to future extreme heat events (Lindquist and Craig 1988, Somero 2002, Sørensen et al. 2003). These results highlight the context-dependent nature of intertidal species' responses to temperature fluctuations, and emphasize the need for further experiments across a broader range of organisms to understand if this is a general pattern. Incorporating this contrast in air-ocean conditions will be crucial for predicting how entire intertidal communities will respond to increasing temperature variability, particularly as land surface temperatures continue to warm at a faster rate than sea surface temperatures (Manabe *et al.*, 1991; Joshi *et al.*, 2008). Our findings further suggest that the growing frequency of extreme heat events and large air-sea disparities may pose new challenges for intertidal ecosystems, necessitating a deeper understanding of species' adaptive responses to thermal stress.

Here, I outline potential community-level changes driven by shifts in keystone predation under climate warming, but I do not directly assess how warming air and seawater conditions affect prey species. Species may respond differently to thermal stress; for example, *Mytilus* spp. have different thermal tolerance limits than *Pisaster* (Pincebourde *et al.*, 2008; Seuront *et al.*, 2019). Such differences in thermal tolerance may disrupt trophic interactions, leading to predator-prey mismatches as one population thrives while the other declines. Future research examining the responses of both predators and prey to contrasting air and seawater temperatures would enhance predictions of species interaction shifts and changes to food webs following extreme heat events, which is a critical knowledge gap for predicting ecological resilience in a warming climate.

In addition to examining the responses of a broader range of organisms to thermal stress, my thesis outlines the need to investigate the effects of temperature variability across different life stages. My findings suggest that juvenile *Pisaster* have a significantly lower upper thermal tolerance limit than adults, aligning with previous research showing ontogenetic shifts in stress tolerance for other intertidal invertebrates (*e.g.*, Gosselin and Qian, 1997; Jenewein and Gosselin, 2013; Hamilton and Gosselin, 2020). Despite their greater vulnerability to climate stressors, studies on juvenile responses to temperature variability remain limited in number when compared to studies focusing on adult stages. Addressing this research gap is important, as climate-driven declines in juvenile survival and recruitment can have severe consequences for species persistence. *Pisaster*, among other species of predatory sea stars, are at risk of both climate- and disease-driven mass mortality events, and without successful post-epidemic recruitment, they may experience local extirpations. A better understanding of juvenile thermal tolerance will be essential for predicting the long-term stability of adult populations.

Although *Pisaster* populations across many areas of their geographic range are experiencing increased thermal stress under future climate change, the results of my infrared thermography (IRT) surveys reveal impressive adaptations that help animals to avoid lethal body temperatures. Regardless of body size, *Pisaster* can maintain body surface temperatures several degrees below the surrounding substrate as well as the ambient air and sea surface. Based on our findings, two key mechanisms are driving this cooling effect: the selection of heat-protected microhabitats and the use of evaporative cooling during low tide. These strategies appear to be very effective under ambient summer conditions, however, I was unable to align my survey days with more extreme thermal conditions. Future studies should aim to measure *Pisaster* body surface temperatures across a wide range of environmental conditions, particularly during periods of extreme heat and direct sun exposure. Additionally, visual inspections of data patterns suggest a potential interaction between humidity and air temperature, but the limited number of observations across the full range of humidity-temperature combinations on the days surveys were conducted limited statistical analysis. A greater focus on the interactions between site-specific environmental variables in future studies would provide further insight to the conditions which are most physiologically stressful for this keystone predator.

Overall, my experiments revealed important deviations from theory, particularly that warmer air and ocean temperatures do not lead to accumulated heat damage. I further demonstrate that infrared thermography is an invaluable tool for assessing the effects of temperature on intertidal invertebrates in the laboratory and field, revealing significant differences between air and body surface temperatures. I recommend its broader application across diverse taxa. This thesis has contributed to our knowledge of thermal stress responses in a keystone predator and has focused on its understudied juvenile life stage. Both laboratory and

field methods may be replicated for a variety of taxa and will hopefully provide a useful framework for investigating the effects of temperature variability on both physiology and behaviour in other key species.

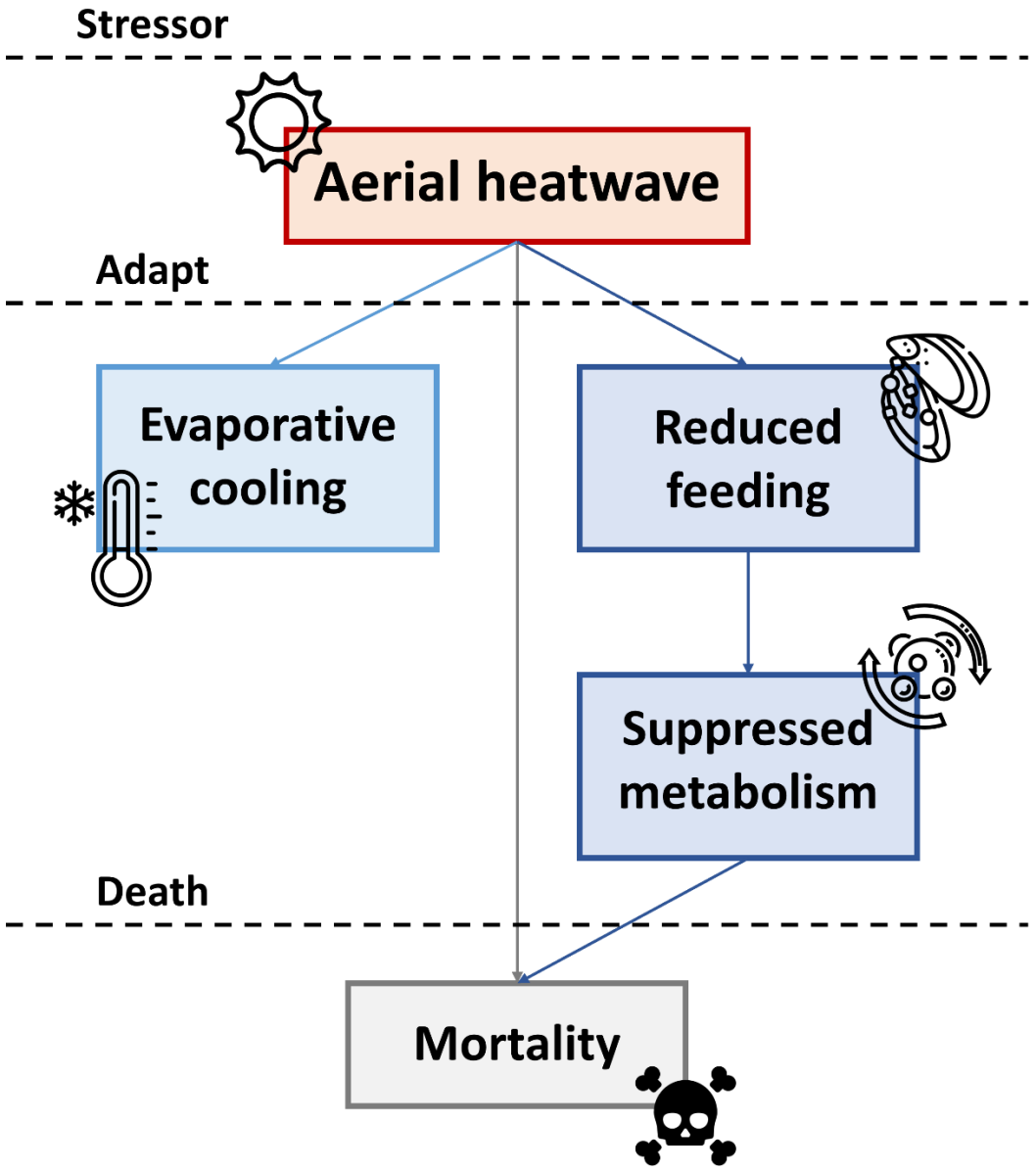

Fig 1. The possible responses of *Pisaster ochraceus* to an aerial heatwave as explored in this thesis.

References

Aguilera, M. A., R. M. Arias and T. Manzur. **2019**. Mapping microhabitat thermal patterns in artificial breakwaters: Alteration of intertidal biodiversity by higher rock temperature. *Ecology and Evolution* **9**: 12915–12927.

Åkesson, A., A. Curtsdotter, A. Eklöf, B. Ebenman, J. Norberg and G. Barabás. **2021**. The importance of species interactions in eco-evolutionary community dynamics under climate change. *Nat Commun* **12**: 4759.

Alexander, J. M., J. M. Diez, S. P. Hart and J. M. Levine. **2016**. When Climate Reshuffles Competitors: A Call for Experimental Macroecology. *Trends in Ecology & Evolution* **31**: 831–841. Elsevier.

Angilletta, M. J. 2009. *Thermal adaptation: A theoretical and empirical synthesis*. Oxford University Press.

Angilletta, M. J., P. H. Niewiarowski and C. A. Navas. **2002**. The evolution of thermal physiology in ectotherms. *Journal of Thermal Biology* **27**: 249–268.

Bartoń, K. 2024. MuMIn: Multi-Model Inference.

Bates, A. E., B. J. Hilton and C. D. G. Harley. **2009**. Effects of temperature, season and locality on wasting disease in the keystone predatory sea star Pisaster ochraceus. *Dis Aquat Organ* **86**: 245–251.

Beever, E. A., L. E. Hall, J. Varner, A. E. Loosen, J. B. Dunham, M. K. Gahl, F. A. Smith and J. J. Lawler. **2017**. Behavioral flexibility as a mechanism for coping with climate change. *Frontiers in Ecology and the Environment* **15**: 299–308.

Boyce, M. S. 2018. Wolves for Yellowstone: dynamics in time and space. *Journal of Mammalogy* **99**: 1021–1031.

Broitman, B. R., P. L. Szathmary, K. A. S. Mislan, C. A. Blanchette and B. Helmuth. **2009**. Predator-Prey Interactions under Climate Change: The Importance of Habitat vs. Body Temperature. *Oikos* **118**: 219–224. [Nordic Society Oikos, Wiley].

Brooks, M. E., K. Kristensen, K. J. van Benthem, A. Magnusson, C. W. Berg, A. Nielsen, H. J. Skaug, M. Mächler and B. M. Bolker. **2017**. glmmTMB balances speed and flexibility among packages for zero-inflated generalized linear mixed modeling. *The R Journal* **9**: 378–400.

Brown, J., J. Gillooly, A. Allen, V. m Savage and G. West. **2004**. Toward a metabolic theory of ecology. *Ecology* **85**: 1771–1789.

Bulova, S. J. 2002. How temperature, humidity, and burrow selection affect evaporative water loss in desert tortoises. *Journal of Thermal Biology* **27**: 175–189.

Byrne, M. 2011. Impact of ocean warming and ocean acidification on marine invertebrate life history stages: Vulnerabilities and potential for persistence in a changing ocean. *An Annual Review* **49**: 1–42.

Caddy-Retalic, S., K. Benkendorff and P. Fairweather. **2011**. Visualizing hotspots: Applying thermal imaging to monitor internal temperatures in intertidal gastropods. *Molluscan Research* **31**.

Carey, N. and J. Harianto. **2023**. respR: Import, process, analyse, and calculate rates from respirometry data.

Cavole, L. M., A. M. Demko, R. E. Diner, A. Giddings, I. Koester, C. M. L. S. Pagniello, M.-L. Paulsen, A. Ramirez-Valdez, S. M. Schwenck, N. K. Yen, *et al.* 2016. Biological Impacts of the 2013–2015 Warm-Water Anomaly in the Northeast Pacific: Winners, Losers, and the Future. *Oceanography* **29**: 273–285.

Chapperon, C., C. Le Bris and L. Seuront. **2013**. Thermally mediated body temperature, water content and aggregation behaviour in the intertidal gastropod Nerita atramentosa. *Ecological Research* **28**: 407–416. John Wiley & Sons, Ltd.

Chapperon, C. and L. Seuront. **2011**. Space-time variability in environmental thermal properties and snail thermoregulatory behaviour. *Functional Ecology* **25**: 1040–1050. British Ecological Society.

Chapperon, C. and L. Seuront. **2012**. Keeping warm in the cold: On the thermal benefits of aggregation behaviour in an intertidal ectotherm. *Journal of Thermal Biology* **37**: 640–647.

Colby, B. R., J. M. Niles, M. H. Persons and M. J. Wilson. **2022**. Shifting thermal regimes influence competitive feeding and aggression dynamics of brook trout (Salvelinus fontinalis) and creek chub (Semotilus atromaculatus). *Ecology and Evolution* **12**: e9056.

Cox, T. and C. Smith. **2011**. Thermal ecology on an exposed algal reef: Infrared imagery a rapid tool to survey temperature at local spatial scales. *Coral Reefs* **30**.

Csik, S. R., B. P. DiFiore, K. Kraskura, E. A. Hardison, J. S. Curtis, E. J. Eliason and A. C. Stier. **2023**. The metabolic underpinnings of temperature-dependent predation in a key marine predator. *Front. Mar. Sci.* **10**. Frontiers.

Currie-Olsen, D., A. V. Hesketh, J. Grimm, J. Kennedy, K. E. Marshall and C. D. G. Harley. **2023**. Lethal and sublethal implications of low temperature exposure for three intertidal predators. *Journal of Thermal Biology* **114**: 103549.

Dahlhoff, E. P., B. A. Buckley and B. A. Menge. **2001**. Physiology of the Rocky Intertidal Predator Nucella ostrina along an Environmental Stress Gradient. *Ecology* **82**: 2816–2829. Ecological Society of America.

Dell, A. I., S. Pawar and V. M. Savage. **2011**. Systematic variation in the temperature dependence of physiological and ecological traits. *Proceedings of the National Academy of Sciences* **108**: 10591–10596. Proceedings of the National Academy of Sciences.

Denny, M. W. and C. D. G. Harley. **2006**. Hot limpets: predicting body temperature in a conductance-mediated thermal system. *J Exp Biol* **209**: 2409–2419.

Deutsch, C. A., J. J. Tewksbury, R. B. Huey, K. S. Sheldon, C. K. Ghalambor, D. C. Haak and P. R. Martin. **2008**. Impacts of climate warming on terrestrial ectotherms across latitude. *Proceedings of the National Academy of Sciences* **105**: 6668–6672. Proceedings of the National Academy of Sciences.

Donelson, J. M., P. L. Munday, M. I. McCormick, N. W. Pankhurst and P. M. Pankhurst. **2010**. Effects of elevated water temperature and food availability on the reproductive performance of a coral reef fish. *Marine Ecology Progress Series* **401**: 233–243.

Dungan, M. L., T. E. Miller and D. A. Thomson. **1982**. Catastrophic decline of a top carnivore in the gulf of california rocky intertidal zone. *Science* **216**: 989–991.

Eisenlord, M. E., M. L. Groner, R. M. Yoshioka, J. Elliott, J. Maynard, S. Fradkin, M. Turner, K. Pyne, N. Rivlin, R. van Hooidonk, *et al.* 2016. Ochre star mortality during the 2014 wasting disease epizootic: role of population size structure and temperature. *Philosophical Transactions of the Royal Society B: Biological Sciences* **371**: 20150212. Royal Society.

Estes, J. A. and D. O. Duggins. **1995**. Sea Otters and Kelp Forests in Alaska: Generality and Variation in a Community Ecological Paradigm. *Ecological Monographs* **65**: 75–100.

Estes, J. A. and J. F. Palmisano. **1974**. Sea Otters: Their Role in Structuring Nearshore Communities. *Science* **185**: 1058–1060. American Association for the Advancement of Science.

Estes, J. A., J. Terborgh, J. S. Brashares, M. E. Power, J. Berger, W. J. Bond, S. R. Carpenter, T. E. Essington, R. D. Holt, J. B. C. Jackson, *et al.* 2011. Trophic Downgrading of Planet Earth. *Science* **333**: 301–306. American Association for the Advancement of Science.

Fernandes, T. and B. C. McMeans. **2019**. Coping with the cold: energy storage strategies for surviving winter in freshwater fish. *Ecography* **42**: 2037–2052.

Fey, S. B., D. A. Vasseur, K. Alujević, K. J. Kroeker, M. L. Logan, M. I. O'Connor, V. H. W. Rudolf, J. P. DeLong, S. Peacor, R. L. Selden, *et al.* 2019. Opportunities for behavioral rescue under rapid environmental change. *Glob Chang Biol* **25**: 3110–3120.

Fitzhenry, T., P. M. Halpin and B. Helmuth. **2004**. Testing the effects of wave exposure, site, and behavior on intertidal mussel body temperatures: applications and limits of temperature logger design. *Marine Biology* **145**: 339–349.

Fly, E. K., C. J. Monaco, S. Pincebourde and A. Tullis. **2012**. The influence of intertidal location and temperature on the metabolic cost of emersion in Pisaster ochraceus. *Journal of Experimental Marine Biology and Ecology* **422–423**: 20–28.

Fox, J., S. Weisberg, B. Price, D. Adler, D. Bates, G. Baud-Bovy, B. Bolker, S. Ellison, D. Firth, M. Friendly, *et al.* 2024. car: Companion to Applied Regression.

Fussmann, K. E., F. Schwarzmüller, U. Brose, A. Jousset and B. C. Rall. **2014**. Ecological stability in response to warming. *Nature Clim Change* **4**: 206–210. Nature Publishing Group.

Galloway, A. W. E., S. A. Gravem, J. N. Kobelt, W. N. Heady, D. K. Okamoto, D. M. Sivitilli, V. R. Saccomanno, J. Hodin and R. Whippo. **2023**. Sunflower sea star predation on urchins can facilitate kelp forest recovery. *Proceedings of the Royal Society B: Biological Sciences* **290**: 20221897. Royal Society.

Gilbert, N. A., J. L. Stenglein, T. R. Van Deelen, P. A. Townsend and B. Zuckerberg. **2022**. Behavioral flexibility facilitates the use of spatial and temporal refugia during variable winter weather. *Behavioral Ecology* **33**: 446–454.

Gillooly, J. F., J. H. Brown, G. B. West, V. M. Savage and E. L. Charnov. **2001**. Effects of size and temperature on metabolic rate. *Science* **293**: 2248–2251. American Association for the Advancement of Science.

Gooding, R. A. and C. D. G. Harley. **2015**. Quantifying the Effects of Predator and Prey Body Size on Sea Star Feeding Behaviors. *Biol Bull* **228**: 192–200.

Gosselin, L. A. 1997. An ecological transition during juvenile life in a marine snail. *Marine Ecology Progress Series* **157**: 185–194.

Gosselin, L. A. and P. Qian. **1997**. Juvenile mortality in benthic marine invertebrates. *Marine Ecology Progress Series* **146**: 265–282.

Hamilton, H. J. and L. A. Gosselin. **2020**. Ontogenetic shifts and interspecies variation in tolerance to desiccation and heat at the early benthic phase of six intertidal invertebrates. *Mar. Ecol.-Prog. Ser.* **634**: 15–28. Inter-Research, Oldendorf Luhe.

Hamilton, S. L., V. R. Saccomanno, W. N. Heady, A. L. Gehman, S. I. Lonhart, R. Beas-Luna, F. T. Francis, L. Lee, L. Rogers-Bennett, A. K. Salomon, *et al.* 2021. Disease-driven mass mortality event leads to widespread extirpation and variable recovery potential of a marine predator across the eastern Pacific. *Proc Biol Sci* **288**: 20211195.

Harley, C. D. G. 2008. Tidal dynamics, topographic orientation, and temperature-mediated mass mortalities on rocky shores. *Marine Ecology Progress Series* **371**: 37–46.

Harley, C. D. G., A. Randall Hughes, K. M. Hultgren, B. G. Miner, C. J. B. Sorte, C. S. Thornber, L. F. Rodriguez, L. Tomanek and S. L. Williams. **2006**. The impacts of climate change in coastal marine systems. *Ecology Letters* **9**: 228–241.

Hartig, F., L. Lohse and M. de S. leite. **2024**. DHARMa: Residual Diagnostics for Hierarchical (Multi-Level / Mixed) Regression Models.

Helmuth, B. 1998. Intertidal Mussel Microclimates: Predicting the Body Temperature of a Sessile Invertebrate. *Ecological Monographs - ECOL MONOGR* **68**: 51–74.

Helmuth, B. 2002. How do we Measure the Environment? Linking Intertidal Thermal Physiology and Ecology Through Biophysics1. *Integrative and Comparative Biology* **42**: 837–845.

Helmuth, B. S. T. and G. E. Hofmann. **2001**. Microhabitats, thermal heterogeneity, and patterns of physiological stress in the rocky intertidal zone. *Biological Bulletin* **201**: 374–384. Marine Biological Laboratory.

Hieb, E. E., C. S. Cloyed, K. P. DaCosta, A. Garelick and R. H. Carmichael. **2023**. Thermal microrefugia and changing climate affect migratory phenology of a thermally constrained marine mammal. *Front. Ecol. Evol.* **11**. Frontiers.

Huey, R. B. and M. Pascual. **2009**. Partial thermoregulatory compensation by a rapidly evolving invasive species along a latitudinal cline. *Ecology* **90**: 1715–1720.

Huey, R. B. and R. D. Stevenson. **1979**. Integrating Thermal Physiology and Ecology of Ectotherms: A Discussion of Approaches. *American Zoologist* **19**: 357–366.

Hui, T. Y., S. Crickenberger, J. W. T. Lau and G. A. Williams. **2022**. Why are 'suboptimal' temperatures preferred in a tropical intertidal ectotherm? *Journal of Animal Ecology* **91**: 1400–1415.

Hunt, H. and R. Scheibling. **1996**. Physical and biological factors influencing mussel (Mytilus trossulus, M. edulis) settlement on a wave-exposed rocky shore. *Marine Ecology Progress Series* **142**: 135–145.

Hurlbert, S. H. 1984. Pseudoreplication and the Design of Ecological Field Experiments. *Ecological Monographs* **54**: 187–211.

Jenewein, B. T. and L. A. Gosselin. **2013**. Ontogenetic shift in stress tolerance thresholds of *Mytilus trossulus*: effects of desiccation and heat on juvenile mortality. *Mar. Ecol.-Prog. Ser.* **481**: 147–159. Inter-Research, Oldendorf Luhe.

Jones, S. M. and R. A. Avery. **1989**. The Use of a Pyroelectric Vidicon Infra-Red Camera to Monitor the Body Temperatures of Small Terrestrial Vertebrates. *Functional Ecology* **3**: 373–377. [British Ecological Society, Wiley].

Joshi, M. M., J. M. Gregory, M. J. Webb, D. M. H. Sexton and T. C. Johns. **2008**. Mechanisms for the land/sea warming contrast exhibited by simulations of climate change. *Clim Dyn* **30**: 455–465.

Judge, R., F. Choi and B. Helmuth. **2018**. Recent Advances in Data Logging for Intertidal Ecology. *Front. Ecol. Evol.* **6**. Frontiers.

Kassambara, A., M. Kosinski, P. Biecek and S. Fabian. **2021**. survminer: drawing survival curves using "ggplot2."

Kidawa, A. 2005. The role of amino acids in phagostimulation in the shallow-water omnivorous Antarctic sea star Odontaster validus. *Polar Biol* **28**: 147–155.

Killick, R., K. Haynes, I. Eckley, P. Fearnhead, R. Long and J. Lee. **2022**. changepoint: methods for changepoint detection.

Kim, H., J.-H. Jo, H.-G. Lee, W. Park, H.-K. Lee, J.-E. Park and D. Shin. **2024**. Inflammatory response in dairy cows caused by heat stress and biological mechanisms for maintaining homeostasis. *PLOS ONE* **19**: e0300719. Public Library of Science.

Kingsolver, J. G., S. E. Diamond and L. B. Buckley. **2013**. Heat stress and the fitness consequences of climate change for terrestrial ectotherms. *Functional Ecology* **27**: 1415–1423.

Kish, N. E., B. Helmuth and D. S. Wethey. **2016**. Physiologically grounded metrics of model skill: a case study estimating heat stress in intertidal populations. *Conservation Physiology* **4**: cow038.

Kordas, R. L., C. D. G. Harley and M. I. O'Connor. **2011**. Community ecology in a warming world: The influence of temperature on interspecific interactions in marine systems. *Journal of Experimental Marine Biology and Ecology* **400**: 218–226.

Lathlean, J. A., D. J. Ayre and T. E. Minchinton. **2012**. Using infrared imagery to test for quadrat-level temperature variation and effects on the early life history of a rocky-shore barnacle. *Limnology and Oceanography* **57**: 1279–1291.

Lathlean, J. and L. Seuront. **2014**. Infrared thermography in marine ecology: methods, previous applications and future challenges. *Mar. Ecol.-Prog. Ser.* **514**: 263–277. Inter-Research, Oldendorf Luhe.

Lenth, R. V. 2016. Least-Squares Means: The R Package lsmeans. *Journal of Statistical Software* **69**: 1–33.

Lindquist, S. and E. A. Craig. **1988**. The heat-shock proteins. *Annual Review of Genetics* **22**: 631–677. Annual Reviews.

López-Urrutia, Á., E. San Martin, R. P. Harris and X. Irigoien. **2006**. Scaling the metabolic balance of the oceans. *Proceedings of the National Academy of Sciences* **103**: 8739–8744. Proceedings of the National Academy of Sciences.

Manabe, S., R. J. Stouffer, M. J. Spelman and K. Bryan. **1991**. Transient Responses of a Coupled Ocean–Atmosphere Model to Gradual Changes of Atmospheric CO2. Part I. Annual Mean Response. *Journal of Climate* **4**: 785–818. American Meteorological Society.

Marshall, D. J., E. L. Rezende, N. Baharuddin, F. Choi and B. Helmuth. **2015**. Thermal tolerance and climate warming sensitivity in tropical snails. *Ecology and Evolution* **5**: 5905–5919.

Martin, T. L. and R. B. Huey. **2008**. Why "suboptimal" is optimal: Jensen's inequality and ectotherm thermal preferences. *Am Nat* **171**: E102-118.

Martínez-De León, G. and M. P. Thakur. **2024**. Ecological debts induced by heat extremes. *Trends in Ecology & Evolution* **39**: 1024–1034.

Mauzey, K. P. 1966. Feeding behavior and reproductive cycles in Pisaster ochraceus. *Biological Bulletin* **131**: 127–144. Marine Biological Laboratory.

McGaw, I. J., A. M. Clifford and G. G. Goss. **2015**. Physiological responses of the intertidal starfish Pisaster ochraceus, (Brandt, 1835) to emersion at different temperatures. *Journal of Experimental Marine Biology and Ecology* **468**: 83–90.

McGaw, I. J. and T. A. Twitchit. **2012**. Specific dynamic action in the sunflower star, *Pycnopodia helianthoides*. *Comparative Biochemistry and Physiology Part A: Molecular & Integrative Physiology* **161**: 287–295.

McKechnie, A. E., P. A. R. Hockey and B. O. Wolf. **2012**. Feeling the heat: Australian landbirds and climate change. *Emu - Austral Ornithology* **112**: i–vii. Taylor & Francis.

McLeod, I. M., J. L. Rummer, T. D. Clark, G. P. Jones, M. I. McCormick, A. S. Wenger and P. L. Munday. **2013**. Climate change and the performance of larval coral reef fishes: the interaction between temperature and food availability. *Conservation Physiology* **1**: cot024.

Menge, B. A., E. L. Berlow, C. A. Blanchette, S. A. Navarrete and S. B. Yamada. **1994**. The Keystone Species Concept: Variation in Interaction Strength in a Rocky Intertidal Habitat. *Ecological Monographs* **64**: 250–286. Ecological Society of America.

Menge, B. A., E. B. Cerny-Chipman, A. Johnson, J. Sullivan, S. Gravem and F. Chan. **2016**. Sea Star Wasting Disease in the keystone predator Pisaster ochraceus in Oregon: insights into differential population impacts, recovery, predation rate, and temperature effects from long-term research. *PLOS ONE* **11**: e0153994. Public Library of Science.

Menge, J. L. and B. A. Menge. **1974**. Role of resource allocation, aggression and spatial heterogeneity in coexistence of two competing intertidal starfish. *Ecological Monographs* **44**: 189–209.

Monaco, C. J., D. S. Wethey and B. Helmuth. **2016**. Thermal sensitivity and the role of behavior in driving an intertidal predator-prey interaction. *Ecol. Monogr.* **86**: 429–447. Wiley, Hoboken.

Monteith, J. L. and M. H. Unsworth (eds). **2008**. Principles of Environmental Physics. In: *Principles of Environmental Physics (Fourth Edition)*, p. i. Academic Press, Boston.

Moore, D., A. Stow and M. R. Kearney. **2018**. Under the weather?—The direct effects of climate warming on a threatened desert lizard are mediated by their activity phase and burrow system. *Journal of Animal Ecology* **87**: 660–671.

Murphy, G. E. P., T. N. Romanuk and B. Worm. **2020**. Cascading effects of climate change on plankton community structure. *Ecology and Evolution* **10**: 2170–2181.

Padfield, D., Genevieve Yvon-Durocher, A. Buckling, S. Jennings and Gabriel Yvon-Durocher. **2016**. Rapid evolution of metabolic traits explains thermal adaptation in phytoplankton. *Ecology Letters* **19**: 133–142.

Paine, R. T. 1966. Food web complexity and species diversity. *The American Naturalist* **100**: 65–75. [University of Chicago Press, American Society of Naturalists].

Paine, R. T. 1969. The Pisaster-Tegula interaction: prey patches, predator food preference, and intertidal community structure. *Ecology* **50**: 950–961. Ecological Society of America.

Paine, R. T. 1974. Intertidal Community Structure. Experimental Studies on the Relationship between a Dominant Competitor and Its Principal Predator. *Oecologia* **15**: 93–120. Springer.

Petchey, O. L., P. T. McPhearson, T. M. Casey and P. J. Morin. **1999**. Environmental warming alters food-web structure and ecosystem function. *Nature* **402**: 69–72. Nature Publishing Group.

Peterson, G., C. R. Allen and C. S. Holling. **1998**. Ecological Resilience, Biodiversity, and Scale. *Ecosystems* **1**: 6–18.

Petes, L. E., M. E. Mouchka, R. H. Milston-Clements, T. S. Momoda and B. A. Menge. **2008**. Effects of environmental stress on intertidal mussels and their sea star predators. *Oecologia* **156**: 671–680.

Pincebourde, S., E. Sanford and B. Helmuth. **2008**. Body temperature during low tide alters the feeding performance of a top intertidal predator. *Limnology and oceanography* **53**: 1562.

Pincebourde, S., E. Sanford and B. Helmuth. **2009**. An intertidal sea star adjusts thermal inertia to avoid extreme body temperatures. *Am Nat* **174**: 890–897.

Pincebourde, S., E. Sanford and B. Helmuth. **2013**. Survival and arm abscission are linked to regional heterothermy in an intertidal sea star. *Journal of Experimental Biology* **216**: 2183–2191.

Pinheiro, J. C., D. J. Bates, S. DebRoy and D. Sakar. **2012**. *The Nlme Package: Linear and Nonlinear Mixed Effects Models, R Version 3*.

Pinsky, M. L., A. M. Eikeset, D. J. McCauley, J. L. Payne and J. M. Sunday. **2019**. Greater vulnerability to warming of marine versus terrestrial ectotherms. *Nature* **569**: 108–111.

Porter, W. P. and D. M. Gates. **1969**. Thermodynamic Equilibria of Animals with Environment. *Ecological Monographs* **39**: 227–244.

Pörtner, H. O., A. F. Bennett, F. Bozinovic, A. Clarke, M. A. Lardies, M. Lucassen, B. Pelster, F. Schiemer and J. H. Stillman. **2006**. Trade-offs in thermal adaptation: the need for a molecular to ecological integration. *Physiol Biochem Zool* **79**: 295–313.

Pörtner, H.-O. 2010. Oxygen- and capacity-limitation of thermal tolerance: a matrix for integrating climate-related stressor effects in marine ecosystems. *Journal of Experimental Biology* **213**: 881–893.

Przeslawski, R., M. Byrne and C. Mellin. **2015**. A review and meta-analysis of the effects of multiple abiotic stressors on marine embryos and larvae. *Glob Chang Biol* **21**: 2122–2140.

R Core Team. **2021**. R: A language and environment for statistical computing. R Foundation for Statistical Computing, Vienna, Austria.

Rall, B. C., O. Vucic-Pestic, R. B. Ehnes, M. Emmerson and U. Brose. **2010**. Temperature, predator–prey interaction strength and population stability. *Global Change Biology* **16**: 2145–2157.

Rebolledo, A. P., C. M. Sgrò and K. Monro. **2021**. Thermal performance curves are shaped by prior thermal environment in early life. *Frontiers in Physiology* **12**.

Richards, C., S. Collins, K. Fisher, R. Blackmore, D. Fifield and A. Bates. **2023**. *Burrows buffer nest temperatures and offer a stable thermal microclimate for threatened seabird chicks during extreme events*.

Ricketts, E. F., J. Calvin, J. W. Hedgpeth and D. W. Phillips. **1985**. *Between Pacific Tides: Fifth Edition*. Stanford University Press.

Ripple, W. J. and R. L. Beschta. **2012**. Trophic cascades in Yellowstone: The first 15years after wolf reintroduction. *Biological Conservation* **145**: 205–213.

Robles, C. 2013. Pisaster ochraceus. In: *Starfish: Biology and Ecology of the Asteroidea*.

Robles, C. D., M. Molina, C. A. Martinez and L. Alvarez. **2021**. Ecological implications of variable energy storage in the keystone predator, Pisaster ochraceus. *Ecosphere* **12**: e03882.

Robles, C., R. Sherwoodstephens and M. Alvarado. **1995**. Responses of a Key Intertidal Predator to Varying Recruitment of Its Prey. *Ecology* **76**: 565–579. Wiley, Hoboken.

Rogers, T. L. and J. K. Elliott. **2013**. Differences in relative abundance and size structure of the sea stars Pisasterochraceus and Evasteriastroschelii among habitat types in Puget Sound, Washington, USA. *Mar Biol* **160**: 853–865.

Sagarin, R. D. and S. D. Gaines. **2002**. Geographical Abundance Distributions of Coastal Invertebrates: Using One-Dimensional Ranges to Test Biogeographic Hypotheses. *Journal of Biogeography* **29**: 985–997. Wiley.

Sanford, E. and B. Menge. **2007**. Reproductive output and consistency of source populations in the sea star Pisaster ochraceus. *Mar. Ecol. Prog. Ser.* **349**: 1–12.

Schindelin, J., I. Arganda-Carreras, E. Frise, V. Kaynig, M. Longair, T. Pietzsch, S. Preibisch, C. Rueden, S. Saalfeld, B. Schmid, *et al.* 2012. Fiji: an open-source platform for biological-image analysis. *Nat Methods* **9**: 676–682. Nature Publishing Group.

Schuster, J. M. and A. E. Bates. **2023**. The role of kelp availability and quality on the energetic state and thermal tolerance of sea urchin and gastropod grazers. *Journal of Experimental Marine Biology and Ecology* **569**: 151947.

Schuster, J. M., A. Kurt Gamperl, P. Gagnon and A. E. Bates. **2022**. Distinct realized physiologies in green sea urchin (Strongylocentrotus droebachiensis) populations from barren and kelp habitats. *FACETS* **7**: 822–842. Canadian Science Publishing.

Seuront, L., K. R. Nicastro, G. I. Zardi and E. Goberville. **2019**. Decreased thermal tolerance under recurrent heat stress conditions explains summer mass mortality of the blue mussel Mytilus edulis. *Sci Rep* **9**: 17498. Nature Publishing Group.

Siegle, M. R., E. B. Taylor and M. I. O'Connor. **2018**. Prior heat accumulation reduces survival during subsequent experimental heat waves. *Journal of Experimental Marine Biology and Ecology* **501**: 109–117.

Silbiger, N. J., G. Goodbody-Gringley, J. F. Bruno and H. M. Putnam. **2019**. Comparative thermal performance of the reef-building coral Orbicella franksi at its latitudinal range limits. *Mar Biol* **166**: 126.

Sohlström, E. H., L. C. Archer, B. Gallo, M. Jochum, R. L. Kordas, B. C. Rall, B. Rosenbaum and E. J. O'Gorman. **2021**. Thermal acclimation increases the stability of a predator-prey interaction in warmer environments. *Glob Chang Biol* **27**: 3765–3778.

Sokolova, I. M., M. Frederich, R. Bagwe, G. Lannig and A. A. Sukhotin. **2012**. Energy homeostasis as an integrative tool for assessing limits of environmental stress tolerance in aquatic invertebrates. *Marine Environmental Research* **79**: 1–15.

Somero, G. N. 2002. Thermal physiology and vertical zonation of intertidal animals: optima, limits, and costs of living. *Integrative and Comparative Biology* **42**: 780–789.

Sørensen, J. G., T. N. Kristensen and V. Loeschcke. **2003**. The evolutionary and ecological role of heat shock proteins. *Ecology Letters* **6**: 1025–1037.

Stoks, R., J. Verheyen, M. Van Dievel and N. Tüzün. **2017**. Daily temperature variation and extreme high temperatures drive performance and biotic interactions in a warming world. *Current Opinion in Insect Science* **23**: 35–42.

Sun, Y.-X., L.-S. Hu and Y.-W. Dong. **2023**. Surviving hot summer: Roles of phenotypic plasticity of intertidal mobile species considering microhabitat environmental heterogeneity. *Journal of Thermal Biology* **117**: 103686.

Szathmary, P., B. Helmuth and D. Wethey. **2009**. Climate change in the rocky intertidal zone: predicting and measuring the body temperature of a keystone predator. *Mar. Ecol. Prog. Ser.* **374**: 43–56.

Therneau, T. M., T. L. (original S.->R port and R. maintainer until 2009), A. Elizabeth and C. Cynthia. **2023**. survival: Survival Analysis.

Traill, L. W., M. L. M. Lim, N. S. Sodhi and C. J. A. Bradshaw. **2010**. Mechanisms driving change: altered species interactions and ecosystem function through global warming. *Journal of Animal Ecology* **79**: 937–947.

Vahl, O. 1984. The relationship between specific dynamic action (SDA) and growth in the common starfish, Asterias rubens. *Oecologia* **61**: 122–125. Springer.

Vasseur, D. A. and K. S. McCann. **2005**. A Mechanistic Approach for Modeling Temperature-Dependent Consumer-Resource Dynamics. *The American Naturalist* **166**: 184–198. The University of Chicago Press.

Vázquez, D. P., E. Gianoli, W. F. Morris and F. Bozinovic. **2017**. Ecological and evolutionary impacts of changing climatic variability. *Biological Reviews* **92**: 22–42.

Wernberg, T., D. A. Smale, F. Tuya, M. S. Thomsen, T. J. Langlois, T. de Bettignies, S. Bennett and C. S. Rousseaux. **2013**. An extreme climatic event alters marine ecosystem structure in a global biodiversity hotspot. *Nature Clim Change* **3**: 78–82. Nature Publishing Group.

Whitman, D. W. 1987. Thermoregulation and daily activity patterns in a black desert grasshopper, *Taeniopoda eques*. *Animal Behaviour* **35**: 1814–1826.

Zeh, J. A., M. M. Bonilla, E. J. Su, M. V. Padua, R. V. Anderson, D. Kaur, D. Yang and D. W. Zeh. **2012**. Degrees of disruption: projected temperature increase has catastrophic consequences for reproduction in a tropical ectotherm. *Global Change Biology* **18**: 1833–1842.

Appendices

Appendix 1: Supplementary Materials for Chapter 2

Lydia N. Walton, Viola R. Watts, Jasmin M. Schuster, and Amanda E. Bates

Section 1: Parameterization and verification of experimental temperature treatments

1.1 Air and sea surface temperatures in Barkley Sound

Air and sea surface temperatures (SST) in Barkley Sound (British Columbia, Canada) supported our selection of the air and seawater temperatures in our experiments. Air temperatures from Eagle Bay (48°50'01.9"N, 125°08'47.7"W; **Fig. S1**) were recorded using an EnvLogger temperature sensor (version T2.4), while SST for the area was recorded by the Amphitrite Point lightstation in Ucluelet (48°55'16.1"N, 125°32'28.1"W; https://open.canada.ca/data/en/dataset/719955f2-bf8e-44f7-bc26-6bd623e82884; **Fig. S1**) during the boreal summer (May to August) of 2022. The maximum air temperature (~30°C, July) and maximum SST (~17°C, August) were used to parameterize the experimental treatments in 2023 and 2024 (**Fig. S1; Table S1**).

To capture finer scale temperature conditions near Bamfield, British Columbia (48°50'5.3844"N, 125°8'7.6452"W) we also recorded air and sea surface temperatures at Eagle Bay (EB), Grappler Narrows (GN), and Strawberry Point (SP) using a handheld temperature probe (INKBIRD IBS-TH2 Plus temperature probe) in 2023. These measurements were used to verify that experimental temperature treatments represented biologically relevant temperatures. The ~20°C and ~25°C experimental air treatments were generally representative of midday low tide conditions in early summer (*i.e.,* May, June) and late summer (*i.e.,* July, August) respectively (**Chapter 2, Table 2**). The ~30°C experimental air treatment represented midday low tide conditions during an aerial heatwave (recorded in 2022; **Fig. S1**). The cooler water treatments (~15°C) were consistent with sea surface temperatures at intertidal sites in early summer while the warmer water treatments (~20°C) were consistent with SST in late summer (**Chapter 2, Table 2**).

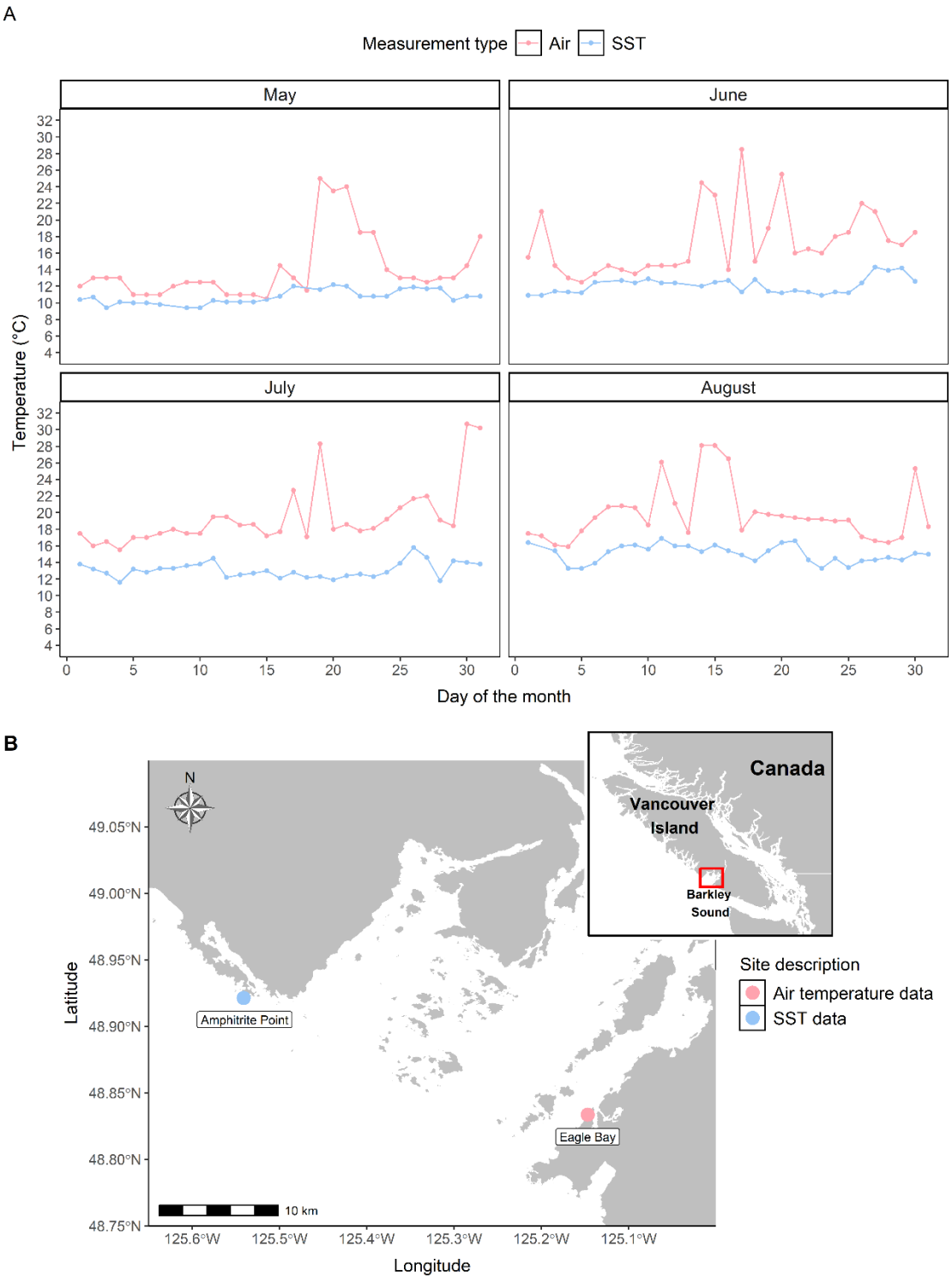

Fig. S1 (A) Daily measurements of the maximum air temperature and sea surface temperature for Barkley Sound during the boreal summer (May – August) of 2022. **(B)** Air temperatures were collected by an EnvLogger temperature sensor deployed at Eagle Bay, Bamfield (48.833739, -125.146825 in the intertidal zone (Baum Lab research group, University of Victoria)). Sea surface temperatures (SST) were obtained from the Amphitrite Point Lightstation (48.921138, -125.540979) dataset (https://www.dfo-mpo.gc.ca/science/data-donnees/lightstations-phares/index-eng.html).

Table S1. Air temperatures (Eagle Bay) and sea surface temperatures (SST; Amphitrite Point lightstation) recorded in Barkley Sound during the boreal summer (May to August) of 2022.

Location	Measurement	Time	Mean temp ± SD (°C)	Min temp (°C)	Max temp (°C)
Eagle Bay	Air temp	May 2022	11.49 ± 1.86	9.0	25.0
Eagle Bay	Air temp	June 2022	13.46 ± 2.11	10.0	28.5
Eagle Bay	Air temp	July 2022	15.71 ± 2.03	11.7	30.7
Eagle Bay	Air temp	August 2022	16.24 ± 1.99	12.2	28.1
Amphitrite Point	SST	May 2022	10.70 ± 0.84	9.4	12.2
Amphitrite Point	SST	June 2022	12.09 ± 0.98	10.9	14.3
Amphitrite Point	SST	July 2022	13.08 ± 0.95	11.6	15.8
Amphitrite Point	SST	August 2022	15.05 ± 1.05	13.3	16.9

Measurements reported are: mean temperature ± standard deviation, minimum temperature, and maximum temperature for each month. Air temperature measurements were recorded using an EnvLogger temperature sensor (version T2.4) deployed by the Baum Lab (University of Victoria) while SST measurements were recorded using daily seawater collections at Amphitrite Point lighstation.

Section 2: Model estimates and supporting statistical analyses

2.1 Experiment 1 (June 2023): Effects of air and seawater temperatures on juvenile *Pisaster* feeding rates

2.1.1 Estimation of mussel biomass

An allometric relationship between mussel shell size and dry tissue weight was determined using a subset of 70 dissected *Mytilus trossulus*. The shell length (mm) and shell width (mm) were used to calculate shell size (length x width). The total wet weight (shell + tissue), empty shell weight (g), tissue wet weight (g), and tissue dry weight (g) were measured for each dissected mussel. Dry weight was calculated as the weight of the dissected tissue following ~24 hours in a drying oven set to 60°C. A polynomial regression was used to determine the relationship between the dry tissue weight and the shell size of the dissected mussels (n = 70) (**Fig. S2**). The resulting equation was applied to the Experiment 1 dataset, as the shell size for every mussel consumed by juvenile *Pisaster* was recorded, and used to estimate the total tissue consumed during Experiment 1. The equation failed to accurately predict tissue mass (unequal variance, particularly with increasing mussel size), therefore, the number of mussels consumed (instead of biomass) was used for statistical analyses of feeding rate in Experiment 1, Experiment 2, and Appendix 3 of this thesis.

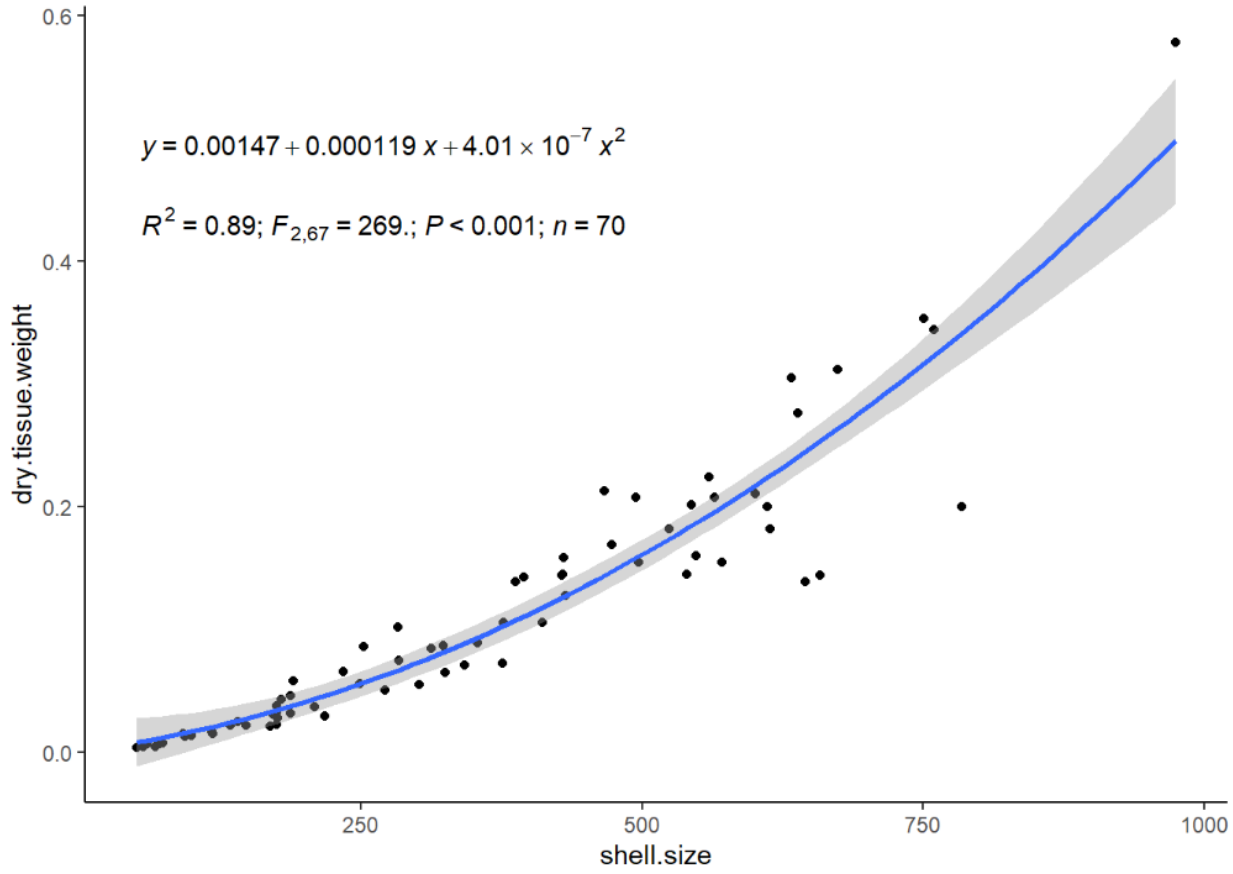

Fig. S2 A polynomial regression relating the dry tissue weight (g) and shell size (mm) of *Mytilus trossulus* (n = 70).

2.1.1 Total mussel consumption (estimate of feeding activity)

Table S2A. Results of a generalized linear mixed model investigating differences in the total number of *Mytilus* spp. consumed by juvenile *Pisaster ochraceus* (n = 63) during the heat stress and recovery periods of Experiment 1 (June 2023).

Model: Total number of mussels consumed ~ Trial type*Treatment + scaled disc diameter (mm) + (1 | day of trial) + (1 | group)			
Model family: Poisson	**AIC:** 2547.8		
Predictors	*Estimate*	*CI*	*p-value*
(Intercept)	0.43	0.32 – 0.57	***
Trial type (Recovery)	1.10	0.73 – 1.65	0.651
Treatment (15°C water and 25°C air)	0.81	0.59 – 1.12	0.205
Treatment (15°C water and 30°C air)	0.16	0.08 – 0.32	***
Treatment (20°C water and 20°C air)	1.18	0.88 – 1.57	0.271
Treatment (20°C water and 25°C air)	1.30	0.98 – 1.73	0.068
Treatment (20°C water and 30°C air)	0.80	0.57 – 1.13	0.211
Scaled disc diameter (mm)	1.01	0.87 – 1.17	0.933
Day of trial	1.01	0.99 – 1.04	0.155
Trial type (Recovery)*Treatment (15°C water and 25°C air)	1.35	0.84 – 2.17	0.221
Trial type (Recovery)*Treatment (15°C water and 30°C air)	4.34	1.82 – 10.35	***
Trial type (Recovery)*Treatment (20°C water and 20°C air)	0.76	0.48 – 1.08	0.266
Trial type (Recovery)*Treatment (20°C water and 25°C air)	0.68	0.42 – 1.08	0.105
Trial type (Recovery)*Treatment (20°C water and 30°C air)	1.23	0.73 – 2.07	0.442
Random Effects			
σ^2	1.10		
$T_{00\ group}$	0.00		
N_{group}	4		
Observations	1447		
Marginal R^2	0.210		

Trial type: heat stress period (16 consecutive days; cycling between submersion (18-hours) and emersion (6-hours)) or recovery period (8 consecutive days; sea stars fully submerged in ambient water temperature (~13°C)). Treatment: six combinations of water temperature (15°C or 20°C) and air temperature (20°C, 25°C, or 30°C). Scaled disc diameter: measurement of body size across the aboral disc of each sea star (mm) which was rescaled in R for comparisons. Day of trial: total of 24 days in the experiment (heat stress and recovery periods). Group: the effect of sea table/tank. Asterisks describe levels of significance ($p < 0.001$***, $p < 0.01$**, $p<0.05$*).

Table S2B. Results of a generalized linear mixed model investigating differences in the total number of *Mytilus* spp. consumed by juvenile *Pisaster ochraceus* (n = 63) during the first half of the heat stress period (days 1-8) of Experiment 1 (June 2023).

Model: Total number of mussels consumed [first half of heat stress period] ~ water treatment*air treatment + scaled disc diameter (mm) + (1 | group)				
Model family: Poisson		**AIC:** 228.3		
Predictors		*Estimate*	*CI*	*p-value*
(Intercept)		4.27	3.21 – 5.69	***
Water treatment (20°C)		0.88	0.58 – 1.32	0.532
Air treatment (25°C)		0.45	0.27 – 0.74	**
Air treatment (30°C)		0.10	0.03 – 0.32	***
Scaled disc diameter (mm)		1.02	0.76 – 1.36	0.918
Water treatment (20°C)*Air treatment (25°C)		2.08	1.08 – 4.01	*
Water treatment (20°C)*Air treatment (30°C)		4.75	1.29 – 17.44	*
Random Effects				
σ^2	0.31			
$T_{00\ group}$	0.00			
N_{group}	4			
Observations	63			
Marginal R^2	0.612			

The heat stress period lasted 16 consecutive days with *Pisaster* cycling between submersion (18-hours) and emersion (6-hours); the first half of the heat stress period includes days 1-8. Water treatment*Air treatment: six combinations of water temperature (15°C or 20°C) and air temperature (20°C, 25°C, or 30°C). Scaled disc diameter: measurement of body size across the aboral disc of each sea star (mm) which was rescaled in R for comparisons. Group: the effect of sea table/tank. Asterisks describe levels of significance ($p < 0.001$***, $p < 0.01$**, $p<0.05$*).

Table S2C. Results of a generalized linear mixed model investigating differences in the total number of *Mytilus* spp. consumed by juvenile *Pisaster ochraceus* (n = 63) during the second half of the heat stress period (days 9-16) of Experiment 1 (June 2023).

Model: Total number of mussels consumed [second half of heat stress period] ~ water treatment* air treatment + scaled disc diameter (mm) + (1 | group)				
Model family: Poisson		**AIC:** 252.4		
Predictors		*Estimate*	*CI*	*p-value*
(Intercept)		3.08	2.20 – 4.31	***
Water treatment (20°C)		1.59	1.04 – 2.43	*
Air treatment (25°C)		1.35	0.87 – 2.09	0.180
Air treatment (30°C)		0.23	0.09 – 0.60	**
Scaled disc diameter (mm)		0.86	0.66 – 1.10	0.228
Water treatment (20°C)*Air treatment (25°C)		0.90	0.52 – 1.58	0.720
Water treatment (20°C)*Air treatment (30°C)		3.46	1.24 – 9.67	*
Random Effects				
σ^2	0.23			
$T_{00\ group}$	0.00			
N_{group}	4			
Observations	63			
Marginal R^2	0.625			

The heat stress period lasted 16 consecutive days with *Pisaster* cycling between submersion (18-hours) and emersion (6-hours); the second half of the heat stress period includes days 9-16. Water treatment*Air treatment: six combinations of water temperature (15°C or 20°C) and air temperature (20°C, 25°C, or 30°C). Scaled disc diameter: measurement of body size across the aboral disc of each sea star (mm) which was rescaled in R for comparisons. Group: the effect of sea table/tank. Asterisks describe levels of significance ($p < 0.001$***, $p < 0.01$**, $p<0.05$*).

Table S2D. Results of a generalized linear mixed model investigating differences in the total number of *Mytilus* spp. consumed by juvenile *Pisaster ochraceus* (n = 63) during the recovery period (days 17-24) of Experiment 1 (June 2023).

Model: Total number of mussels consumed [recovery period] ~ water treatment* air treatment + scaled disc diameter (mm) + (1 | group)				
Model family: Poisson		**AIC:** 252.4		
Predictors		*Estimate*	*CI*	*p-value*
(Intercept)		5.07	3.90 – 6.59	***
Water treatment (20°C)		0.90	0.62 – 1.31	0.588
Air treatment (25°C)		1.08	0.75 – 1.54	0.683
Air treatment (30°C)		0.67	0.42 – 1.08	0.102
Scaled disc diameter (mm)		1.16	0.92 – 1.45	0.204
Water treatment (20°C)*Air treatment (25°C)		0.91	0.54 – 1.53	0.724
Water treatment (20°C)*Air treatment (30°C)		1.68	0.90 – 3.13	0.102
Random Effects				
σ^2	0.19			
$T_{00\ group}$	0.00			
N_{group}	4			
Observations	63			
Marginal R^2	0.113			

The recovery period lasted eight consecutive days where sea stars were fully submerged in ambient water temperature (~13°C). Water treatment*Air treatment: six combinations of water temperature (15°C or 20°C) and air temperature (20°C, 25°C, or 30°C). Scaled disc diameter: measurement of body size across the aboral disc of each sea star (mm) which was rescaled in R for comparisons. Group: the effect of sea table/tank. Asterisks describe levels of significance ($p < 0.001$***, $p < 0.01$**, $p<0.05$*).

2.2 Experiment 2 (May 2024): Effects of air and seawater temperatures on juvenile Pisaster feeding rates, metabolism, and attachment tenacity

2.2.1 Total mussel consumption (estimate of feeding activity)

Table S2A. Results of a generalized linear mixed model investigating differences in the total number of *Mytilus* spp. consumed by juvenile *Pisaster ochraceus* (n = 72) during Experiment 2 (May 2024).

Model: Total number of mussels consumed ~ Trial type*treatment + scaled disc diameter (mm) + (1 | day of trial) + (1 | group/individual) + (1| $\dot{M}O_2$ measured)			
Model family: Poisson	**AIC:** 2884.7		
Predictors	*Estimate*	*CI*	*p-value*
(Intercept)	0.42	0.27 – 0.64	***
Trial type (Heat stress)	1.13	0.68 – 1.88	0.631
Trial type (Recovery)	2.12	1.21 – 3.69	**
Treatment (15°C water and 30°C air)	1.49	1.01 – 2.19	*
Treatment (20°C water and 25°C air)	1.24	0.83 – 1.85	0.289
Treatment (20°C water and 30°C air)	1.41	0.96 – 2.09	0.083
Scaled disc diameter (mm)	0.79	0.69 – 0.91	***
Trial type (Heat stress)*Treatment (15°C water and 30°C air)	0.09	0.04 – 0.17	***
Trial type (Recovery)*Treatment (15°C water and 30°C air)	0.30	0.17 – 0.51	***
Trial type (Heat stress)*Treatment (20°C water and 25°C air)	1.15	0.72 – 1.83	0.570
Trial type (Recovery)*Treatment (20°C water and 25°C air)	0.73	0.44 – 1.20	0.208
Trial Type (Heat stress)*Treatment (20°C water and 30°C air)	0.27	0.16 – 0.47	***
Trial type (Recovery)*Treatment (20°C water and 30°C air)	0.66	0.40 – 1.08	0.099
Random Effects			
σ^2	1.24		
$T_{00\ day\ of\ trial}$	0.14		
$N_{day\ of\ trial}$	25		
$T_{00\ group}$	0.00		
N_{group}	4		
$T_{00\ \dot{M}O2\ measured}$	0.00		
$N_{\dot{M}O2\ measured}$	1		
Observations	1800		
Marginal R^2	0.367		

Trial type: adjustment period, heat stress period, or recovery period; sea stars were fed mussels *ad libidum* and alternated between water temperatures and air temperatures in a simulated high-tide (submerged for 18 hours) and low-tide (emersed for 6 hours). Treatment: four combinations of water temperature (15°C or 20°C) and air temperature (25°C or 30°C). Scaled disc diameter: measurement of body size across the aboral disc of each sea star

(mm) which was rescaled in R for comparisons. Day of trial: total of 39 days in the experiment. Group: the effect of sea table/tank with each individual *Pisaster* included as a nested random effect. $\dot{M}O_2$ measured: the effect of animal handling during $\dot{M}O_2$ measurements; *Pisaster* were either in the control group (no $\dot{M}O_2$ measurements) or the $\dot{M}O_2$ group ($\dot{M}O_2$ measured four times during the experiment). Asterisks describe levels of significance ($p < 0.001$***, $p < 0.01$**, $p<0.05$*).

Table S3B. Results of a generalized linear mixed model investigating differences in the total number of *Mytilus* spp. consumed by juvenile *Pisaster ochraceus* (n = 72) during the adjustment period (days 1-10) of Experiment 2 (May 2024).

Model: Total number of mussels consumed [adjustment period] ~ water treatment* air treatment + scaled disc diameter (mm) + (1 | group) + (1| $\dot{M}O_2$ measured)				
Model family: Poisson		**AIC:** 289.8		
Predictors		*Estimate*	*CI*	*p-value*
(Intercept)		2.39	1.77 – 3.22	***
Water treatment (20°C)		1.26	0.84 – 1.87	0.265
Air treatment (30°C)		1.53	1.04 – 2.25	*
Scaled disc diameter (mm)		0.99	0.77 – 1.29	0.962
Water treatment (20°C) x Air treatment (30°C)		0.72	0.43 – 1.24	0.237
Random Effects				
σ^2	0.28			
$T_{00\ group}$	0.00			
$T_{00\ \dot{M}O2\ measured}$	0.00			
N_{group}	4			
$N_{\dot{M}O2\ measured}$	1			
Observations	72			
Marginal R^2	0.084			

The adjustment period lasted 10 consecutive days with *Pisaster* alternating between 15°C water temperatures and 20°C air temperatures in a simulated high-tide (submerged for 18 hours) and low-tide (emersed for 6 hours) cycle. Treatment: four combinations of water temperature (15°C or 20°C) and air temperature (25°C or 30°C). Scaled disc diameter: measurement of body size across the aboral disc of each sea star (mm) which was rescaled in R for comparisons. Group: the effect of sea table/tank. $\dot{M}O_2$ measured: the effect of animal handling during $\dot{M}O_2$ measurements; *Pisaster* were either in the control group (no $\dot{M}O_2$ measurements) or the $\dot{M}O_2$ group ($\dot{M}O_2$ measured four times during the experiment). Asterisks describe levels of significance ($p < 0.001$***, $p < 0.01$**, $p<0.05$*).

Table S3C. Results of a generalized linear mixed model investigating differences in the total number of *Mytilus* spp. consumed by juvenile *Pisaster ochraceus* (n = 72) during the first half of the heat stress period (days 11-20) of Experiment 2 (May 2024).

Model: Total number of mussels consumed [first half heat stress period] ~ water treatment* air treatment + scaled disc diameter (mm) + (1 | group) + (1| $\dot{M}O_2$ measured)				
Model family: Poisson		**AIC:** 193.5		
Predictors		*Estimate*	*CI*	*p-value*
(Intercept)		2.15	1.56 – 2.97	***
Water treatment (20°C)		1.27	0.82 – 1.94	0.280
Air treatment (30°C)		0.15	0.06 – 0.35	***
Scaled disc diameter (mm)		0.71	0.47-1.08	0.109
Water treatment (20°C) x Air treatment (30°C)		0.98	0.30 – 3.17	0.974
Random Effects				
σ^2	0.54			
$T_{00\ group}$	0.00			
$T_{00\ \dot{M}O2\ measured}$	0.00			
N_{group}	4			
$N_{\dot{M}O2\ measured}$	1			
Observations	72			
Marginal R^2	0.644			

The heat stress period lasted 20 consecutive days where *Pisaster* alternated between treatment water temperatures and air temperatures in a simulated high-tide (submerged for 18 hours) and low-tide (emersed for 6 hours) cycle; the first half of the heat stress period included days 11-20. Treatment: four combinations of water temperature (15°C or 20°C) and air temperature (25°C or 30°C). Scaled disc diameter: measurement of body size across the aboral disc of each sea star (mm) which was rescaled in R for comparisons. Group: the effect of sea table/tank. $\dot{M}O_2$ measured: the effect of animal handling during $\dot{M}O_2$ measurements; *Pisaster* were either in the control group (no $\dot{M}O_2$ measurements) or the $\dot{M}O_2$ group ($\dot{M}O_2$ measured four times during the experiment). Asterisks describe levels of significance ($p < 0.001$***, $p < 0.01$**, $p<0.05$*).

Table S3D. Results of a generalized linear mixed model investigating differences in the total number of *Mytilus* spp. consumed by juvenile *Pisaster ochraceus* (n = 72) during the second half of the heat stress period (days 21-30) of Experiment 2 (May 2024).

Model: Total number of mussels consumed [second half heat stress period] ~ water treatment* air treatment + scaled disc diameter (mm) + (1 | group) + (1| $\dot{M}O_2$ measured)				
Model family: Poisson		**AIC:** 266.6		
Predictors		*Estimate*	*CI*	*p-value*
(Intercept)		3.74	2.95 – 4.75	***
Water treatment (20°C)		1.5	1.11 – 2.04	**
Air treatment (30°C)		0.11	0.05 – 0.23	***
Scaled disc diameter (mm)		0.66	0.49 – 0.88	**
Water treatment (20°C) x Air treatment (30°C)		3.07	1.33 – 7.05	**
Random Effects				
σ^2	0.30			
$T_{00\ group}$	0.00			
$T_{00\ \dot{M}O2\ measured}$	0.00			
N_{group}	4			
$N_{\dot{M}O2\ measured}$	1			
Observations	72			
Marginal R^2	0.772			

The heat stress period lasted 20 consecutive days where *Pisaster* alternated between treatment water temperatures and air temperatures in a simulated high-tide (submerged for 18 hours) and low-tide (emersed for 6 hours) cycle; the second half of the heat stress period included days 21-30. Treatment: four combinations of water temperature (15°C or 20°C) and air temperature (25°C or 30°C). Scaled disc diameter: measurement of body size across the aboral disc of each sea star (mm) which was rescaled in R for comparisons. Group: the effect of sea table/tank. $\dot{M}O_2$ measured: the effect of animal handling during $\dot{M}O_2$ measurements; *Pisaster* were either in the control group (no $\dot{M}O_2$ measurements) or the $\dot{M}O_2$ group ($\dot{M}O_2$ measured four times during the experiment). Asterisks describe levels of significance ($p < 0.001$***, $p < 0.01$**, $p<0.05$*).

Table S3E. Results of a generalized linear mixed model investigating differences in the total number of *Mytilus* spp. consumed by juvenile *Pisaster ochraceus* (n = 72) during the recovery period (days 31-39) of Experiment 2 (May 2024).

Model: Total number of mussels consumed [recovery period] ~ water treatment* air treatment + scaled disc diameter (mm) + (1 | group) + (1| $\dot{M}O_2$ measured)				
Model family: Poisson		**AIC:** 293.9		
Predictors		*Estimate*	*CI*	*p-value*
(Intercept)		4.97	4.04 – 6.11	***
Water treatment (20°C)		0.90	0.67 – 1.21	0.482
Air treatment (30°C)		0.43	0.30 – 0.63	***
Scaled disc diameter (mm)		0.69	0.53 – 0.88	**
Water treatment (20°C) x Air treatment (30°C)		2.42	1.49 – 3.93	***
Random Effects				
σ^2	0.22			
$T_{00\ group}$	0.00			
$T_{00\ \dot{M}O2\ measured}$	0.00			
N_{group}	4			
$N_{\dot{M}O2\ measured}$	1			
Observations	72			
Marginal R^2	0.393			

The recovery period lasted 9 consecutive days where *Pisaster* alternated between 15°C water temperatures and 20°C air temperatures in a simulated high-tide (submerged for 18 hours) and low-tide (emersed for 6 hours) cycle. Treatment: four combinations of water temperature (15°C or 20°C) and air temperature (25°C or 30°C). Scaled disc diameter: measurement of body size across the aboral disc of each sea star (mm) which was rescaled in R for comparisons. Group: the effect of sea table/tank. $\dot{M}O_2$ measured: the effect of animal handling during $\dot{M}O_2$ measurements; *Pisaster* were either in the control group (no $\dot{M}O_2$ measurements) or the $\dot{M}O_2$ group ($\dot{M}O_2$ measured four times during the experiment). Asterisks describe levels of significance ($p < 0.001$***, $p < 0.01$**, $p<0.05$*).

2.2.2 Thermal stress

Table S4. Results of a generalized linear mixed model investigating differences in the attachment of juvenile *Pisaster ochraceus* (n = 72) to experimental aquaria during the heat stress and recovery periods of Experiment 2 (May 2024).

Model: Attachment to substrate ~ Trial block*treatment + scaled disc diameter (mm) + MO2 measured + (1 | individual) + (1 | group)				
Model family: Binomial		**AIC:** 1709.4		
Predictors		*Estimate*	*CI*	*p-value*
(Intercept)		0.13	0.06 – 0.28	***
Trial type (Second half of heat stress)		1.39	0.76 – 2.53	0.287
Trial type (Recovery)		0.45	0.21 – 0.99	*
Treatment (15°C water and 30°C air)		8.47	3.70 – 19.40	***
Treatment (20°C water and 25°C air)		0.56	0.22 – 1.45	0.236
Treatment (20°C water and 30°C air)		3.41	1.48 – 7.87	**
Scaled disc diameter (mm)		0.72	0.43 – 1.19	0.201
MO2 measured (Y)		1.73	1.03 - 2.89	*
Trial type (Second half of heat stress)*Treatment (15°C water and 30°C air)		8.46	3.56 – 20.08	***
Trial type (Recovery)*Treatment (15°C water and 30°C air)		0.68	0.27 – 1.72	0.417
Trial type (Second half of heat stress)*Treatment (20°C water and 25°C air)		0.90	0.34 – 2.33	0.821
Trial type (Recovery)*Treatment (20°C water and 25°C air)		1.20	0.35 – 4.08	0.775
Trial Type (Second half of heat stress)*Treatment (20°C water and 30°C air)		4.68	2.16 – 10.12	***
Trial type (Recovery)*Treatment (20°C water and 30°C air)		0.77	0.29 – 2.04	0.595
Random Effects				
σ^2	3.29			
$T_{00\ group}$	0.00			
$T_{00\ individual}$	0.82			
N_{group}	4			
$N_{individual}$	72			
Observations	2016			
Marginal R^2	0.463			

Trial type: first half of heat stress period, second half of heat stress period, or recovery period; sea stars were fed mussels *ad libidum* and alternated between water temperatures and air temperatures in a simulated high-tide (submerged for 18 hours) and low-tide (emersed for 6 hours). Treatment: four combinations of water temperature (15°C or 20°C) and air temperature (25°C or 30°C). Scaled disc diameter: measurement of body size across the aboral disc of each sea star (mm) which was rescaled in R for comparisons. $\dot{M}O_2$ measured: the effect of animal handling during $\dot{M}O_2$ measurements; *Pisaster* were either in the control group (no $\dot{M}O_2$ measurements) or the $\dot{M}O_2$ group ($\dot{M}O_2$ measured four times during the experiment). Day of trial: total of 39 days in the experiment. Group: the effect of sea table/tank. Asterisks describe levels of significance ($p < 0.001$***, $p < 0.01$**, $p<0.05$*).

2.2.3 Aquatic oxygen consumption ($\dot{M}O_2$)

Table S5. Results of a linear mixed model investigating differences in the mass-corrected $\dot{M}O_2$ of juvenile *Pisaster ochraceus* (n = 9 per treatment) during the adjustment, heat stress and recovery periods of Experiment 2 (May 2024). Treatments were re-leveled and the 15°C water/30°C air treatment was used as the intercept for the model.

Model: AFDM-corrected $\dot{M}O_2$ ~ Treatment*measurement number + scaled disc diameter (mm) + total mussels consumed per individual, random = (~1| individual), weights = varIdent(form = ~1|Treatment)				
AIC: 290.2755				
Predictors		*Estimate*	*CI*	*p-value*
(Intercept)		0.29	0.24 – 0.34	***
Treatment (15°C water and 25°C air)		-0.07	-0.13 – -0.02	**
Treatment (20°C water and 25°C air)		-0.07	-0.12 – -0.01	*
Treatment (20°C water and 30°C air)		-0.04	-0.11 – -0.02	0.191
Measurement number (M2)		-0.08	-0.14 – -0.02	**
Measurement number (M3)		-0.11	-0.17 – -0.05	***
Measurement number (M4)		-0.06	-0.12 – 0.00	0.069
Scaled disc diameter (mm)		-0.03	-0.05 – 0.00	*
Total number of mussels consumed per individual		0.01	0.00 – 0.01	**
Treatment (15°C water and 25°C air)*Measurement number (M2)		0.05	-0.02 – 0.11	0.180
Treatment (20°C water and 25°C air)*Measurement number (M2)		0.14	0.07 – 0.20	***
Treatment (20°C water and 30°C air)*Measurement number (M2)		0.13	0.05 – 0.21	**
Treatment (15°C water and 25°C air)*Measurement number (M3)		0.08	0.01 – 0.15	*
Treatment (20°C water and 25°C air)*Measurement number (M3)		0.16	0.09 – 0.24	***
Treatment (20°C water and 30°C air)*Measurement number (M3)		0.08	-0.01 – 0.16	0.70
Treatment (15°C water and 25°C air)*Measurement number (M4)		0.07	0.00 – 0.14	*
Treatment (20°C water and 25°C air)*Measurement number (M4)		0.09	0.02 – 0.16	**
Treatment (20°C water and 30°C air)*Measurement number (M4)		0.04	-0.04 – 0.12	0.346
Random Effects				
σ^2	0.00			
$T_{00\ individual}$	0.00			
ICC	0.43			
$N_{individual}$	36			
Observations	130			
Marginal R^2	0.616			

During the adjustment (M1), heat stress (M2, M3), and recovery (M4) periods *Pisaster* were fed mussels *ad libidum* and alternated between water temperatures and air temperatures in a simulated high-tide (submerged for 18 hours) and low-tide (emersed for 6 hours). Treatment: four combinations of water temperature (15°C or 20°C) and air temperature (25°C or 30°C). Measurement number: four measurements of $\dot{M}O_2$ during the experiment (M1: adjustment period; M2: first half of the heat stress period; M3: second half of the heat stress period; M4: recovery period). Scaled disc diameter: measurement of body size across the aboral disc of each sea star (mm) which was rescaled in R for comparisons. Total mussels: the total number of mussels consumed per individual during the adjustment, first half of the heat stress, second half of the heat stress, and recovery periods. Weights modelled the variance structure of each Treatment and was used to improve the model fit. Asterisks describe levels of significance ($p < 0.001$***, $p < 0.01$**, $p<0.05$*).

2.2.4 Aerial oxygen consumption ($\dot{M}O_2$)

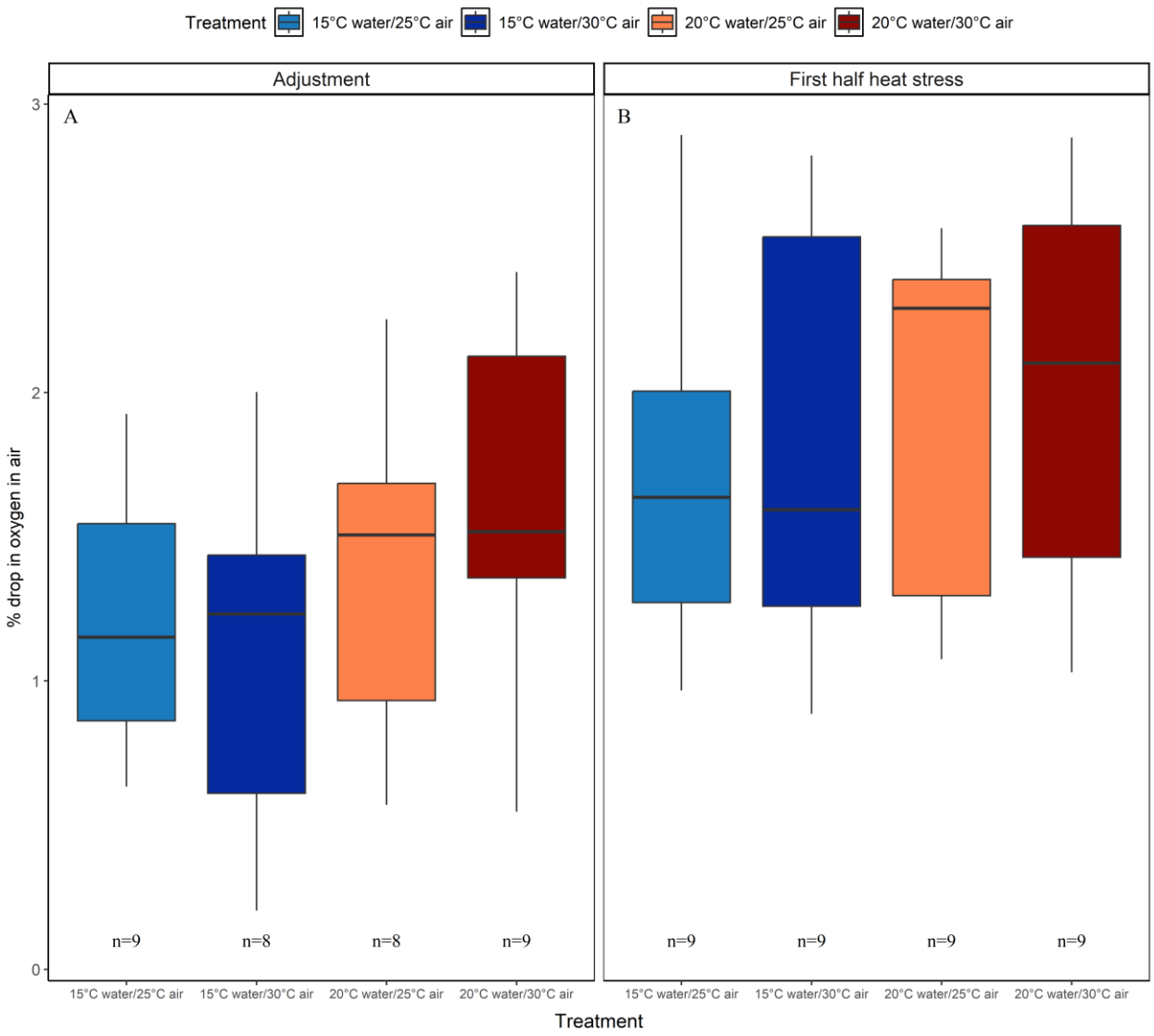

Fig. S3 The percent drop in oxygen by juvenile *Pisaster ochraceus* over 2-hours of aerial exposure in Experiment 2 (May 2024). Treatment (colour) corresponds to the assigned temperature treatments crossing different water (15 and 20°C) and air (25 and 30°C) temperature exposures (respectively, water/air temperatures in °C: 15/25, 15/30, 20/25, 25/30). Two measurements were excluded from analyses as the sea stars were on top of the oxygen probes and a proper reading could not be obtained. **(A)** Adjustment period, days 1-10; cycled between ~15°C seawater (18-hours) and ~20°C air (6-hours). **(B)** first half of the heat stress period, days 11-20; cycled between ~15°C or 20°C seawater (18-hours) and ~25°C or 30°C air (6-hours).

2.2.5 Metabolic kit set-up

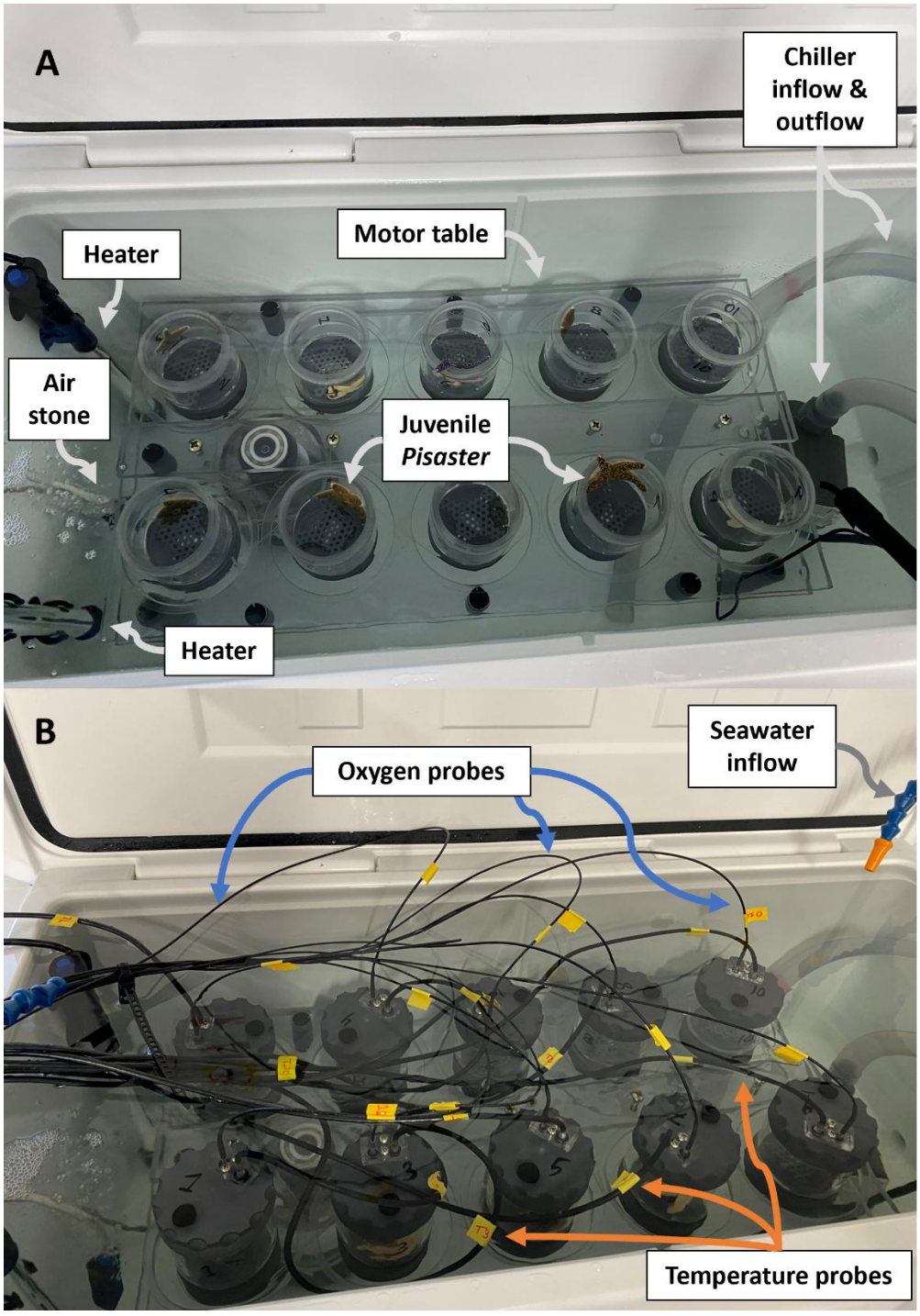

Fig. S4 Set up of the metabolic kit **(A)** prior to and **(B)** during measurements of oxygen consumption. Juvenile *Pisaster ochraceus* were placed in individuals chambers on the motor table during measurements. To begin a measurement, the lids of the chambers were sealed and oxygen (blue lines) and temperature (orange lines) probes were placed inside each chamber. There were nine chambers total each with an oxygen and temperature probe.

2.2.6 Body surface temperatures (submerged and emersed)

Table S6. Body surface temperatures of juvenile *Pisaster ochraceus* (n = 72) measured using an infrared camera during Experiment 2 (May 2024).

Treatment	Trial period	Measurement type	Body surface temperature (°C)	Sea table temperature (°C)	Incubator temperature (°C)
15°C water and 25°C air	Heat stress	Submerged	15.5 ± 0.7	15.0	NA
15°C water and 30°C air	Heat stress	Submerged	14.4 ± 0.4	15.0	NA
20°C water and 25°C air	Heat stress	Submerged	19.5 ± 0.6	19.2	NA
20°C water and 30°C air	Heat stress	Submerged	19.8 ± 0.8	19.2	NA
15°C water and 25°C air	Heat stress	Emersed	22.5 ± 0.7	NA	24.4
15°C water and 30°C air	Heat stress	Emersed	26.7 ± 0.8	NA	28.9
20°C water and 25°C air	Heat stress	Emersed	22.3 ± 0.8	NA	24.4
20°C water and 30°C air	Heat stress	Emersed	26.5 ± 0.6	NA	28.9
15°C water and 25°C air	Recovery	Submerged	15.4 ± 0.7	14.7	NA
15°C water and 30°C air	Recovery	Submerged	14.8 ± 0.8	14.7	NA
20°C water and 25°C air	Recovery	Submerged	14.4 ± 0.9	14.7	NA
20°C water and 30°C air	Recovery	Submerged	14.4 ± 0.5	14.7	NA
15°C water and 25°C air	Recovery	Emersed	19.3 ± 0.8	NA	20.0
15°C water and 30°C air	Recovery	Emersed	19.2 ± 0.4	NA	20.0
20°C water and 25°C air	Recovery	Emersed	18.9 ± 0.3	NA	20.0
20°C water and 30°C air	Recovery	Emersed	19.0 ± 0.6	NA	20.0

Treatment corresponds to the assigned temperature treatments crossing different water (15 and 20°C) and air (25 and 30°C) temperature exposures (respectively, water/air temperatures in °C: 15/25, 15/30, 20/25, 25/30). Trial period refers to either the heat stress or recovery period of the experiment. Measurement type corresponds to the type of body surface temperature measurement with “submerged” measurements taken immediately after an 18-hour submersion in seawater and “emersed” measurements taken immediately after a 6-hour emersion in air.

Appendix 2: Supplementary Materials for Chapter 3

Lydia N. Walton, Valesca de Groot, and Amanda E. Bates

Table S1. Results of a generalized linear mixed model testing the relationship between body surface temperature and body size of *Pisaster* at eight different sites on Vancouver Island (British Columbia, Canada).

Model: Body surface temperature (°C) ~ Arm length (scaled)*Location + (1 | Site)				
Model family: Gaussian		**AIC:** 2962.5		
Predictors		*Estimate*	*CI*	*p-value*
(Intercept)		16.92	15.28 – 18.55	***
Arm length		0.19	-0.9 – 0.48	0.188
Location [Sidney]		0.20	-2.13 – 2.52	0.869
Arm length*Location[Sidney]		-0.28	-1.12 – 0.55	0.504
Random Effects				
σ^2	3.02			
$\tau_{00\ site}$	2.76			
ICC	0.48			
N_{site}	8			
Observations	740			
Marginal R^2/ Conditional R^2	0.003/0.479			

Body surface temperature: temperature of the central aboral disc in °C; Arm length (scaled): standardized arm length measured from the centre of the aboral disc to the tip of the longest/most visible arm; Location: Bamfield or Sidney; Site: eight survey sites (four in Bamfield and four in Sidney) included as a random effect.

Table S2. Results of a generalized linear mixed model testing the relationship between body surface temperature and aggregating behaviour of *Pisaster* at eight different sites on Vancouver Island (British Columbia, Canada).

Model: Body surface temperature (°C) ~ Aggregated*Location + (1 | Site)				
Model family: Gaussian		**AIC:** 2954.8		
Predictors		*Estimate*	*CI*	*p-value*
(Intercept)		16.91	15.15 – 18.67	***
Aggregated [solitary]		0.05	-0.25 – 0.34	0.762
Location [Sidney]		-0.16	-2.68 – 2.35	0.898
Aggregated[solitary]*Location[Sidney]		0.95	0.25 – 1.65	**
Random Effects				
σ^2	2.98			
$\tau_{00\ site}$	3.18			
ICC	0.52			
N_{site}	8			
Observations	740			
Marginal R^2/ Conditional R^2	0.007/0.520			

Body surface temperature: temperature of the central aboral disc in °C; Aggregated: *Pisaster* classified as "aggregated" if touching at least one other conspecific or "solitary" if not; Location: Bamfield or Sidney; Site: eight survey sites (four in Bamfield and four in Sidney) included as a random effect.

Table S3. Results of a generalized linear mixed model testing the relationship between *Pisaster* body surface temperature and transect (low tide line or high tide line) at eight different sites on Vancouver Island (British Columbia, Canada).

Model: Body surface temperature (°C) ~ Transect*Site + (1 | Location)				
Model family: Gaussian		**AIC:**1904		
Predictors		*Estimate*	*CI*	*p-value*
(Intercept)		16.09	15.77 – 16.42	***
Transect [Low tide line]		-1.37	-1.82 – -0.93	***
Site [Brady's Beach]		0.84	0.37 – 1.31	***
Site [Chalet Beach]		-0.13	-1.04 – 0.79	0.783
Site [Eagle Bay]		2.23	1.62 – 2.84	***
Site [Glass Beach]		-3.49	-5.08 – -1.90	***
Site [Grappler Narrows]		3.10	2.52 – 3.67	***
Site [Moses Point]		4.01	3.19 – 4.83	***
Site [Seabreeze Road]		1.64	0.33 – 2.95	*
Transect [Low tide line]*Site [Brady's Beach]		-0.11	-0.77 – 0.55	0.744
Transect [Low tide line]*Site [Chalet Beach]		3.82	2.44 – 5.20	***
Transect [Low tide line]*Site [Eagle Bay]		0.66	-0.10 – 1.42	0.087
Transect[Low tide line]*Site [Glass Beach]		3.22	1.30 – 5.14	***
Transect [Low tide line]*Site [Grappler Narrows]		-0.45	-1.27 – 0.37	0.280
Transect [Low tide line]*Site [Moses Point]		0.84	-0.14 – 1.82	0.093
Transect [Low tide line]*Site [Seabreeze Road]		1.11	-0.28 – 2.51	0.118
Random Effects				
σ^2	2.52			
$\tau_{00\ locality}$	0.00			
$N_{locality}$	2			
Observations	738			
Marginal R^2/ Conditional R^2	0.491/NA			

Body surface temperature: temperature of the central aboral disc in °C; Aggregated: *Pisaster* classified as "aggregated" if touching at least one other conspecific or "solitary" if not; Air temperature: air temperature measured at the start of each transect in °C; Humidity: humidity measured at the start of each transect in %; SST: sea surface temperature measured at the start of each transect in °C; Substrate temperature: the average temperature in °C across a ~3cm line measurement placed on the substrate directly underneath each *Pisaster*; Microhabitat: the type of microhabitat each *Pisaster* was found in, classified during thermal image processing. Random effects were Site: eight survey sites (four in Bamfield and four in Sidney) and Location: Bamfield or Sidney.

Table S4. Results of a generalized linear mixed model testing the relationship between *Pisaster* body surface temperature and several predictors at eight different sites on Vancouver Island (British Columbia, Canada).

Model: Body surface temperature (°C) ~ Aggregated + Air temperature (°C) + Humidity (%) + SST (°C) + Substrate temperature (°C) + Average wind speed (km/h) + Microhabitat type + (1 | Site)				
Model family: Gaussian		**AIC:**1904		
Predictors		*Estimate*	*CI*	*p-value*
(Intercept)		14.75	10.50 – 19.00	***
Aggregated [solitary]		0.23	0.10 – 0.37	***
Air temperature (°C)		0.26	0.17 – 0.36	***
Humidity (%)		0.05	0.02 – 0.08	***
SST (°C)		-0.38	-0.63 – -0.12	**
Substrate temperature (°C) (scaled and centred)		3.28	3.12 – 3.44	***
Average wind speed (km/h)		0.10	-0.02 – 0.23	0.111
Microhabitat [partly exposed]		-1.02	-1.40 – -0.65	***
Microhabitat [shaded]		-1.11	-1.38 – -0.84	***
Microhabitat [tidepool]		-1.04	-1.56 – -0.51	***
Microhabitat [under rock]		-1.34	-1.58 – -1.10	***
Random Effects				
σ^2	0.71			
$\tau_{00\ site}$	0.57			
N_{site}	8			
ICC	0.44			
Observations	738			
Marginal R^2/ Conditional R^2	0.715/0.841			

Body surface temperature: temperature of the central aboral disc in °C; Aggregated: *Pisaster* classified as "aggregated" if touching at least one other conspecific or "solitary" if not; Air temperature: air temperature measured at the start of each transect in °C; Humidity: humidity measured at the start of each transect in %; SST: sea surface temperature measured at the start of each transect in °C; Substrate temperature: the average temperature in °C across a ~3cm line measurement placed on the substrate directly underneath each *Pisaster*; Average wind speed: the average daily wind speed recorded by the Bamfield Marine Sciences weather station (for sites in Bamfield) and the Victoria International Airport weather station (for sites in Sidney) on the day of each survey in km/h; Microhabitat: the type of microhabitat each *Pisaster* was found in, classified during thermal image processing. Site was included as a random effect.

Appendix 3: Effects of food availability and air temperature on the aquatic oxygen consumption of juvenile *Pisaster ochraceus*

Lydia N. Walton, Viola R. Watts, Jasmin M. Schuster, and Amanda E. Bates

Background and objectives

Environmental temperatures and food consumption are major drivers of metabolic rate in ectotherms. Metabolism varies predictably with temperature, increasing from a critical lower thermal limit up to a thermal optimum before dropping towards a critical upper thermal limit (Gillooly *et al.*, 2001; Brown *et al.*, 2004; Dell *et al.*, 2011; Rebolledo *et al.*, 2021). Additionally, metabolic rates increase following food consumption to facilitate the digestion, absorption and assimilation of nutrients, known as specific dynamic action (SDA; Brody, 1945; Secor, 2001). At higher temperatures, these processes are accelerated, enhancing metabolic efficiency (Plasman *et al.*, 2019).

In this experiment we investigated the combined effects of warming air and seawater temperatures on the aquatic metabolic rate (estimated through measurements of aquatic oxygen consumption) of juvenile *Pisaster* when fed mussels *ad libidum* and when fasted. We predicted that *Pisaster* metabolic rates would increase with rising temperatures and mussel consumption. As fasted organisms are expected to be more susceptible to thermal stress (Dahlhoff *et al.*, 2001), we also predicted high levels of mortality in fasted Pisaster experiencing warmer air temperatures (~30°C).

Materials and methods

Collections and experimental design

Juvenile *Pisaster* were haphazardly hand-collected in early August 2023 from Eagle Bay, Bamfield and transported by boat (in water-filled buckets) to the Bamfield Marine Sciences Centre (BMSC) in Bamfield, British Columbia. All *Pisaster* had a wet mass between 1 g and 18 g (mean ± SD = 6.39 ± 4.33 g, n = 56) and were classified as juveniles based on size (Mauzey, 1966; Menge and Menge, 1974; Robles, 2013). Animals were randomly assigned to one of four treatments (n = 14 per treatment) crossing different food (+ mussels and - mussels) and air (25°C and 30°C) temperature exposures (respectively, food/air temperatures: +mussels/25°C, +mussels/30°C, -mussels/25°C, -mussels/30°C).

Water temperature was held constant at 20°C across all four treatments. *Pisaster* in the +mussels treatments were provided mussels *ad libidum* throughout the experiment while individuals in the -mussels treatments were given no access to food (*i.e.*, fasted). Mussels (*Mytilus* spp.) were collected from docks and pilings within the Bamfield Inlet and had shell lengths ranging from 6.2 mm to 32.3 mm (mean ± SD = 15.0 ± 5.65 mm, n = 96) and shell widths ranging from 3.8 mm to 18.8 mm (mean ± SD = 8.6 ± 3.25 mm, n = 96). This experiment consisted of two parts: **(1)** a 16-day period during which individuals acclimated to food/air treatments and **(2)** an experimental estimation of metabolic rates for all surviving *Pisaster* using a closed respirometry system.

Acclimating to food and air treatments

A set of four sea tables and two temperature-controlled incubators (as described in **Chapter 2**) were used during the acclimation period of the experiment, with sea tables heated to 20°C and incubators heated to 25°C or 30°C. Temperature probes (INKBIRD IBS-TH2 Plus) remained in each sea table and incubator for the duration of the experiment with temperatures recorded daily (**Table 1**). Following collection, *Pisaster* were assigned to individual holding containers and submerged in the heated sea tables for 24 h to recover from handling stress. Animals were then alternated between sea tables and incubators in a simulated tidal cycle (as described in **Chapter 2**) that was repeated for 16 consecutive days. Empty mussel shells were counted every 24 h to determine if there were any differences in feeding activity between the air treatments. To mitigate sea table effects, *Pisaster* holding containers were swapped systematically between sea tables corresponding to the same feeding treatment. Following the acclimation period, *Pisaster* remained submerged in heated sea tables until metabolic testing began.

Pre-measurement procedures

A custom-built experimental system was used to measure the oxygen consumption ($\dot{M}O_2$) of individual *Pisaster* after the acclimation period was completed (see **Chapter 2** for detailed description). A maximum of nine individuals could be assayed per day (due to space constraints of the respirometry system), thus measurements of $\dot{M}O_2$ for all surviving individuals (n = 18) were staggered over two assay days. On the evening before the assay, the mass and volume of each individual was measured by

displacement [volumetric displacement = volume of seawater with *Pisaster* - volume without *Pisaster*]. Animals were randomly drawn from all treatments and distributed individually into each of the nine chambers, while the tenth chamber remained empty to account for background respiration (*i.e.*, due to microorganisms). The chambers were covered with mesh-fabric to prevent escape and placed into a holding tank overnight. The holding tank was supplied with filtered (10 μm) flow-through seawater at the treatment temperature (~20°C). Oxygen consumption measurements were started the subsequent morning.

Oxygen consumption measurements

Oxygen consumption was measured for all *Pisaster* at the treatment water temperature (~20°C). The insulated cooler was filled with fresh, filtered (10 μm) seawater and maintained at the treatment temperature for each run. To initiate a measurement run, the lids to each chamber (9 *Pisaster*, one blank) were sealed. Oxygen consumption ($\dot{M}O_2$ in % air saturation) was recorded until oxygen levels dropped by 5 to 10%. The total measurement time varied from 30 min to approximately 1.5 h, with longer measurement times for *Pisaster* with lower masses of metabolically active tissue. Once the measurements were completed for each of the 10 chambers, all *Pisaster* included in the measurement run were removed from their chambers and immediately frozen prior to ash-free dry mass (AFDM) determination. The chambers were emptied and cleaned. The same evening, nine fresh organisms were placed into the chambers (after having their mass and volume measured) and placed into the overnight holding tank, repeating the same measurement procedure as before. The seawater tank was emptied, rinsed with warm freshwater, and refilled with fresh seawater to prepare for the next assay day.

Ash-free dry mass (AFDM)

Pisaster AFDM was determined to quantify the amount of organic tissue, or metabolically active tissue, of each ochre star. Empty aluminum weigh boats were placed in a muffle furnace (500°C) for 12 h to remove any organic matter and stored in a sealed container. Animals frozen at the end of the metabolic testing were thawed and placed on pre-weighed (to 0.01 g accuracy) weigh boats prior to drying. *Pisaster* were dried in a combustion oven (60°C) for 12 – 24 h until their dry mass had stabilized and then ashed in a muffle furnace (500°C) for 24 – 48 h. AFDM (*i.e.*, metabolically active tissue) was calculated as the dry

mass (including the weigh boat) minus the ashed mass (including the weigh boat) while individual dry mass (*i.e.*, organic and inorganic mass) was calculated as the dry mass minus the weight of the empty weigh boat. The inorganic mass, primarily representing the ochre star's calcified endoskeleton, was calculated as the ashed mass minus the weight of the empty weigh boat.

Data processing and statistical analyses

Absolute and mass-specific $\dot{M}O_2$ were calculated for each individual *Pisaster* using the "respR" package in R (Carey and Harianto, 2023). All $\dot{M}O_2$ measurements were adjusted for salinity and water volume in the chamber by correcting for each individual's volumetric displacement. The $\dot{M}O_2$ values in the blank chamber of each run (< 0.1 mL O_2/h) were used to correct for background respiration in the absolute and mass-specific $\dot{M}O_2$ values. Mass-specific values were adjusted for both wet mass and AFDM (*i.e.*, absolute $\dot{M}O_2$ divided by mass). The $\dot{M}O_2$ data was visually inspected to ensure that a linear decrease in water % air saturation of 5-10% occurred and a minimum r^2 of 0.98 was set to identify nonlinear measurements (Schuster *et al.*, 2022). One measurement was discarded as it represented an extreme outlier in the data (n = 1/18; $\dot{M}O_2$ value 8x greater than all other values).

Results

Pisaster mortality

No significant differences in *Pisaster* mortality were found between treatments, with all treatments exhibiting some level of mortality (**Fig. 1;** Cox proportional-hazards model, $p = 0.2$). There was a trend towards higher mortality in fasted *Pisaster* compared to *Pisaster* that were fed *ad libidum* (**Fig. 1;** +mussels/25°C = 6 individuals died, +mussels/30°C air = 11 individuals died, -mussels/25°C = 9 individuals died, -mussels/30°C = 12 individuals died).

Pisaster feeding activity

There was no significant difference in *Pisaster* feeding activity (*i.e.*, the total number of mussels consumed by each juvenile ochre star) found between treatments where mussels were provided *ad libitum* (**Fig. 2b;** t-test, $p = 0.059$). Even so, *Pisaster* in the +mussels/30°C air treatment did consume fewer mussels than those in the +mussels/25°C air treatment **(Fig. 2a, b)**. Lack of statistical power is expected

as only 8 (of 14) individuals survived the +mussels/25°C air treatment and only 3 (of 14) individuals survived in the +mussels/30°C air treatment. Overall, *Pisaster* that consumed mussels during the experiment tended to have a lower probability of mortality compared with individuals that were fasted (**Fig. 3**).

Pisaster metabolic rate

In general, *Pisaster* did not differ in body mass or oxygen consumption between treatments. There was no difference found in wet mass (WM), ash-free dry mass (AFDM), or ADFM:WM ratio between treatments at any point of the experiment (ANOVA, $p > 0.05$). The $\dot{M}O_2$ per g of wet mass was significantly higher for *Pisaster* with access to mussels than for *Pisaster* that were fasted (Two-factor ANOVA, $p = 0.02$), with no differences found in $\dot{M}O_2$ between air treatments (**Fig. 4a)**. There were no significant differences detected in absolute $\dot{M}O_2$ or $\dot{M}O_2$ per g of AFDM between treatments (**Fig. 4b, c**).

Conclusions

Here we find that elevated aerial temperatures combined with reduced food availability led to lower metabolic rates and increased mortality in juvenile *Pisaster*. These findings highlight the vulnerability of juvenile *Pisaster* to food scarcity, especially under climate warming. The widespread mortality of mussels (*Mytilus* spp.) as a result of extreme heat events (Tsuchiya, 1983; Harley, 2008) further emphasizes the potential impacts of rising aerial temperatures on *Pisaster* populations. Understanding the interactions between multiple stressors and their effect on various species is crucial for predicting broader shifts in community structure and ecosystem functioning.

References

Brody, S. 1945. Bioenergetics and Growth.

Brown, J., J. Gillooly, A. Allen, V. m Savage and G. West. **2004**. Toward a Metabolic Theory of Ecology. *Ecology* **85**: 1771–1789.

Carey, N. and J. Harianto. **2023**. respR: Import, Process, Analyse, and Calculate Rates from Respirometry Data.

Dahlhoff, E. P., B. A. Buckley and B. A. Menge. **2001**. Physiology of the Rocky Intertidal Predator Nucella ostrina along an Environmental Stress Gradient. *Ecology* **82**: 2816–2829. Ecological Society of America.

Dell, A. I., S. Pawar and V. M. Savage. **2011**. Systematic variation in the temperature dependence of physiological and ecological traits. *Proceedings of the National Academy of Sciences* **108**: 10591–10596. Proceedings of the National Academy of Sciences.

Gillooly, J. F., J. H. Brown, G. B. West, V. M. Savage and E. L. Charnov. **2001**. Effects of size and temperature on metabolic rate. *Science* **293**: 2248–2251.

Harley, C. D. G. 2008. Tidal dynamics, topographic orientation, and temperature-mediated mass mortalities on rocky shores. *Marine Ecology Progress Series* **371**: 37–46.

Mauzey, K. P. 1966. Feeding Behavior and Reproductive Cycles in Pisaster ochraceus. *Biological Bulletin* **131**: 127–144. Marine Biological Laboratory.

Menge, J. L. and B. A. Menge. **1974**. Role of Resource Allocation, Aggression and Spatial Heterogeneity in Coexistence of Two Competing Intertidal Starfish. *Ecological Monographs* **44**: 189–209.

Plasman, M., M. D. McCue, V. H. Reynoso, J. S. Terblanche and S. Clusella-Trullas. **2019**. Environmental temperature alters the overall digestive energetics and differentially affects dietary protein and lipid use in a lizard. *Journal of Experimental Biology* **222**: jeb194480.

Rebolledo, A. P., C. M. Sgrò and K. Monro. **2021**. Thermal Performance Curves Are Shaped by Prior Thermal Environment in Early Life. *Frontiers in Physiology* **12**.

Robles, C. 2013. Pisaster ochraceus. In: *Starfish: Biology and Ecology of the Asteroidea*.

Secor, S. M. 2001. Regulation of digestive performance: a proposed adaptive response. *Comp Biochem Physiol A Mol Integr Physiol* **128**: 565–577.

Tsuchiya, M. 1983. Mass mortality in a population of the mussel *Mytilus edulis* L. Caused by high temperature on rocky shores. *Journal of Experimental Marine Biology and Ecology* **66**: 101–111.

Figures and Tables

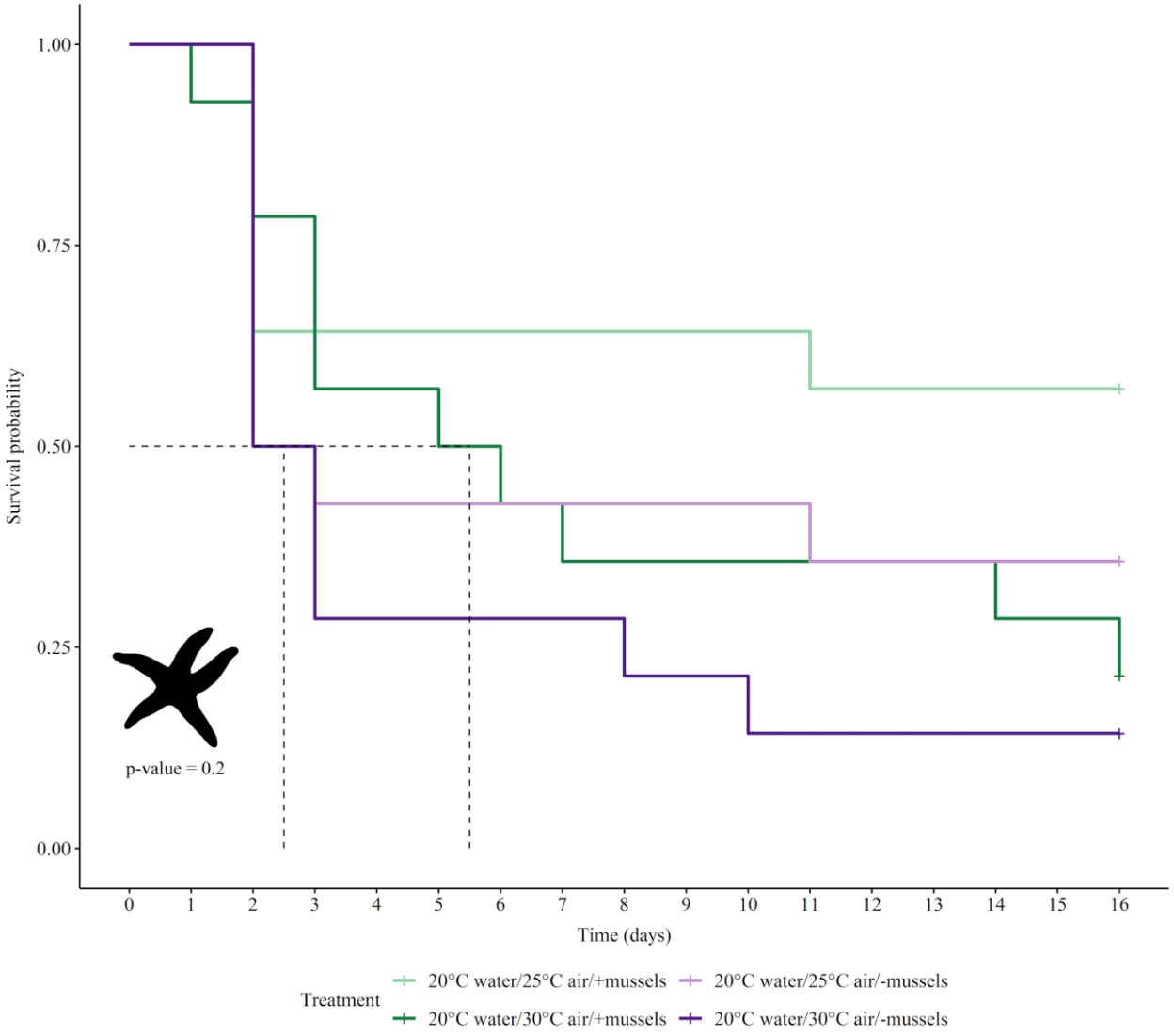

Fig. 1 Kaplan-Meier survival curves for juvenile *Pisaster ochraceus* (n = 56). *Pisaster* were separated into four treatments (+mussels/25°C air, +mussels/30°C air, -mussels/25°C air, -mussels/30°C air). Individuals in the "+ mussels" treatments were fed mussels *ad libidum* for the duration of the experiment while individuals in the "- mussels" treatments were given no food (*i.e.*, fasted). *Pisaster* alternated between sea tables (20°C fixed water temperature) and incubators (25°C or 30°C air temperature) in a simulated high-tide (submerged for 18 hours) and low-tide (emersed for 6 hours) cycle. Dotted lines represent the median survival probability for each temperature treatment. No significant difference in *Pisaster* survival probability was found between treatments (Cox proportional-hazards model; p = 0.2).

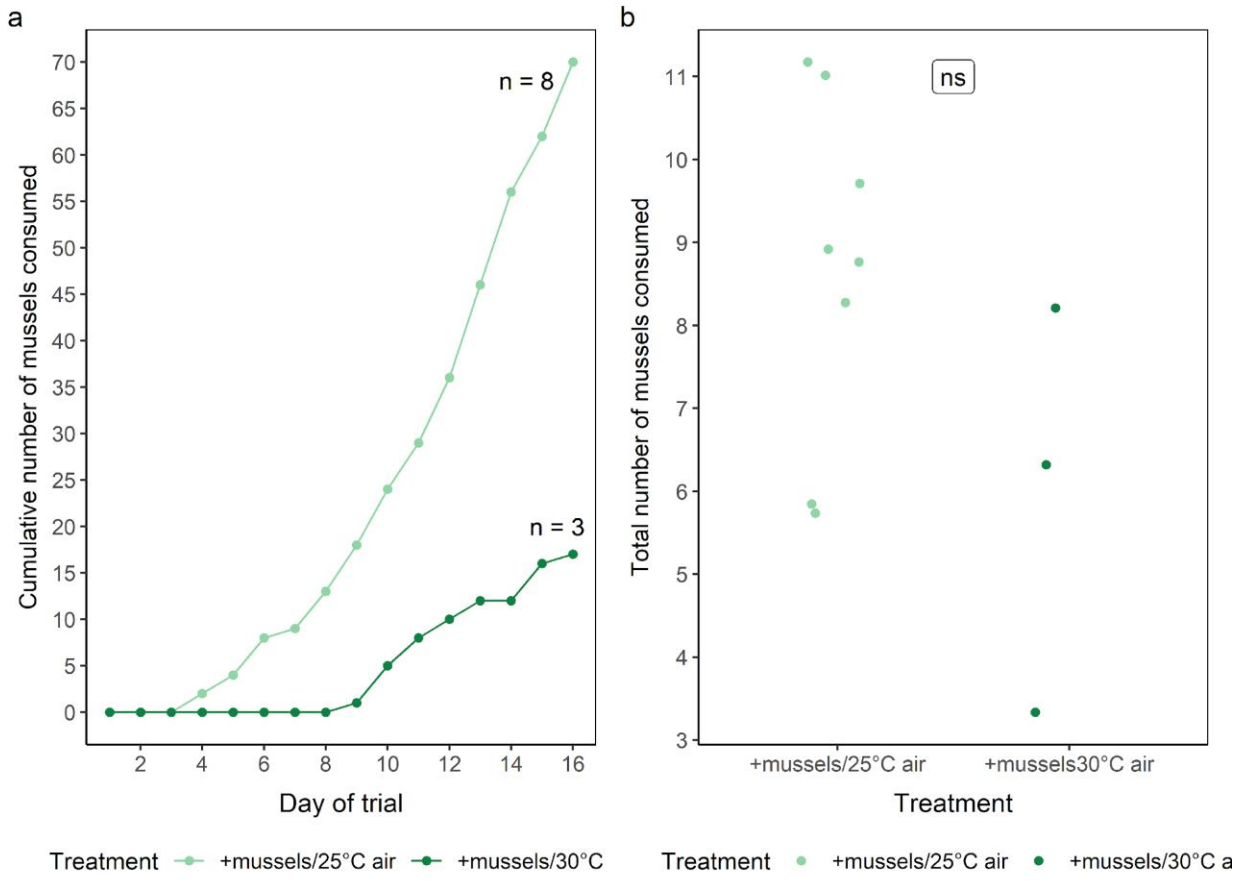

Fig. 2 Feeding activity of *Pisaster ochraceus* (n = 11) during the metabolic rate experiment conducted in August 2023. **(a)** Cumulative consumption of *Mytilus* spp. by *Pisaster* in "+ mussels" treatments (+mussels/25°C air, +mussels/30°C air) on each day of the experiment. **(b)** Total consumption of *Mytilus* spp. by *Pisaster* in "+mussels" treatments. Points represent the total number of mussels consumed by each individual over the course of the entire experiment (16 days total). There was no significant difference in mussel consumption found between treatments (t-test, $p = 0.059$).

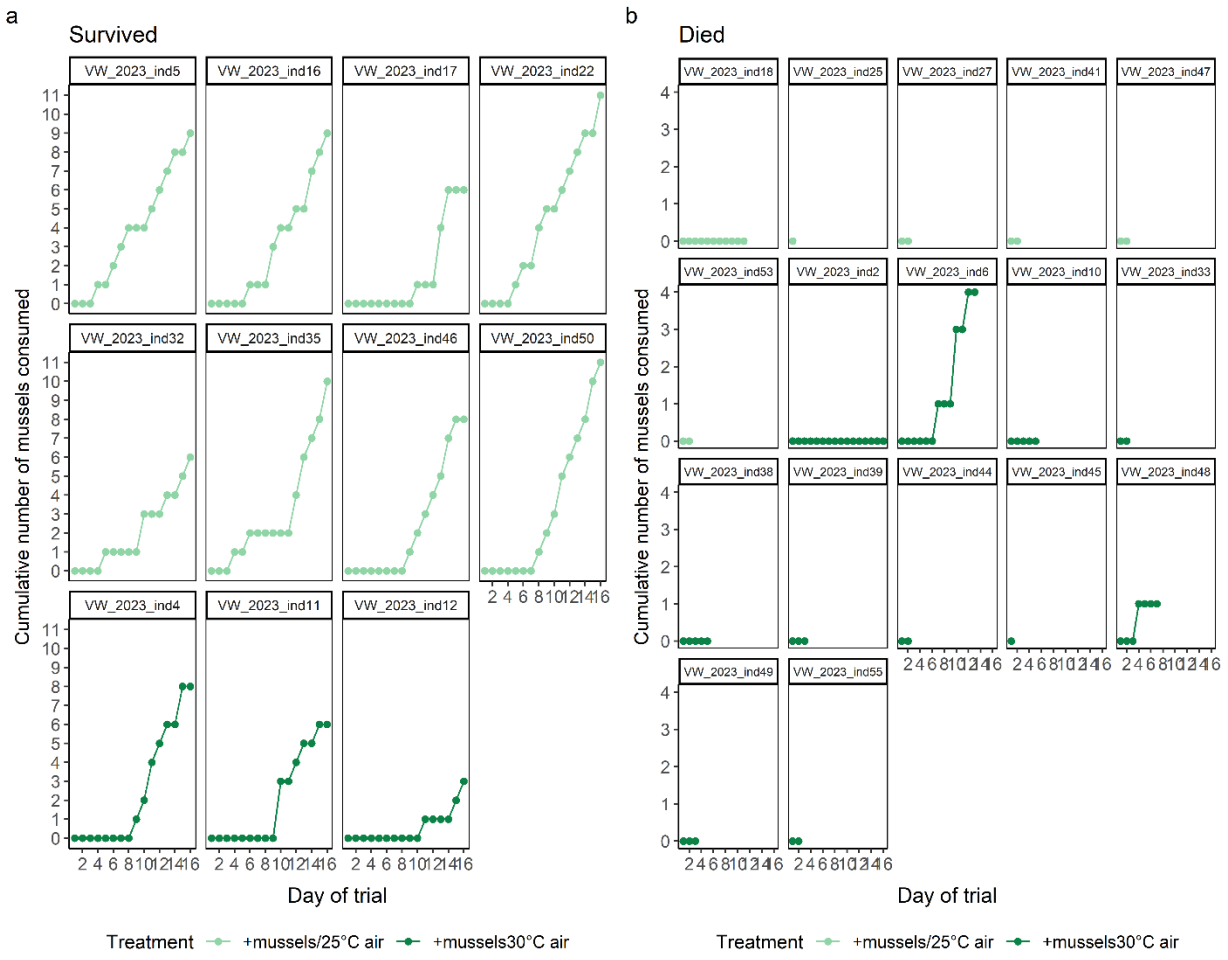

Fig. 3 The cumulative consumption of *Mytilus* spp. by juvenile *Pisaster ochraceus* in "+ mussels" treatments (+mussels/25°C air, +mussels/30°C air) of the metabolic rate experiment conducted in August 2023. **(a)** Cumulative consumption of mussels by *Pisaster* that survived until the end of the experiment. **(b)** Cumulative consumption of mussels by *Pisaster* that died before the end of the experiment

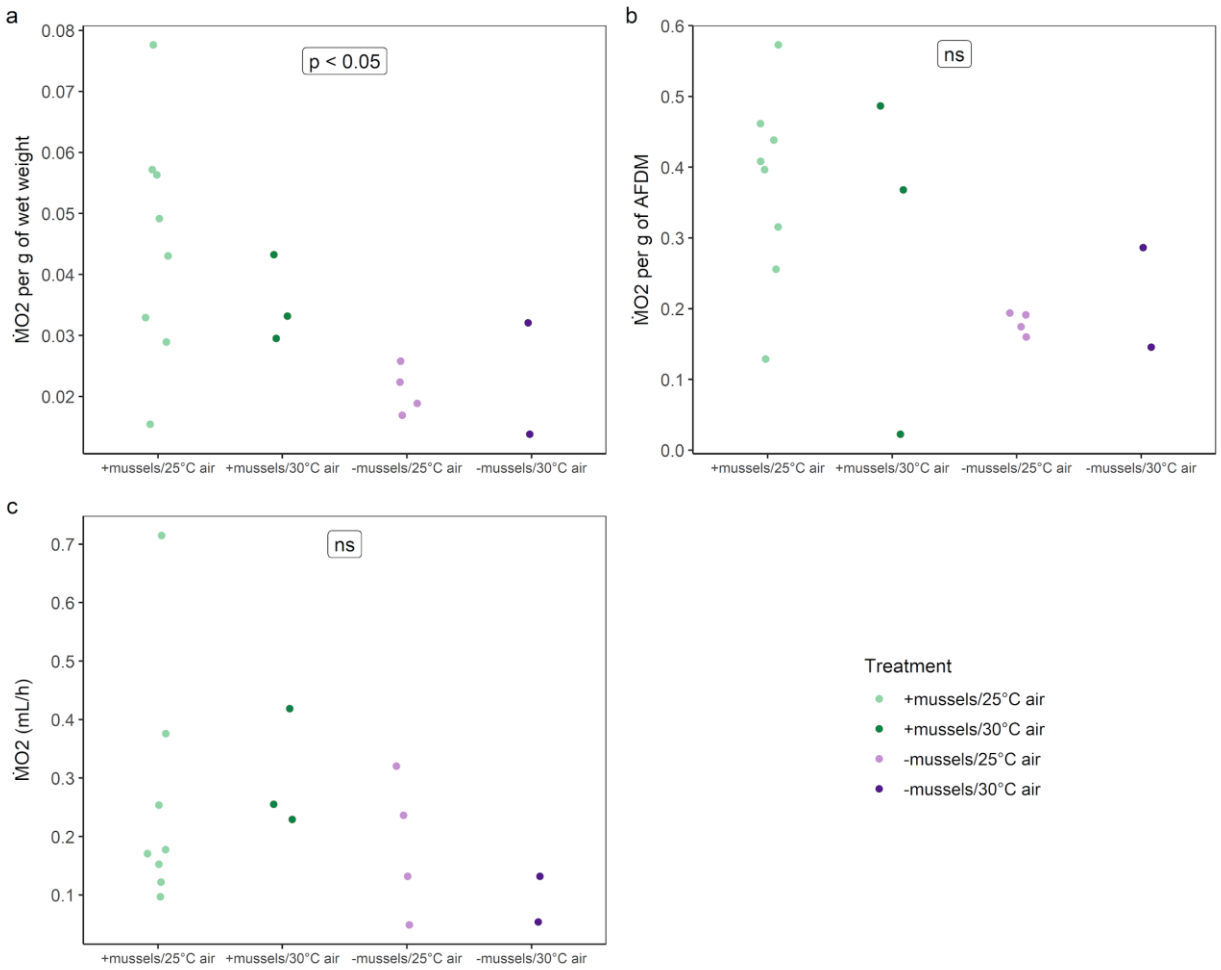

Fig. 4 The metabolic rates of juvenile *Pisaster ochraceus* that survived the metabolic rate experiment conducted in August 2023. *Pisaster* were assigned to four different treatments: 25°C air/+mussels, 30°C air/+mussels, 25°C air/-mussels, 30°C air/-mussels. **(a)** $\dot{M}O_2$ per g of wet mass. There was a significant difference in $\dot{M}O_2$ between the "+mussels" and "-mussels" treatments but not between air treatments (ANOVA, $p = 0.02$); **(b)** $\dot{M}O_2$ per g of ash-free dry mass (AFDM). No significant difference was found between treatments (Kruskall-Wallace test, $p = 0.41$); **(c)** Absolute $\dot{M}O_2$. No significant difference was found between treatments (Kruskall-Wallace test, $p = 0.25$)

Appendix 4: The relationship between juvenile *Pisaster ochraceus* body size, body surface temperature, and metabolic rate in air and seawater

Lydia N. Walton and Amanda E. Bates

Background and objectives

The body temperature of ectotherms is influenced by thermal inertia, which describes the time needed for an organism to return to its equilibrium body temperature following a change in environmental temperatures (Monteith and Unsworth, 2008). Larger organisms tend to have a higher thermal inertia and are better able to buffer rapid environmental changes than smaller organisms (Helmuth, 1998). Some ectotherms (*e.g.*, reptiles, marine invertebrates) can also modulate their thermal inertia in response to unfavourable conditions (Bakken and Gates, 1975; Seebacher and Franklin, 2005; Pincebourde *et al.*, 2009). Following exposure to high aerial temperatures, the sea star *Pisaster ochraceus* can increase the amount of cool fluid in its coelomic cavity when resubmerged in seawater, reducing its body temperature during the next aerial exposure at low tide (Pincebourde *et al.*, 2009).

Metabolic rates increase positively with both body temperature and body size (Brown *et al.*, 2004). Thus, smaller organisms may be more sensitive to extreme temperatures than larger organisms as body temperatures approach critical thermal limits more rapidly. The effect of adult *Pisaster* body temperature on metabolic rate has been measured previously (Fly *et al.*, 2012; McGaw *et al.*, 2015), however, impacts on the oxygen consumption of smaller, juvenile *Pisaster* has yet to be investigated.

The objectives of this experiment were to: (1) determine how much oxygen is consumed by juvenile *Pisaster* during a 6-hour aerial emersion, (2) investigate the relationship between juvenile *Pisaster* body size and oxygen consumption (when animals are submerged during high tide and emersed at low tide), and (3) investigate the relationship between juvenile *Pisaster* body size and body surface temperature immediately following submersion in seawater (~15°C) and emersion in air (~20°C and 30°C). We predicted that aerial oxygen consumption would be significantly lower than aquatic oxygen consumption as *Pisaster* have less surface area for respiration during emersion (tube feet retract and dermal papulae become limp; Murphy and Jones, 1987; Fly *et al.*, 2012). We also predicted that larger

individuals would have higher metabolic rates in both air and water (Brown *et al.*, 2004). Given that larger *Pisaster* are expected to have greater thermal inertia, we predicted that body surface temperatures would be lower in animals with higher mass under extreme aerial temperatures (~30°C), but remain consistent across different sizes at temperatures within their critical thermal limits (~15°C water and ~20°C air).

Materials and methods

The experiment was completed in two parts: (1) measuring the oxygen consumption of juvenile *Pisaster* in air and in seawater and (2) estimating the body surface temperatures of juvenile *Pisaster* after submersion in ~15°C seawater and aerial emersion in ~20°C air and ~30 air.

Collections and experimental design

Juvenile *Pisaster ochraceus* (hereafter *Pisaster*) were haphazardly hand-collected in late June 2024 from Eagle Bay, Bamfield and immediately transported by boat (in water-filled buckets) to the Bamfield Marine Sciences Centre (BMSC) in Bamfield, British Columbia. All *Pisaster* had a wet mass between 23 g and 56 g (mean ± SD = 38.72 ± 10.73 g, n = 9) and were classified as juveniles based on size (Mauzey, 1966; Menge and Menge, 1974; Robles, 2013). At BMSC, *Pisaster* were placed in individual holding containers (750 mL) and housed in a flow-through seawater table (holding tank) heated to ~15°C using 200 W aquarium heaters (AEH3617090 Jager aquarium thermostat heater, Eheim). *Pisaster* were not fed at any point during the experiment.

Experimental assay system for measuring oxygen consumption in air and seawater

A custom-built experimental system was used to measure the oxygen consumption ($\dot{M}O_2$) of individual *Pisaster* (described in detail in **Chapter 2**). This system consisted of a table with 10 removable acrylic chambers (650 mL) with magnetic stir plates, placed inside a temperature -insulated seawater tank (for aquatic measurements) or a temperature-controlled incubator (for aerial measurements).

Pre-measurement procedures

The mass and volume of each animal was measured by displacement [volumetric displacement = volume of seawater with animal - volume without animal] on the evening before the assay. Animals were

randomly distributed into each of the nine chambers, while the tenth chamber remained empty to account for background respiration (*i.e.*, due to microorganisms). The chambers were covered with mesh-fabric to prevent escape and placed into a holding tank overnight. The holding tank was supplied with filtered (10 µm) flow-through seawater at ~15°C. Oxygen consumption measurements were started the subsequent morning.

Oxygen consumption measurements

Oxygen consumption was measured for all *Pisaster* in seawater (~15°C) and in air (~20°C). The insulated cooler was filled with fresh, filtered (10 µm) seawater and maintained at ~15°C for aquatic measurements of $\dot{M}O_2$. To initiate a measurement run, the lids to each chamber (9 *Pisaster*, one blank) were sealed. Oxygen consumption ($\dot{M}O_2$ in % air saturation) was recorded until oxygen levels dropped by 5 to 10%. The total measurement time varied from 30 min to approximately 60 min, with longer measurement times for *Pisaster* with lower masses of metabolically active tissue. Once the measurements were completed for each of the 10 chambers, the chambers were drained of seawater (with the animals inside) and all chambers (9 Pisaster, one blank) were moved into a temperature-controlled incubator maintained at ~20°C for measurements of $\dot{M}O_2$ in air. Aerial oxygen consumption was recorded for ~6 hr as *Pisaster* in our study area are typically exposed to aerial conditions only during the lowest daily tide (lasting approximately 6 hr).

Calculating aerial and aquatic oxygen consumption

Aerial oxygen consumption was calculated by subtracting the O_2 value recorded at minute 366 from the O_2 value recorded at minute 20 (starting at minute 20 accounted for the stabilization of oxygen in the chambers once the lids were sealed). For aquatic measurements, the absolute $\dot{M}O_2$ was calculated for each individual *Pisaster* using the "respR" package in R (Carey and Harianto, 2023). The $\dot{M}O_2$ values in the blank chamber of each run (< 0.1 mL O2/h) were used to correct for background respiration. The $\dot{M}O_2$ data was visually inspected to ensure that a linear decrease in water % air saturation of 5 – 10% occurred and a minimum r^2 of 0.98 was set to identify nonlinear measurements (Schuster et al., 2022).

Absolute MO_2 was not calculated for aerial oxygen consumption as approximately half of the animals did not achieve a linear decrease in % air saturation greater than 5% after 6-hours.

Body surface temperatures in air and seawater

The body surface temperatures of juvenile *Pisaster* were estimated using a handheld infrared camera (FLIR ONE Pro (iOS), Teledyne FLIR; iPhone 13 Pro, Apple Inc.). The pixel resolution of the infrared camera is 19200px (160 x 120px) and the accuracy is ±3°C or ±5% when the unit is within 15°C - 35°C and the scene is within 5°C - 120°C. Emissivity was set at 0.95 consistent with previous studies demonstrating that the emissivity of intertidal rocky substrate and invertebrates varies between 0.95 and 1 (Denny and Harley, 2006; Chapperon and Seuront, 2011; Cox and Smith, 2011). Three infrared images were taken of each animal (first image: immediately after the animal was removed from the temperature-controlled incubator measuring aerial oxygen consumption at ~20°C; second image: immediately after the animal was removed from the sea table (following an 18-hour submersion; the day after metabolic measurements); third image: immediately after the animal was removed from a temperature-controlled incubator maintained at ~30°C (following a 6-hour aerial emersion; the day after metabolic measurements)). Infrared images were analyzed using Thermal Studio Pro (Teledyne FLIR) to determine the relative body surface temperatures of Pisaster across treatments. Spot measurements were placed on the central disc (aboral side) and on each visible arm ray (approximately ¾ length down the arm ray from its attachment to the central disc).

Statistical analyses

The relationship between *Pisaster* body size and oxygen consumption, and the relationship between *Pisaster* body size and body surface temperature were assessed using linear regressions (R Core Team, 2021).

Results

Aerial oxygen consumption

The percent drop in oxygen for juvenile *Pisaster* in 20°C air ranged from 2.51 – 7.54% with a mean drop of 5.20 ± 1.38% (n = 9) during a 6-hour emersion period. There was a significant positive

relationship between body size (ash-free dry mass) and aerial oxygen consumption (linear regression; $p < 0.01$, adjusted $R^2 = 0.62$).

Aquatic oxygen consumption

The metabolic rate of juvenile *Pisaster* in 15°C seawater ranged from 0.37 – 0.97 mL O_2 with a mean rate of 0.58 ± 0.19 mL O_2 (n = 9). There was a significant positive relationship between body size (ash-free dry mass) and aquatic metabolic rate (linear regression; $p < 0.01$, adjusted $R^2 = 0.59$).

Relationship between Pisaster body size and body surface temperature

There was no relationship found between juvenile *Pisaster* body size (ash-free dry mass) and aerial body surface temperature at ~20°C (linear regression; $p = 0.79$, adjusted $R^2 = -0.15$) or ~30°C (linear regression; $p = 0.14$, adjusted $R^2 = 0.19$). Similarly, no relationship was found between juvenile *Pisaster* body size and aquatic body surface temperature at ~15°C (linear regression; $p = 0.44$, adjusted $R^2 = -0.04$).

Pisaster had a mean body surface temperature of 18.9 ± 0.8°C (min = 17.5°C, max = 20°C, n = 9) following the 20°C aerial emersion. The mean body surface temperature of animals following the 30°C emersion was 27.3 ± 0.5°C (min = 26.6°C, max = 28°C, n = 9). After submersion in 15°C seawater, the mean body surface temperature of *Pisaster* was 15.8°C ± 0.9°C (min = 14.4°C, max = 17°C, n = 9).

Conclusions

Here we find that aerial and aquatic oxygen consumption increase with body size in juvenile *Pisaster,* while body surface temperature remains consistent across sizes. As *Pisaster* grow, their metabolic demands rise and more energy is required to sustain physiological functions. This has important implications for populations facing warming aerial temperatures, as extreme heat events can suppress feeding, limiting the intake of energy needed for survival. Notably, the body surface temperature of juvenile *Pisaster* was consistent across sizes in each temperature treatment. It may be that a larger increase in mass is needed to achieve thermal inertia, suggesting that future research should directly compare the body surface temperatures of juvenile and adult *Pisaster* under thermally stressful conditions.

References

Bakken, G. S. and D. M. Gates. **1975**. Heat-Transfer Analysis of Animals: Some Implications for Field Ecology, Physiology, and Evolution. In: *Perspectives of Biophysical Ecology* (D. M. Gates and R. B. Schmerl, eds), pp. 255–290. Springer, Berlin, Heidelberg.

Brown, J., J. Gillooly, A. Allen, V. m Savage and G. West. **2004**. Toward a Metabolic Theory of Ecology. *Ecology* **85**: 1771–1789.

Fly, E. K., C. J. Monaco, S. Pincebourde and A. Tullis. **2012**. The influence of intertidal location and temperature on the metabolic cost of emersion in Pisaster ochraceus. *Journal of Experimental Marine Biology and Ecology* **422–423**: 20–28.

Helmuth, B. 1998. Intertidal Mussel Microclimates: Predicting the Body Temperature of a Sessile Invertebrate. *Ecological Monographs - ECOL MONOGR* **68**: 51–74.

Mauzey, K. P. 1966. Feeding Behavior and Reproductive Cycles in Pisaster ochraceus. *Biological Bulletin* **131**: 127–144. Marine Biological Laboratory.

McGaw, I. J., A. M. Clifford and G. G. Goss. **2015**. Physiological responses of the intertidal starfish Pisaster ochraceus, (Brandt, 1835) to emersion at different temperatures. *Journal of Experimental Marine Biology and Ecology* **468**: 83–90.

Menge, J. L. and B. A. Menge. **1974**. Role of Resource Allocation, Aggression and Spatial Heterogeneity in Coexistence of Two Competing Intertidal Starfish. *Ecological Monographs* **44**: 189–209.

Monteith, J. L. and M. H. Unsworth (eds). **2008**. Principles of Environmental Physics. In: *Principles of Environmental Physics (Fourth Edition)*, p. i. Academic Press, Boston.

Murphy, C. T. and M. B. Jones. **1987**. Some factors affecting the respiration of intertidal Asterina gibbosa (Echinodermata: Asteroidea). *Journal of the Marine Biological Association of the United Kingdom* **67**: 717–727.

Pincebourde, S., E. Sanford and B. Helmuth. **2009**. An intertidal sea star adjusts thermal inertia to avoid extreme body temperatures. *Am Nat* **174**: 890–897.

R Core Team. **2021**. R: A language and environment for statistical computing. R Foundation for Statistical Computing, Vienna, Austria.

Robles, C. 2013. Pisaster ochraceus. In: *Starfish: Biology and Ecology of the Asteroidea*.

Schuster, J. M. and A. E. Bates. **2023**. The role of kelp availability and quality on the energetic state and thermal tolerance of sea urchin and gastropod grazers. *Journal of Experimental Marine Biology and Ecology* **569**: 151947.

Schuster, J. M., A. Kurt Gamperl, P. Gagnon and A. E. Bates. **2022**. Distinct realized physiologies in green sea urchin (Strongylocentrotus droebachiensis) populations from barren and kelp habitats. *FACETS* **7**: 822–842. Canadian Science Publishing.

Seebacher, F. and C. E. Franklin. **2005**. Physiological mechanisms of thermoregulation in reptiles: a review. *J Comp Physiol B* **175**: 533–541.

Figures and Tables

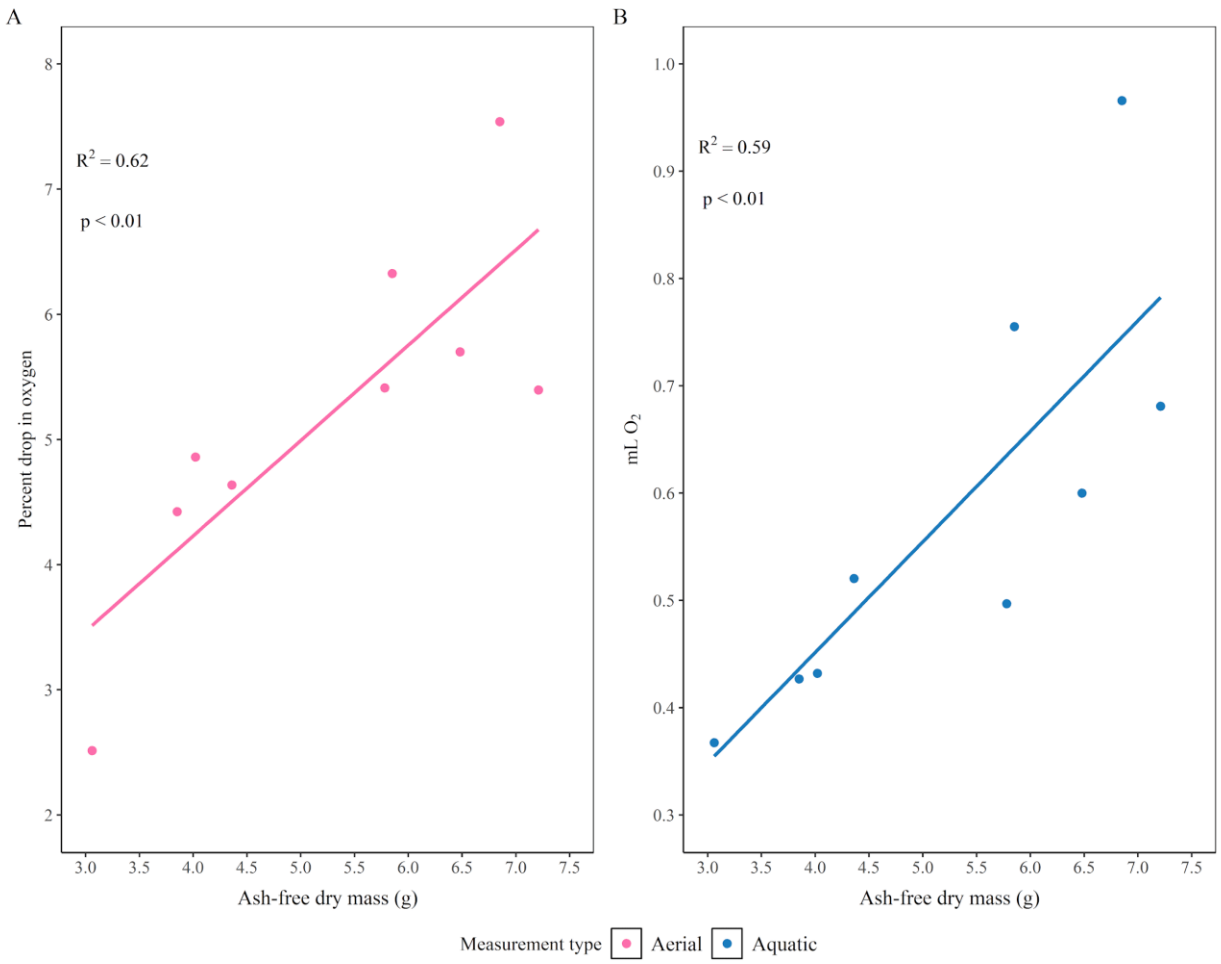

Fig. 1 The relationship between *Pisaster* body size (ash-free dry mass) and **(A)** the percent drop in aerial oxygen and **(B)** aquatic metabolic rate (estimated using aquatic oxygen consumption). Lines represent the linear relationship between variables (linear regression) with the p-value and adjusted R^2 included on the plot. **(A)** Aerial oxygen consumption was recorded for 6-hours while juvenile *Pisaster* were emersed in 20°C air. **(B)** Aquatic oxygen consumption was recorded while juvenile *Pisaster* were submerged in 15°C seawater until a 5 – 10% drop in oxygen was reached in all animals (30 – 60 min).

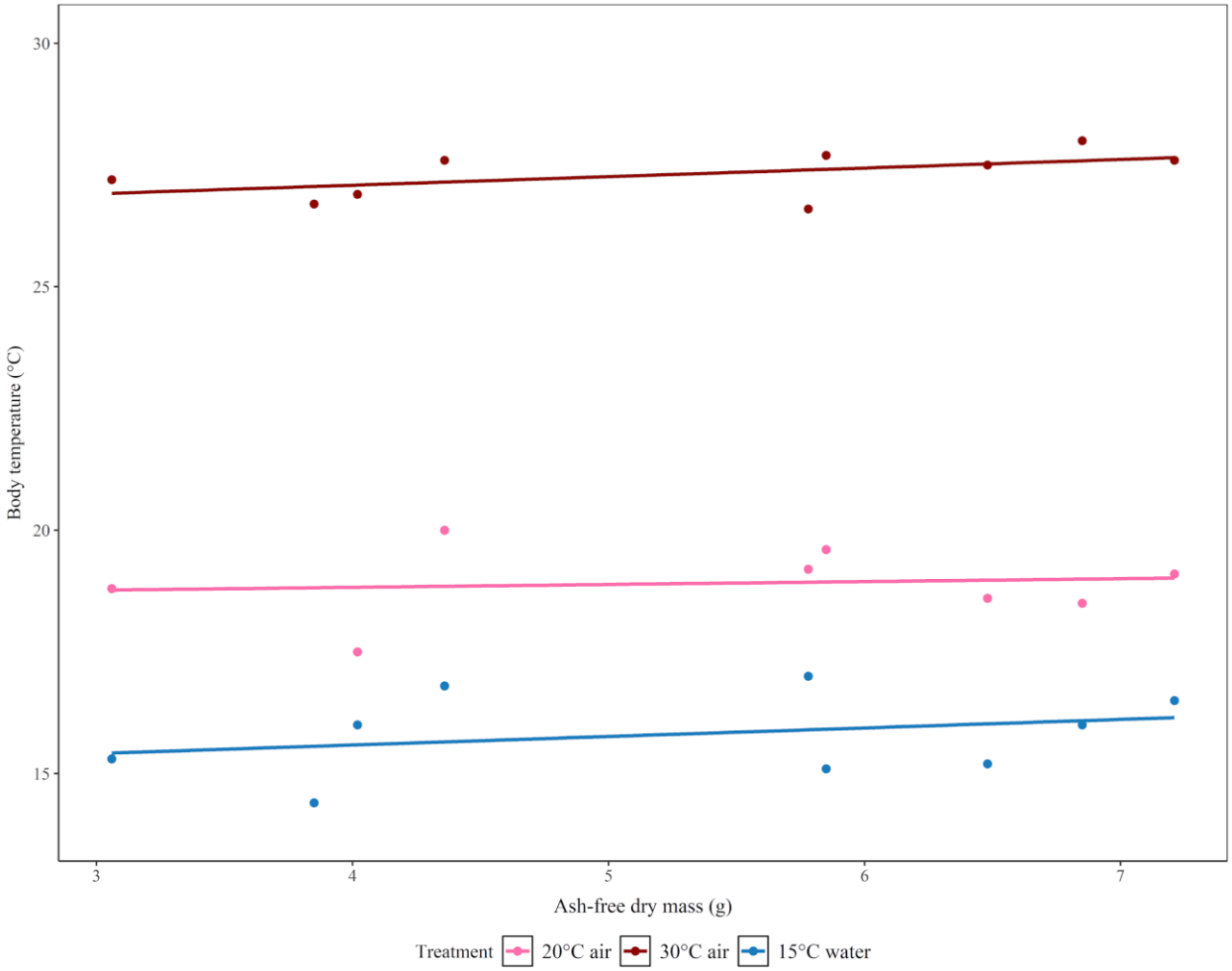

Fig. 2 The body surface temperatures of juvenile *Pisaster* immediately after a 6-hour emersion in 20°C air (actual air temperature = 18.8°C; pink), a 6-hour emersion in 30°C air (actual air temperature = 28.8°C; red), and **(C)** an 18-hour submersion in 15°C seawater (actual water temperature = 15.2°C; blue). Lines represent the linear relationship between variables (linear regression); no significant relationships were found between *Pisaster* body surface temperature and body size (ash-free dry mass).

Appendix 5: Lactic acid in juvenile *Pisaster* coelomic fluid following thermal stress

Lydia N. Walton, Iain J. McGaw, and Amanda E. Bates

Background and objectives

We investigated whether anaerobic respiration follows metabolic suppression under oxygen-limited conditions by measuring the concentration of lactic acid (a byproduct of anaerobic respiration; see review by Allen and Holm, 2008) in the coelomic fluid of juvenile *Pisaster* exposed to aerial heatwave temperatures. We predicted that L-lactate concentrations would be highest in animals exposed to 30°C air temperatures.

Materials and methods

Collections and experimental design

The following experiment was conducted in May 2024 alongside measurements of juvenile *Pisaster* feeding and metabolic rates (Experiment 2; n = 72).

Anaerobic respiration (measuring lactic acid)

Coelomic fluid was extracted from the perivisceral coelomic cavity ~36 hours after aquatic $\dot{M}O_2$ measurements, when *Pisaster* were emersed in air. Samples were transferred to 1.5 mL Eppendorf tubes under mineral oil and stored at -80°C. The maximum amount of coelomic fluid extracted from each animal was 2% of the total wet body weight (*i.e.*, 100 µL for *Pisaster* between 5 g and 10 g, and 200 µL for *Pisaster* between 10 g and 20 g). This amount is comparable to current recommendations for safe withdrawal of total blood volume (10%) in small vertebrates, assuming coelomic fluid volume makes up 20% of *Pisaster*'s total wet weight (Wahltinez *et al.*, 2023). All animals were euthanized and frozen after the last coelomic fluid extraction (day 39).

Lactate concentrations were measured enzymatically using an L-Lactate assay kit (MAK443, Sigma-Aldrich) and microplate spectrophotometry. Coelomic fluid samples were thawed at room temperature and diluted 100x (1 µL of coelomic fluid to 99 µL of distilled H_2O). 50 µL of each sample and 50 µL of L-Lactate standards (see MAK443 protocols) were added to separate wells in a black-walled 96-well plate. 50 µL of working reagent (assay buffer, enzyme A, enzyme B, NAD, and probe) was then

added to every well (with either the sample or standard inside). The plate was tapped to mix and incubated for 60 minutes at room temperature, protected from light. Fluorescence intensity (λEx = 530 nm and λEm = 585 nm) was measured and compared to a standard curve for L-lactate concentrations. The concentration of L-lactate (μM) was calculated as: $(F_{Sample} - F_{Blank}) / (Slope) * DF$ where F_{Sample} is the fluorescence intensity of the sample well, F_{Blank} is the fluorescence intensity of the water blank well, Slope is the slope of the L-lactate standard curve, and DF is the dilution factor of the sample (DF = 100).

Results

Lactic acid in *Pisaster* coelomic fluid was below the detectable limits of the assay (1 μM) for 93% of samples (n = 28/30), and differences between treatments could not be tested statistically.

Conclusions

Here we find that juvenile *Pisaster* do not produce detectable amounts of lactic acid in their coelomic fluid when exposed to 25°C or 30°C air temperatures. While lactate production has been observed in the coelomic fluid of the sea urchin *Mesocentrotus nudus* (Drozdov and Drozdov, 2015), it has not been reported in any other echinoderm, including adult *Pisaster* (McGaw *et al.*, 2015), at the time of this study. *Pisaster* likely rely on alternative strategies to anaerobic respiration during low tide, such as metabolic depression, use of stored energy reserves, or behavioural evasion of thermal stress.

References

Allen, S. E. and J. L. Holm. 2008. Lactate: physiology and clinical utility. *Journal of Veterinary Emergency and Critical Care* 18: 123–132.

Drozdov, K. A. and A. L. Drozdov. 2015. Variation in the contents of lactate and alanine in the coelomic fluid of the sea urchin *Mesocentrotus nudus* (A. Agassiz, 1863) indicates anaerobic glycolysis. *Russ J Mar Biol* 41: 311–314.

McGaw, I. J., A. M. Clifford and G. G. Goss. 2015. Physiological responses of the intertidal starfish Pisaster ochraceus, (Brandt, 1835) to emersion at different temperatures. *Journal of Experimental Marine Biology and Ecology* 468: 83–90.

Wahltinez, S. J., M. Byrne and N. I. Stacy. 2023. Coelomic fluid of asteroid echinoderms: Current knowledge and future perspectives on its utility for disease and mortality investigations. *Vet Pathol* 60: 547–559. SAGE Publications Inc.